Institut für Tierwissenschaften

Effect of an inflammatory stimulus on mitochondrial functionality in liver cells of dairy cows

Inaugural – Dissertation

zur

Erlangung des Grades

Doktor der Agrarwissenschaften

(Dr. agr.)

der

Landwirtschaftlichen Fakultät

der

Rheinischen Friedrich-Wilhelms-Universität Bonn

von

MohamadTaher Alaedin, M.Sc

aus

Gorgan, Iran

Bonn, 2021

Referentin: Prof. Dr. Dr. Helga Sauerwein

Korreferent: Prof. Dr. Karl-Heinz Südekum

Fachnahes Mitglied: Prof. Dr. Bernt Guldbrandtsen

Tag der mündlichen Prüfung: 28.04.2021

Angefertigt mit Genehmigung der Landwirtschaftlichen Fakultät der Universität Bonn.

ENGLISH ABSTRACT

Mitochondria are essential organelles with key roles in metabolism and health; their function is influenced by various exogenous and endogenous factors. Dairy cows undergo a negative energy balance (EB) and a systemic inflammation around parturition that is interrelated with the metabolism of nutrients like fatty acids (FA) and can ultimately affect the productive efficiency of the animals. The oxidation of FA is localized in the mitochondria and L-Carnitine (CAR) is required for their transport into the mitochondria for generating energy. The objective of this study was to evaluate the effects of a controlled inflammation induced by lipopolysaccharide (LPS) in mid lactation when the EB has turned positive on pathways related to mitochondrial FA metabolism in the liver of dairy cows receiving a dietary CAR supplement or not (CON, control). Holstein cows (n = 43, parity: 2-5) were randomly assigned to either CON (n = 21) or CAR (n = 22; 25 g CAR/cow/day) from day - 42 until day +112 relative to calving. At day +111, all cows were intravenously infused with LPS (0.5 µg/kg body weight). To identify potential changes of hepatic FA metabolism, mRNA abundance of genes involved in FA metabolism were determined in liver biopsy samples taken at day -42, +100, +112, and +126. The Microfluidic qPCR technology was used to quantify the mRNA abundance of 41 genes involved in FA metabolism and 8 endogenous reference genes. Besides, the hepatic abundance of 3 target proteins related to the FA metabolism was assessed on d +100 and +112 (equal to -11 and +1 days relative to the LPS challenge) from 22 cows (n =11 per group) by a capillary Western blotting method. The effectiveness of the CAR supplementation was confirmed by elevated CAR concentrations in the CAR but not the CON groups. The mRNA and protein data were statistically evaluated by mixed models, using time and treatment as well as their interaction as fixed effects. The CAR supplementation at the used dosage did not affect the mRNA of genes related to hepatic FA metabolism, with the exception of solute carrier family 27 member 2 (*SLC27A2*) and carnitine palmitoyltransferase 1 (*CPT1*) that are related to the activation of FA to FA-acyl-CoA esters and to mitochondrial FA oxidation, respectively. In contrast, LPS affected the mRNA abundance of more genes, among which were enoyl-CoA hydratase 1 (*ECH1*) and acyl-CoA oxidase 2 (*ACOX2*) that are involved in peroxisomal β-oxidation. This may point to a shift in hepatic FA metabolism from mitochondrial towards peroxisomal β-oxidation. In addition, changes in protein abundance were solely observed with LPS, independent of treatment: acetyl-CoA carboxylase alpha (ACACA, mitochondrial FA oxidation pathway) was downregulated during inflammation. The results show the effects of inflammation during a balanced energy status on hepatic FA metabolism at the level of pathway-selected mRNA and protein. They thus contribute to understanding the interplay of energy metabolism and immune reaction in dairy cows.

Key words: lipopolysaccharide, L-carnitine, inflammatory stress, hepatic fatty acid metabolism, mitochondria, mRNA abundance, protein abundance, mid-lactation, dairy cow

Deutsche Kurzfassung

Mitochondrien sind essenzielle Organellen, die für Stoffwechsel und Gesundheit zentrale Bedeutung haben. Ihre Funktion wird durch verschiedene exogene und endogene Faktoren beeinflusst. Um den Zeitpunkt der Kalbung sinkt die Energiebilanz (EB) von Milchkühen ins Negative; gleichzeitig läuft eine systemische Entzündungsreaktion, die auch mit dem Metabolismus von Nährstoffen wie etwa Fettsäuren (FA) in Verbindung steht und letztlich auch die Produktionseffizienz der Tiere beeinflussen kann. Damit die Oxidation von FA in den Mitochondrien ablaufen kann, müssen diese zunächst über L-Carnitin (CAR) in die Mitochondrien transportiert werden. Ziel dieser Arbeit war es, die Effekte einer kontrollierten Entzündungsreaktion, herbeigeführt durch Infusion von Lipopolysaccharid (LPS), auf den mitochondrialen FA-Stoffwechsel in der Mitte der Laktation, wenn die EB wieder ausgeglichen ist, von Milchkühen, die entweder CAR als Futterzusatz erhielten (n = 21), oder kein Supplement bekamen (CON, n =), zu untersuchen. Die Gabe von CAR (25 g/Tier/Tag) erfolgte von Tag -42 bis +112 relativ zur Kalbung. Am Tag +111 wurde allen Kühen LPS (0.5 µg/kg Körpergewicht) intravenös verabreicht. Um potenzielle Veränderungen im Leber-Fettsäurestoffwechsel zu erfassen, wurde die mRNA-Menge von Genen, die für Komponenten des FA-Metabolismus kodieren, in Leber-Bioptaten von Tag -42, +100, +112, and +126 bestimmt. Die mRNA-Menge von insgesamt 41 Zielgenen aus dem FA-Stoffwechsel sowie von 8 Referenzgenen wurde mittels der *Microfluidic qPCR*-Technologie quantifiziert. Zudem wurde von 3 Zielgenen auch die Proteinexpression in den Leberbiopsien von Tag 100 and 112 (N = 11/Gruppe) mittels eines Kapillar-basierten Western Blot-Verfahrens gemessen. Die Wirksamkeit der CAR-Supplementierung wurde anhand der erhöhten CAR-Konzentrationen im Blut der CAR, nicht aber der CON-Tiere, bestätigt. Die mRNA- und Proteindaten wurden über gemischte Modelle mit Zeit, Gruppe und der entsprechenden Interaktion als fixen Faktoren statistisch ausgewertet. Von den untersuchten Zielgenen waren lediglich "*Solute Carrier Family 27 Member 2" (SLC27A2)* und Carnitin-Palmitoyltransferase 1 (*CPT1*), die an der Aktivierung von FA zu FA-Acyl-CoA-Estern bzw. der mitochondrialen FA-Oxidation beteiligt sind, durch die CAR-Supplementierung beeinflusst. Dagegen war unter LPS-Stimulation die mRNA-Menge von mehreren Genen verändert, darunter auch Enoyl-CoA-Hydratase 1 (*ECH1*) und Acyl-CoA Oxidase 2 (*ACOX2*), die an der peroxisomalen ß-Oxidation beteiligt sind. Dies deutet möglicherweise auf eine Verschiebung des hepatischen FA-Metabolismus von den Mitochondrien zu den Peroxisomen. Zudem ergaben sich ausschließlich unter LPS-Simulation unabhängig von CAR bzw. CON auch Veränderungen bei einem der untersuchten Zielproteine: die Acetyl-CoA-Carboxylase-alpha (ACACA) aus dem Stoffwechselpfad der mitochondrialen FA-Oxidation war unter LPS reduziert. Die Ergebnisse beschreiben die Wirkung einer entzündlichen Reaktion während einer ausgeglichenen EB auf den Leber-FA-Stoffwechsel auf mRNA- und Proteinebene ausgewählter Zielgene. Damit liefern sie einen Beitrag zum Verständnis der Beziehung zwischen Energiestoffwechsel und Immunreaktion bei der Milchkuh.

Contents

List of abbreviations

ACACA	Acetyl-CoA carboxylase alpha
ACAD10	Acyl-CoA dehydrogenase family member 10
ACADM	Acyl-CoA dehydrogenase medium-chain
ACADS	Acyl-CoA dehydrogenase short-chain
ACADVL	Acyl-CoA dehydrogenase very-long-chain
ACAT1	Acetyl-CoA acetyltransferase 1
ACAT1	Acetyl-CoA acetyltransferase 1
ACOX1	Acyl-CoA oxidase 1
ACOX2	Acyl-CoA oxidase 2
ACOX3	Acyl-CoA oxidase 3
AICAR	5-Aminoimidazole4-carboxamide riboside
ALDH3A1	Aldehyde dehydrogenase 9 family member A1
AMP	Adenosine monophosphate
ap	Ante partum
APOB	Apolipoprotein B
AU	Arbitrary unit
BB	γ-butyrobetaine
BBOX1	γ-butyrobetaine dioxygenase
bp	Base pair
C16:0	Palmitic acid
C18:0	Stearic acid
C18:1n9c	Oleic acid
CACT	Carnitine-acylcarnitine translocase
cAMP	Cyclic AMP
CAR	Carnitine group
CD	Cluster of differentiation
cDNA	Complementary DNA
CLA	Conjugated linoleic acid
CLP	Cecal ligation and puncture
CoA	Coenzyme A
CON	Control group
COX	Mammalian cytochrome C oxidase
COX4I1	Cytochrome C oxidase subunit 4I1
Cp	Crossing point
CPT1	Carnitine palmitoyltransferase 1
CPT-1	Carnitine palmitoyltransferase-1
CPT2	Carnitine palmitoyltransferase 2
CPT-2	Carnitine palmitoyltransferase-2
CRAT	Carnitine O-acetyltransferase
CROT	Carnitine O-octanoyltransferase
Ct	Cycle threshold
DAVID	Database for annotation, visualization, and integrated discovery
DGAT1	Acyl CoA:diacylglycerol acyltransferase
DM	Dry matter
DMI	Dry matter intake

DPPH	1-Diphenyl- 2-picryl-hydrazyl
ECH1	Enoyl-CoA hydratase 1
ECHDC2	Enoyl-CoA hydratase domain containing 2
ECHDC3	Enoyl-CoA hydratase domain containing 3
ECHS1	Enoyl-CoA hydratase, short-chain 1
EIF3K	Eukaryotic translation initiation factor 3 subunit K
EMD	Emerin
ER	Endoplasmic reticulum
ETC	Electron transport chain
FADH	Flavin adenine dinucleotide
FAO	Fatty acid oxidation
FAS	Fatty acid synthase
FATP	Fatty acid transport proteins
FGF21	Fibroblast growth factor 21
FOXO1	Forkhead box protein O1
GAPDH	Glyceraldehyde-3-phosphate dehydrogenase
GD	Glutaryl-CoA dehydrogenase
GE	Gene expression
GPAD	Glycerol-3-phosphate acyltransferase
HADHA	Hydroxyacyl-CoA dehydrogenase trifunctional multienzyme complex subunit alpha
HMGCL	3-Hydroxy-3-methylglutaryl-CoA lyase
HMGCS2	3-Hydroxy-3-methylglutaryl-CoA synthase 2
HNE	4-Hydroxynonenal
HNE	4-Hydroxy-2-nonenal
HPCAL1	Hippocalcin-like 1
HPLC	High-performance liquid chromatography
HSL	Hormone-sensitive lipase
i2VD	Iso(2)valeryl-CoA dehydrogenase
i3VD	Iso(3)valeryl-CoA dehydrogenase
iBD	Isobutyryl-CoA dehydrogenase
IFC	Integrated fluidic circuits
IGF1	Insulin-like growth factor 1
IRS-1	Insulin receptor substrate 1
KEGG	Kyoto encyclopedia of genes and genomes
LBP	Lipopolysaccharide binding protein
LCFA	Long-chain fatty acid
LOX	Lipoxygenase
LPL	Lipoprotein lipase
LPS	Lipopolysaccharides
LRP10	LDL receptor-related protein 10
LRP10	Low-density lipoprotein receptor-related protein 10
LSM	Least square means
MAPK	Mitogen-activated protein kinases
MARVELD1	MARVEL domain containing 1
MCKAT	Medium-chain 3-ketoacyl-coa thiolase
MIQE	Minimum information for publication of qPCR experiments
MLYCD	Malonyl-CoA decarboxylase

mTOR	Mammalian target of rapamycin
MTOR	Mechanistic target of rapamycin kinase
MTP	Mitochondrial trifunctional protein
MTTP	Microsomal triglyceride transfer protein
MUFA	Monounsaturated fatty acid
MUT	Methylmalonyl-CoA mutase
NADPH	Nicotinamide adenine dinucleotide phosphate hydrogen
NDF	Neutral detergent fiber
EB	Energy balance
NEFA	Non-esterified fatty acid
NEL	Net energy requirement for lactation
NEM	Net energy requirement for maintenance
NF-kB	Nuclear factor kappa-light-chain-enhancer of activated B cells
NMN	Nicotinamide mononucleotide
NRF1	Nuclear respiratory factor 1
OCTN	Organic cation transporters
OD	Optical density
PAMP	Pathogen-associated molecular patterns
PCCA	Propionyl-CoA carboxylase subunit alpha
PCCB	Propionyl-CoA carboxylase subunit beta
PCI	Peritoneal contamination and infection
PKA	Protein kinase A
PMR	Partial mixed ration
POLR2A	RNA polymerase II subunit A
pp	Postpartum
PPARGC1A	Peroxisome proliferator-activated receptor-gamma coactivator 1
PPARα	Peroxisome proliferator-activated receptor alpha
PRKAG1	Protein kinase AMP-activated non-catalytic subunit gamma 1
RIN	RNA integrity number
Rn	Normalized reporter value
ROS	Reactive oxygen species
RPS6KB1	Ribosomal protein S6 kinase B1
rs	Correlation coefficient
RT	Rectal temperature
RT-qPCR	Reverse-transcription quantitative polymerase chain reaction
SARA	Subacute ruminal acidosis
SCHAD	Short-chain 3-hydroxyacyl-CoA dehydrogenase
SEM	Standard error of the mean
SFA	Saturated fatty acid
SIRS	Systemic inflammatory response syndrome
SLC22A5	Solute carrier family 22 member 5
SLC25A20	Solute carrier family 25 member 20
SLC27A2	Solute carrier family 27 member 2
SLC27A3	Solute carrier family 27 member 3
SLC27A4	Solute carrier family 27 member 4
sn	Stereospecific position number
TAG	Triacylglycerol

TCA	Tricarboxylic acid
TFAM	Mitochondrial transcription factor A
TLR	Toll-like receptors
TML	Trimethyllysine
TMLHE	Trimethyllysine hydroxylase
VFA	Volatile Fatty Acid
VLDL	Very-low-density lipoprotein
YWHAZ	Tyrosine 3-monooxygenase/tryptophan 5-monooxygenase activation protein zeta

List of Tables

List of Figures

1 INTRODUCTION

1.1 Metabolism and inflammation of dairy cows during different stages of lactation

1.1.1 General overview

During the past 25 years, energy metabolism research has resolved numerous doubts regarding energy use by lactating cows. Tensed metabolic conditions are triggered at all stages of lactation by the great lactation performance in cows of modern intensive dairy production systems. The energy metabolism of dairy cows in all its complexity is central to performance and production as well as animal health. It is particularly evident that in the transition period when the energy requirements rapidly increase, and metabolic capacity is challenged. During the rest of the lactation cycle, the interaction between metabolism and the relation with the immune system are also very important.

1.1.1.1 Nutrient metabolism and inflammation in transition cows (pre-, peri- and early postpartum period)

The transition period for dairy cows is characterized as about 3 weeks prepartum through 3 weeks postpartum and is indicated by significant physiological and immunologic adjustments as the cow shifts from a gestational non-lactating state to the onset of lactation (Grummer, 1995). It should be noted that several studies have presented that all cows practice some degree of systemic inflammation in the days after parturition (Bradford et al., 2015b). Dairy cows are susceptible to increased incidence and severity of diseases during the transition period and health disorders occurring at this point which is exceptionally problematic as they extremely impact the productive efficiency of cows in the ensuing lactation (Ingvartsen, 2006; Pinedo et al., 2010). Indeed, approximately 75% of disease incidence within herds occurs within the first month of lactation including disorders of economic significance such as mastitis, metritis, ketosis, and displaced abomasum (LeBlanc et al., 2006). Numerous studies have been conducted to comprehend the underlying causes of both metabolic and infectious diseases at the time of parturition to design more persuasive management practices for reducing transition cow health disorders (Burke et al., 2010; Roche et al., 2013). Accordingly, several health disorders of dairy cows may be explained by the dramatic diversities in nutrient requirements that occur around the time of calving. During late pregnancy, as an example, glucose and amino acid are required to increase supporting fetal development (Bell, 1995; Bell et al., 2000). The onset of copious milk synthesis and secretion during the periparturient period also requires increased demands for energy, protein, and minerals (Bauman and Currie, 1980). Nutrient

metabolism must adjust accordingly to meet the rigorous production demands of the early lactation of cows. On the other hand, failure to adapt to these nutrient demands, however, it was found to be related to the development of many metabolic and inflammatory transition cow disorders (Sordillo and Raphael, 2013). Over the past decade, the notion evolved that a link might be existed between metabolic and immune pathways during times of altered nutrient metabolism that can broaden the risk of disease while the transition period. To acknowledge this theory, metabolic and infectious diseases tend to occur in parallel rather than as isolated events in cows during early lactation. Increased incidence of any disorder will increase the chance that cows will succumb to other health issues (Curtis et al., 1983). For instance, cows suffering from ketosis were twice as likely to develop mastitis than healthy cows (Oltenacu and Ekesbo, 1994). Epidemiological studies also indicated an association between the development of the retained placenta and the incidence of mastitis (Emanuelson et al., 1993). There are detailed shreds of evidence to suggest that increase of both metabolic and infectious diseases during the transition period points to altered energy metabolism, oxidative stress, and dysfunctional host immune defenses (Sordillo and Mavangira, 2014; Sordillo et al., 2009; Sordillo and Raphael, 2013).

It is apparent that inflammatory signaling is elevated in several organs in the postpartum cow, with no obvious focal organ. Therefore, this growing body of evidence suggests that the processes of parturition and galactopoiesis or infections (and/or LPS absorption) induce inflammation (Bradford et al., 2015b). Unlike the inflammation associated with acute infection, the postpartum inflammatory state is often low grade without the classical signs of inflammation, which is consistent with the notion of metabolic inflammation (Hotamisligil, 2006). The wide variety of signals that converge to drive inflammatory processes are derived from a broad list of systemic stressors, namely social and heat stress which is able to promote inflammatory transcription patterns via autonomic catecholamine release and bloodborne heat shock proteins, respectively (Kumar et al., 2015; Patki et al., 2015). Consequently, tissue damage associated with parturition and subsequent uterine involution, as well as infections such as metritis and mastitis, result in leukocyte activation and release of inflammatory cytokines and eicosanoids (Contreras et al., 2012). Various dietary and environmental conditions can decrease the barrier function of the gut, and allow translocation of LPS into the bloodstream (Kvidera et al., 2017a). Accordingly, excess circulating lipids and low antioxidant status are associated with oxidative stress, which occurs when free radicals cause chain

reactions, thus producing reactive oxygen species (ROS) that promote inflammation (Bradford et al., 2015b; Figure 1).

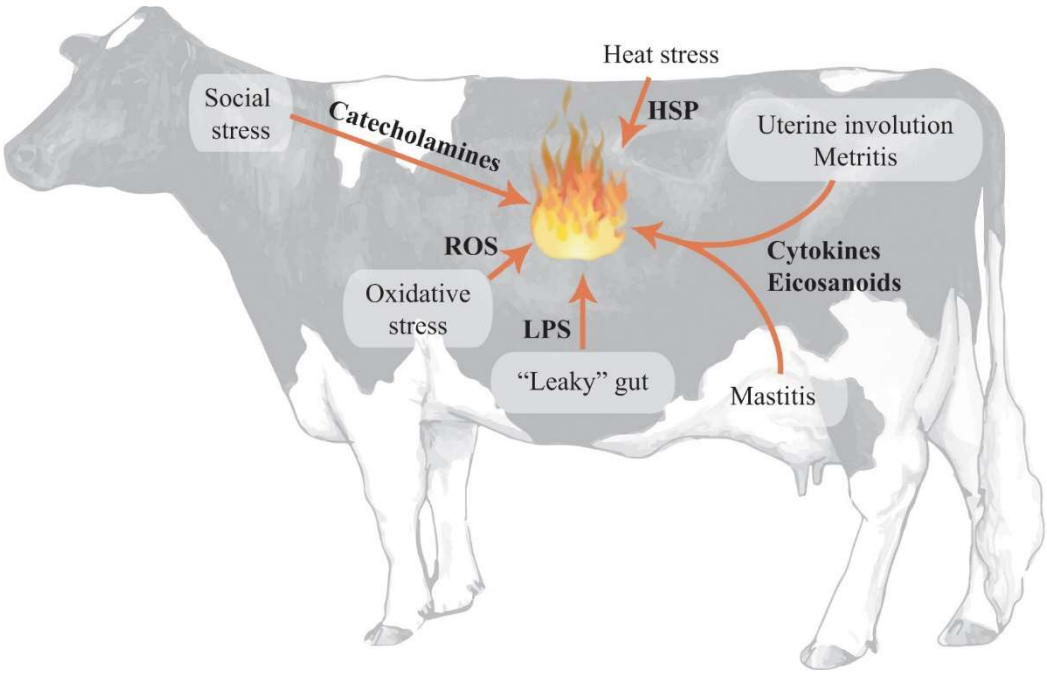

Figure 1. Diverse stressors may contribute to systemic inflammation at different stages of lactation (Bradford et al., 2015b).

Despite the harmful effects of excessive inflammation, a certain degree of inflammation seems to be beneficial for normal physiological adaptations in the transition period that can give inflammatory signals a central role not only during diseases and disorders but in developmental physiology (Bradford et al., 2015b). At parturition, there is a massive flow of macrophages and neutrophils into the myometrium; making a proinflammatory environment that promotes dilation of the cervix, contraction of the uterus, cleavage of the fetal membranes, and removal of the placenta. The other benefit of inflammation is its role in stimulating mechanisms for pathogens clearance and resolving infections. Activation of inflammatory pathways may help cows to overthrow diseases, knowing that infections increase during early lactation. Inflammation was also shown to contribute to wound healing by promoting keratinocyte (the main cells in the epidermis) migration to close the wound. Since inflammation of muscle and adipose tissue are thought to be tightly linked to insulin resistance, endogenous inflammation in early lactation is likely necessary to improve insulin resistance and protect metabolic homeostasis as nutrient demands for the mammary gland increase. It has also been suggested that inflammation as a likely mechanism for regulating nutrient partitioning and energy balance, is involved in the homeorhetic shifts in metabolism required for a successful transition period when the shifts in nutrient demand are dramatic. Subsequently, it has been shown that

inflammatory signals play identified critical roles in normal tissue development and rebuilt like the central role of inflammatory signals in mammary gland development, lactogenesis, galactopoiesis, and involution (Bradford et al., 2015b).

1.1.1.2 Nutrient metabolism and inflammation in mid and late lactation

During mid to late lactation, energy intake is usually higher than energy requirements for maintenance and lactation (Figure 2).

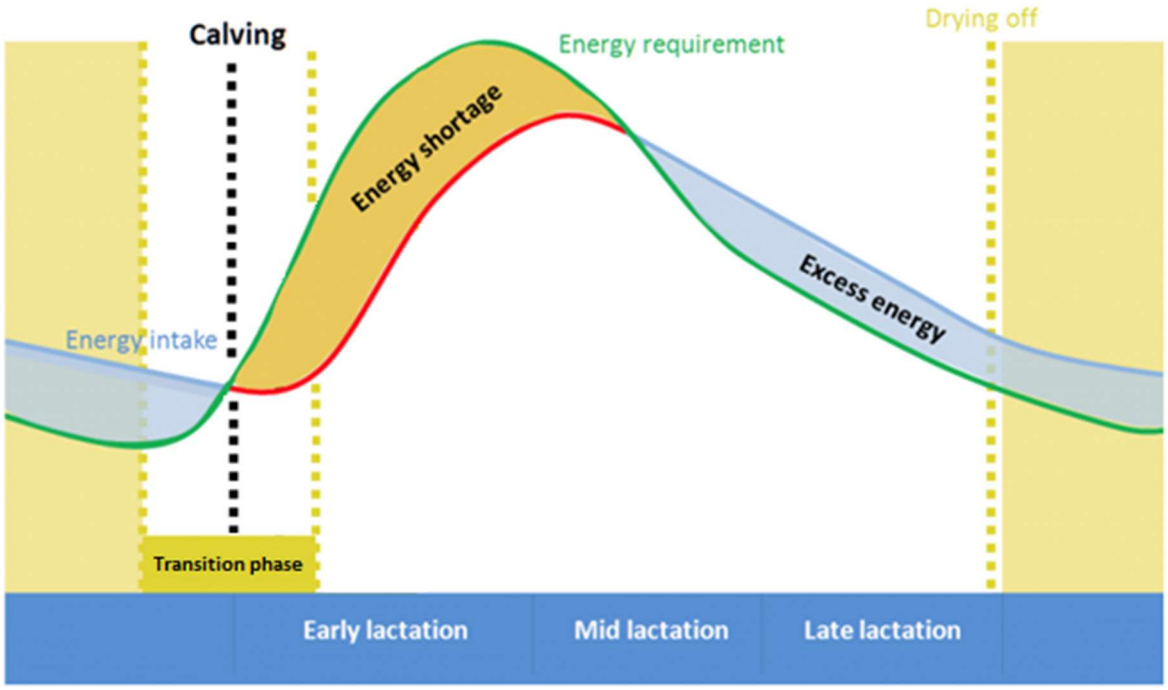

Figure 2. Energy supply and requirements during the lactation cycle in the dairy cow. The green curve represents the energy that is needed for the maintenance of vital body functions and milk production. In the transition phase from dry off till 3 weeks after calving (black dotted line) a shift happens in the balance of energy from positive (the blue area between 2 curves) to negative (the brown area between 2 curves). The feed intake increases slowly after calving, but the energy demand is also very high that in taken energy cannot cover it (red curve). The energy needed for milk production is highest when milk production reaches a peak. After that, when the milk production decreases during mid-lactation the energy is taken in through food can meet and exceed the energy requirements for milk production till the end of lactation and through the dry off period (khaki area) resulting in positive energy balance (Strucken et al., 2015).

During this period, the cow can replenish her body fat stores for the next lactation. Moe (1981) estimated that the efficiency of dietary energy utilization to replenish body fat stores would be higher during the last two-thirds of lactation (75%) than the dry period (60%). Nevertheless, in high producing dairy cows, it is difficult for replenishing body fat stores during mid to late lactation. High energy diets fed during mid to late lactation might be required to help restore body fat stores for the next lactation. Two approaches to increase the energy content

of diets fed to cows not only in early lactation but also in mid to late lactation are to increase the grain content of the diet or to supplement the diet with fat. It is worth to mention that these two approaches may not influence metabolism in the same manner. By increasing propionate production in the rumen (Davis and Brown, 1970), high grain diets can elicit an insulin response (Gaynor et al., 1995), resulting in the partitioning of nutrients toward body fat and away from the mammary gland (Davis and Brown, 1970). In contrast, moderate fat supplementation should not influence rumen fermentation. However, by providing long-chain fatty acids (LCFA) to the mammary gland, supplemental fat might spare glucose oxidation for nicotinamide adenine dinucleotide phosphate hydrogen (NADPH) production, increase glucose availability for lactose synthesis, and increase milk production (Grummer, 1995). There are some disadvantages to high energy diets. High grain diets have been associated with acidosis (Harmon et al., 1991). Afterward, they switch cattle from a high-forage to a high-starch diet results in decreases in rumen pH that are characteristic of subacute ruminal acidosis (SARA) because volatile fatty acids (VFA) including acetate, propionate, and butyrate, as well as other organic acids such as lactate, accumulate in the rumen (Goad et al., 1998; Iqbal et al., 2009). Respectively, the increase in non-structural carbohydrates in the diet of cattle during gradual grain adaptation results in microbiological changes in the rumen. The cornerstone among the changes is the increase in lactate-utilizing bacteria such as *Megasphaera elsdenii* (Counotte et al., 1981). These are relatively slow-growing bacteria found in low numbers in ruminants fed high-forage diets, and they increase in number only when lactate is a major product of rumen fermentation. If the rate of concentrate inclusion in the diet is higher than the rate at which lactate-utilizing bacteria can increase, then lactic acid accumulates in the rumen and depresses rumen pH more drastically than similar amounts of VFA (Owens et al., 1998). Accordingly, a survey on 15 dairy farms in Wisconsin, USA showed the presence of SARA in 19% of early-lactation cows and 26% of mid-lactation cows (Garrett et al., 1997). Furthermore, Oetzel et al. (1999) surveyed 14 dairy farms in the same region that detected SARA in 20.1% of early- and peak-lactation cows. Additionally, the results from several studies show that feeding concentrate increases ruminal LPS (e.g. Gozho et al., 2005, 2006, 2007). It can be stated that SARA can result in damage to the rumen epithelium, which leads to pathogen infiltration and subsequently to the abscessation of various organs in the body. The presence of pathogens and LPS in blood circulation sets off inflammatory responses (Gozho et al., 2007).

Significantly, high grain diets have been also related to milk fat depression – by the reduction of the content of fat, the nutrient, which is the most variable and represents the major

energy cost in the milk production – (Gaynor et al., 1995; Schlegel et al., 2012), and lameness (Groehn et al., 1992). Long-term fat supplementation may chronically elevate plasma non-esterified fatty acids (NEFA) (Grummer, 1995), which may increase liver triglyceride, plasma ketone bodies concentrations, or both. From early on, it had been assumed that fat supplementation is necessary only during the period of lactation when cows are in negative energy balance. However, some studies revealed that supplemental fat feeding from parturition depressed feed intake (Jerred et al., 1990; Ruegsegger and Schultz, 1985). These studies suggest that fat should not be fed until after 6 weeks of lactation. It was doubted that perhaps the total supplemental and mobilized fat was greater than the ability of the cow to metabolize the fat (Palmquist, 1994). Recent research has shown that in early lactation, supplemental fat-fed with high neutral detergent fiber (NDF) diets is deposited in body reserves, perhaps via insulin stimulation, whereas supplemental fat-fed with low NDF diets increases milk yield (Piantoni et al., 2015; Weiss and Pinos-Rodríguez, 2009). Important in these studies is that SFA was supplemented at low levels (< 3% of DM). Even at low levels of fat supplementation, fats may depress ruminal fiber digestion, or more likely promote the formation of fatty acid isomers that cause milk fat depression (Palmquist and Jenkins, 2017). Jenkins and Harvatine (2014) conducted a formula to calculate the amount of unsaturated fat (UFA) that may be safely added to lactation rations. It considers the total UFA in the supplement and the NDF content of the dietary DM as follows:

Fat include in the ratio (%) = 4 × %NDF ÷ SUM of % UFA in the supplement

Inflammatory challenges can change the health status of the animal through a dual risk factor including altered nutrient metabolism and dysfunctional inflammation (Sordillo and Mavangira, 2014). Even though the milk production is the most important consumer of nutrients and energy, altered nutrient metabolism at inflammation can be triggered with negative energy balance which is a result of a reduction in dry matter intake (DMI) during inflammation and increased demand for energy due to increased activity of the immune system. Increased lipid mobilization as a consequence of negative energy balance may increase inflammatory responses and the generation of reactive oxygen species (ROS; Sordillo and Raphael, 2013). A pro-oxidant change in the redox balance can occur due to An imbalance between the ROS production and decreased intake of dietary antioxidants because of a decrease in feed intake (Sordillo and Aitken, 2009). When excessive ROS can damage cellular macromolecules such as lipids, protein, and DNA (Castillo et al., 2005; Celi, 2011), oxidative stress in dairy cattle

can cause increased disease susceptibility, longer durations of clinical disease, and slower return to peak production (Bertoni et al., 2008; Jóźwik et al., 2012; Sordillo and Raphael, 2013).

High-yielding dairy cows are commonly fed concentrate-based diets to meet their energy requirements. However, it was shown that feeding excessively high grain diets (21% of the DM) increases the concentration of free ruminal and plasma lipopolysaccharides (LPS) (Khafipour et al., 2009) attributable to increased lyses of gram-negative bacteria cells, developed by a rise in rumen acidity (Plaizier et al., 2012). Several researchers have revealed that LPS in the rumen may reach circulation (Bilal et al., 2016; Sato, 2015). Once translocated, LPS in blood interacts with lipopolysaccharide-binding protein (LBP) (Plaizier et al., 2012) and subsequently, immune activation and systemic inflammatory responses begin, after the LPS-LBP complex is transferred to a cluster of differentiation 14 (CD14) and recognized by immune cells. It has been shown that inflammation can decrease milk yield because of decreased DMI, and the increased energy demands of the immune system. Immune system activation is an energy-demanding process that necessitates a reallocation of nutrients and energy from dispensable functions such as growth and production (Zhao et al., 2018).

1.1.2 Physiological aspects of inflammation throughout the lactation cycle

Like all mammals, dairy cattle have a complex network of immune cells and soluble factors that interact in a highly coordinated fashion to provide optimal resistance to tissue injury and disease (Dänicke et al., 2018). Inflammation is an essential component of the initial immune response that often determines if the source of tissue insult is eliminated promptly and affected areas are returned to normal function. Acute inflammation can be characterized by a series of responses involving vascular tissue including the release of soluble inflammatory mediators, vasodilation, increased blood flow, extravasation of serum components, leukocyte influx into affected areas, and elevated cellular metabolism. Each of these responses contributes to the classical clinical symptoms associated with inflammation including heat, redness, swelling, and pain (Chen et al., 2017). The initial step that triggers the inflammatory cascade during microbial infections is the recognition of invading pathogens through highly conserved pathogen recognition receptors on host cells (Jungi et al., 2011). Pattern recognition receptors can be expressed on cell surfaces, within cells, or secreted by cells with the capability to recognize a range of microbial factors associated with infectious pathogens. Collectively, this diverse array of conserved motifs unique to specific groups of microbes are referred to as pathogen-associated molecular patterns (PAMP) and including, for example, lipopeptides of Gram-positive bacteria and lipopolysaccharide of Gram-negative bacteria (Jungi et al., 2011; Kumar

et al., 2011). Some examples of pattern recognition receptors found in both immune and non-immune cells that can differentiate a range of PAMP are CD14, nucleotide-binding oligomerization domains, and the family of toll-like receptors (TLR) including TLR2, TLR4, TLR5, and TLR9 (Kumar et al., 2011). After binding to their ligand, pattern recognition receptors can initiate intracellular signaling through the release of potent pro-inflammatory factors including eicosanoids and other oxylipids, nitric oxide, and cytokines. These soluble mediators act locally on the vascular endothelium to increase permeability and facilitate chemotaxis of leukocytes from the blood to the site of infection. Newly recruited (neutrophils) and pre-existing (monocytes) leukocytes eliminate microbial pathogens through phagocytosis and intracellular killing mechanisms. Neutrophils destroy internalized microbes by degradative enzymes and toxic amounts of ROS. Oxylipids and cytokines can also elicit systemic inflammatory responses that include the release of acute-phase proteins from the liver, increased body temperature, increased heart rate, and reduced feed intake (Lumeng and Saltiel, 2011). Inflammation is a finite process that should be self-limiting as soon as the source of tissue injury is neutralized, and adequate tissue repair is completed. Processes that self-limit or resolve inflammation include the cessation of pro-inflammatory signaling cascades, apoptosis and clearance of neutrophils, and the eventual return of tissue mononuclear cells (macrophages and lymphocytes) back to normal numbers. Historically, the resolution of inflammation was thought to be a passive event that was a consequence of a spent immune reaction. Correspondigly, Serhan (2009) discovered that the resolution of inflammation is a tightly controlled process of the immune system orchestrated, in part, by novel families of lipid-derived mediators that have anti-inflammatory, pro-resolving, and protective properties. In other words, metabolites derived from fatty acids (FA) include lipoxins, resolvins, and protectins. To emphasize, the timely resolution of inflammation is essential to prevent collateral damage to host tissues as a consequence of an overly robust or prolonged inflammatory response. The transition period is characterized as a time of dramatic alternations in the efficiency of the bovine immune system. Numerous studies have recorded adjustments in several facets of both innate and adaptive immunity that can influence the susceptibility to new diseases in the transition cow (Aitken et al., 2011). Dysfunctional inflammatory reactions occur at both the systemic and the local levels which are especially problematic through the direct impact on disease pathogenesis in cows including metritis and mastitis (Contreras and Sordillo, 2011; Sordillo et al., 2009). Derangements in inflammatory responses can consist of a hypo-responsive state characterized by delayed migration of functionally adequate neutrophils and other innate immune factors during the early stages of the disease. Conversely, the lack of an

appropriate balance between the initiation and resolution of inflammation can result in an overly robust or chronic inflammatory response characterized by extensive damage to host tissues (Aitken et al., 2011). The underlying causes of dysfunctional inflammation during the transition period have been the subject of considerable research, with evidence to support a role for both endocrine and metabolic factors. For example, increases in several steroid hormones around the time of parturition are at least partially responsible for the altered function of neutrophils (Burton et al., 1995). Glucocorticoids are known to have potent immunosuppressive functions and plasma concentrations increase around the time of calving. A mechanism by which glucocorticoids can impair blood neutrophil function is by inducing downregulation of L-selectin and CD18 adhesion molecules needed for effective activation and migration to sites of tissue injury (Burton et al., 1995). Furthermore, changes in oestradiol and progesterone concentrations just before calving were reported to have direct and indirect effects on the functional capabilities of immune cell populations (Roth et al., 1982). Changes in these steroid hormones do not overlap with the entire transition period; it is clear, therefore, that other factors like several homeorhetic hormones including prolactin, growth hormone, IGF, and insulin associated with the transition period also contribute to inflammatory dysfunction (Kelley et al., 2007; Sordillo, 2016).

1.1.3 Interactions between metabolism and inflammation

The conversion of nutrients into an energy source needed to fuel normal physiological functions occurs through a series of metabolic reactions collectively referred to as cellular respiration. Oxygen is required for aerobic cellular respiration and ROS are metabolites formed in the mitochondria during this as by-products of the electron transport chain. Molecular oxygen is required as an electron acceptor for efficient energy production and ROS are formed as normal end products of cellular metabolism. Superoxide anion is a major free radical produced within mitochondria during cellular respiration that can interact with other molecules to generate other ROS, including hydrogen peroxide and hydroxyl radicals (Valko et al., 2007). Although the majority of ROS present in tissues follow increased cellular metabolism and energy generation, other potential sources include oxidizing enzyme pathways associated with host inflammatory responses. To point out, phagocytosis is an essential part of the inflammatory response that involves the generation of toxic ROS needed to kill microbes through an oxygen-dependent mechanism. Hence, the NADPH oxidase system localized within the phagosomal membranes of neutrophils and macrophages generates ROS needed to destroy engulfed pathogens (Babior, 1999). Oxygenation of FA substrates during oxylipid biosynthesis is another

significant source of ROS associated with inflammation. Following the release of poly-unsaturated FA from membrane phospholipids, the initial oxygenation step through either the cyclooxygenase or lipoxygenase (LOX) enzymatic pathways results in the generation of highly reactive ROS. For example, enzymatic oxidization of free arachidonic acid through the 15-LOX enzymatic pathway generates not only the FA hydroperoxide but also superoxide anion as a by-product of the reaction (Sordillo and Raphael, 2013). The production of low to moderate amounts of ROS is essential for the regulation of normal cellular processes including those that regulate inflammation. The production of ROS by NADPH oxidase during phagocytosis is an essential host defense mechanism needed to kill infectious pathogens. The ROS also plays a critical role in a variety of redox-regulated signal transduction pathways that lead to the production of cytokines, oxylipids, and other immunoregulatory factors essential for normal inflammatory responses (Finkel, 2011). For example, hydrogen peroxide as a result of autoxidation of the reduced components in the mitochondrial electron transport chain (Nulton-Persson and Szweda, 2001), can diffuse out of mitochondria and into the cytoplasm where it can react with nuclear factor kappa-light-chain-enhancer of activated B cells (NF-kB) (Bolisetty and Jaimes, 2013). Normally localized in the cytoplasm, NF-kB will become activated and translocate to the nucleus in response to ROS accumulation where it can interact with gene promoters that regulate the expression of pro-inflammatory genes (Mittal et al., 2013). Another significant inflammatory signaling pathway that is responsive to ROS activation is the mitogen-activated protein kinases (MAPK) pathway. Elements of the MAPK pathways become phosphorylated when the kinase apoptosis-signal kinase-1 is activated through ROS-mediated oxidation (Mittal et al. 2014). Thus, the moderate production of intracellular ROS is essential to elicit normal inflammatory responses during infection or other tissue injuries. As mentioned before, some ROS production is optimal for normal cellular functions, but the overproduction of ROS can cause cell and tissue injury and lead to a condition referred to as oxidative stress (Sordillo and Aitken, 2009). The amount of ROS is kept to nontoxic levels by a complex series of antioxidant mechanisms that have the capability to quench oxidants directly or form part of enzymatic redox couples (the pair of an oxidizing and reducing agent that are involved in a particular reaction) that covert ROS to less reactive metabolites. Some examples of antioxidants that act as radical scavengers include tocopherols, ascorbic acid, carotenoids, alpha-lipoic acid (ALA), and glutathione. Important ROS detoxifying enzyme systems include catalase, superoxide dismutase, and the selenium-dependent antioxidant enzymes glutathione peroxidase and thioredoxin reductase (Sordillo and Aitken, 2009). During the transition period, however, the total antioxidant potential in the sera of dairy cows is diminished and ROS accumulation

occurs resulting in oxidative stress (Bernabucci et al., 2002). Cellular FA is the primary target of ROS oxidation, and oxidative stress is often measured by the formation of plasma lipid hydroperoxides that are also highly reactive metabolites. Studies in both humans and cows suggest that increased plasma NEFA concentrations can contribute to enhanced ROS production and further increase the formation of lipid hydroperoxides that exacerbate oxidative stress (Bernabucci et al., 2005; Hotamisligil and Erbay, 2008). Enhanced oxidative stress may then cause additional lipolysis and that can contribute to higher plasma NEFA concentrations in cows (Sordillo and Raphael, 2013). Both increased plasma NEFA concentrations and lipid hydroperoxide formation are hallmarks of metabolic stress and represent important risk factors for health disorders in cows, such as ketosis, fatty liver, mastitis, and retained placenta (Herdt, 2000; Sordillo and Raphael, 2013). Oxidative stress in dairy cattle is also thought to be a contributing factor to dysfunctional inflammatory responses especially during the transition period (Sordillo and Aitken, 2009). Oxidative stress increases inflammation by constantly activating redox-sensitive transcription factors such as NF-kB, which leads to increased expression of pro-inflammatory mediators that can cause damage to host tissues (Sordillo and Mavangira, 2014). Thus, oxidative stress forms a common link between increased lipolysis during negative energy balance and dysfunctional inflammatory responses that together form destructive feedback loops resulting in metabolic stress.

1.1.4 Fatty acid metabolism, mitochondria, and related pathways

White adipose tissue represents the body's predominant energy reserve and consists of triglyceride-filled cells known as adipocytes (Bell, 1995). These cells contain lipid droplets which are lipid-rich cellular organelles that regulate the storage of lipids and are involved in energy homeostasis (Olzmann and Carvalho, 2019). Mainly within adipocytes, and in hepatocytes, two metabolic processes, lipolysis, and lipogenesis are continuously occurring, resulting in intracellular triglycerides constantly being degraded and resynthesized (Figure 3).

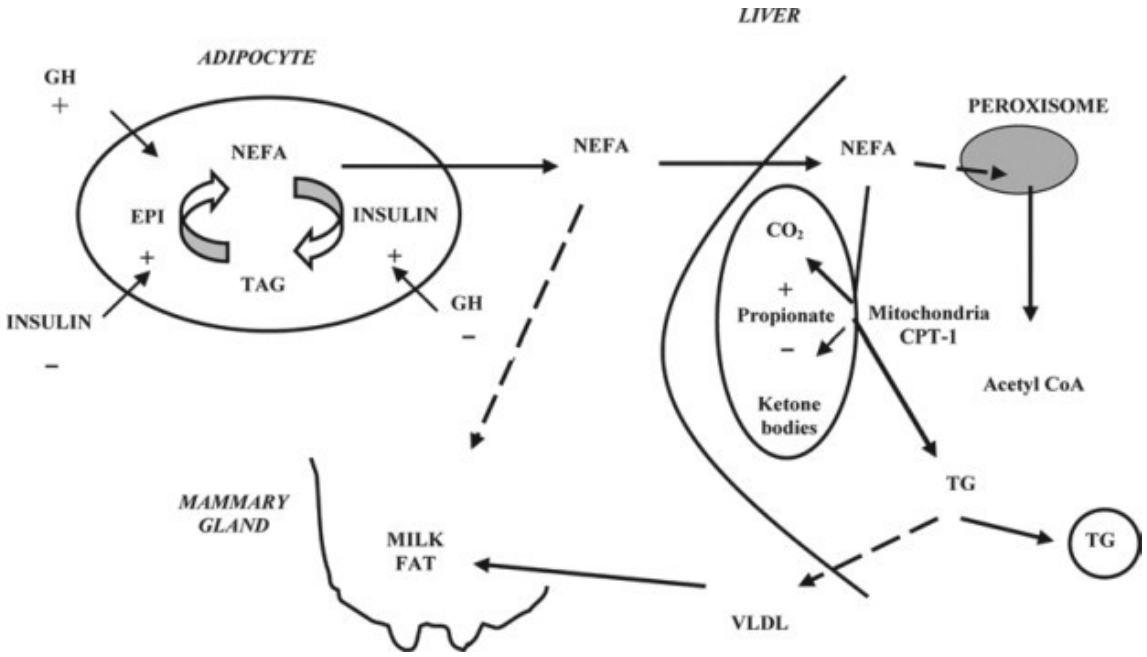

Figure 3. Schematic representation of lipid metabolism in the transition dairy cow. Positive signs (+) indicate stimulation and negative signs (–) indicate inhibition. Dashed lines are processes that occur at low rates or only during certain physiological states. CPT1 = carnitine palmitoyltransferase 1, EPI = epinephrine, GH = growth hormone, TG = triglycerides, TAG = triacylglycerol, and VLDL = very-low-density lipoproteins (Drackley, 1999b).

1.1.4.1 FA synthesis

FA synthesis occurs in ruminant adipocytes and hepatocytes via two pathways: de novo synthesis and the uptake of preformed FA from circulation (Bauman and Currie, 1980). Compared with monogastric animals, that use glucose, ruminants use acetate (derived from rumen fermentation) as the predominant carbon source for de novo FA synthesis. Acetyl CoA carboxylase (ACC), the rate-limiting enzyme in de novo FA synthesis (Bauman et al., 1988), catalyzes the formation of malonyl-CoA, the first committed step in FA synthesis. Malonyl-CoA is then condensed with acetyl-CoA by fatty acid synthetase (FAS) to produce the first 4-carbon acyl unit, butyrate. Acetate is the primary carbon source for FA elongation, and additional malonyl-CoAs (produced by ACC) is condensed with the growing acyl chain (via FAS) to produce longer chain FA (LCFA), with the primary product being palmitate (C16:0; Bauman and Davis, 1974).

In the case of FA uptake from circulating lipids, lipoprotein lipase (LPL) hydrolyses plasma triacylglycerides (TAG), producing NEFA and monoacylglycerides (Fielding and Frayn, 1998). Uptake and intracellular transport of both NEFA and monoglycerides in hepatocyte and adipocyte are thought to be mediated by FA binding protein 1 (FABP1) and 4 (FABP4) respectively (Elis et al., 2016; Zhu et al., 2019). Adipose TAG is synthesized through

either the phosphatidic pathway or the monoacylglycerol pathway, depending upon the availability of glycerol-3-phosphate and monoacylglycerides (Lehner and Kuksis, 1996). In the phosphatidic pathway, the initial step is the formation of lysophosphatidic acid catalyzed by glycerol-3-phosphate acyltransferase (GPAT) which occurs in both the endoplasmic reticulum (ER) and mitochondria. Lysophosphatidic acid is further esterified and converted into phosphatidic acid in the reaction catalyzed by lysophosphatidate acyltransferase, an enzyme mainly present in the ER. Phosphatidic acid is then shunted into the synthesis of various phospholipids or the synthesis of TAG (Ahmadian et al., 2007). In the monoacylglycerol pathway, the monoacylglycerol is first acylated by an acyl CoA: monoacylglycerol acyltransferase with the formation of *sn*-1,2-diacylglycerols mainly as the first intermediate in the process, and *sn*-2,3-diacylglycerols. Finally, the acyl CoA: diacylglycerol acyltransferase (DGAT1) reacts with the *sn*-1,2-diacylglycerols to form triacylglycerols (Yang and Kuksis, 1991).

1.1.4.2 Lipolysis

During lipolysis, hormone-sensitive lipase (HSL) acts as a catalyst at the lipid droplet surface in the adipocyte to hydrolyze FA at the stereospecific position number 1 (sn-1) and sn-3. Control of HSL by lipolytic hormones like insulin and endothelin-1 is mediated by reversible phosphorylation via cyclic AMP (cAMP)-dependent protein kinase A (PKA) (Lan et al., 2019). Additional regulation occurs via perilipin, a hydrophobic protein associated with the lipid droplet. Perilipin phosphorylation (via cAMP-dependent PKA) is believed to be essential for HSL translocation from the cytosol to the surface of the lipid droplet, enabling FA hydrolysis to occur (Yeaman, 2004). Monoacylglycerol lipase then hydrolyses the remaining FA at the sn-2 position generating 3 NEFA and a glycerol backbone which are taken up by the liver for re-synthesis of TAGs (Herrera and Desoye, 2016; Stipanuk, 2000). Consistent with the increased lipolysis in early lactation, as Sumner and McNamara (2007) reported upregulation in HSL and perilipin mRNA in adipose tissue in lactating cows relative to cows prepartum. However, these data do not reflect a downregulation of these lipolytic factors through mid-lactation (Roche et al., 2009).

Once mobilized, NEFA quickly attaches to serum albumin for transport to various tissues. During high rates of lipolysis, the ratio of NEFA to albumin increases, and NEFA occupy the lower affinity binding sites on the albumin molecule. This weak connection favors the delivery and uptake of NEFA by energy and lipid requiring tissues (Stipanuk, 2000).

1.1.4.3 Metabolism of NEFA

Circulating NEFA is metabolized via three pathways: they can be oxidized by many tissues, including the liver and skeletal muscle as an energy source; re-esterified to triglyceride in the liver; or used by the mammary gland as a source of milk fat (Figure 3; Drackley, 1999).

1.1.4.3.1 Mitochondrial β-oxidation

The β-oxidation of FA in the liver is localized in the mitochondrial compartment of hepatic cells and produces acetyl-CoA and reduced forms of NADH and flavin adenine dinucleotide (FADH); these generate energy via ATP production in the citric acid cycle and electron transport chain respectively (Stipanuk, 2000). The CPT1 is the rate-limiting enzyme responsible for transporting cytosolic FA to the mitochondria for β-oxidation (McGarry and Brown, 1997). Activity of CPT1 and subsequent FA β-oxidation rates increase during negative energy balance, probably because of decreased concentrations of, and reduced sensitivity to, malonyl-CoA, a potent allosteric CPT1 inhibitor (Brindle et al., 1985; Jesse et al., 1986). Malonyl Co-A is a FA synthesis intermediate and concentrations decrease during periods of negative energy balance, when the insulin to glucagon ratio (anabolic and catabolic hormones in the order given involved in the metabolism of glucose and FA) is low and lipogenesis is limited (McGarry and Brown, 1997).

Also, FA oxidation in the mitochondrial matrix is a major source of energy and not only fuels the TCA cycle and oxidative phosphorylation but also stimulates hepatic synthesis of the ketone bodies [ß-hydroxybutyrate (BHB), acetone, and acetoacetate] especially when physiological energy demand is increased and exceeds what can be provided via feed, through glycolysis and glycogenolysis (Ciapaite et al., 2011; Liang and Nishino, 2010). A series of enzymes, transporters, and other facilitating proteins are involved in FA oxidation. To be more specific, approximately 20 different proteins play specific roles in FA oxidation (van Houten et al., 2016). This system requires L-carnitine and is composed of two acyltransferases, carnitine palmitoyltransferases 1 and 2 (CPT1 and CPT2), and carnitine acylcarnitine translocase (CACT), which is a member of the mitochondrial carrier family of proteins. To explain, CACT carries out the transport of acylcarnitines across the inner mitochondrial membrane in exchange for a free carnitine molecule (van Houten et al., 2016). Likewise, carnitine behaves as a carrier of fatty acyl groups from the cytoplasm to the mitochondrion. Long-chain acyl-CoA derivatives do not penetrate the inner mitochondrial membrane. CPT1 which is located on the external surface of the mitochondrial inner membrane catalyzes the

conversion of cytoplasmic long-chain acyl-CoA and carnitine into acylcarnitine followed by transport of this complex into the mitochondrial matrix in exchange for free carnitine as mediated by the inner mitochondrial membrane protein CACT. The acylcarnitine is re-converted to intramitochondrial acyl-CoA by the action of CPT2 located in the inner membrane. Thereby the acyl-CoA is available for β-oxidation in the matrix. In the liver, malonyl-CoA, the first committed intermediate produced during FA synthesis, is proposed to regulate the activity of CPT1 (Bartlett and Eaton, 2004; Drackley et al., 2001; Hoppel, 1982; van Houten et al. 2016). Besides, Malonyl-CoA decreases in response to lowered blood concentrations of insulin and glucagon/adrenalin and increases in line with enhanced blood insulin concentration in ruminants (Bell, 1995; Brindle et al., 1985; Knapp and Baldwin Jr, 1990). The most pronounced effects of various hormones like insulin, glucagon, and somatotropin (involved in growth stimulation, cell reproduction and metabolism of glucose and FA) are on the supply of NEFA to the liver rather than on its intracellular disposal (Adewuyi et al., 2005; Drackley et al., 2001).

Acyl-CoA dehydrogenases are a class of at least 11 enzymes most of which perform a function in FA oxidation or amino acid catabolism in the mitochondria of cells (Swigoňová et al., 2009; van Houten et al. 2016). Their action appears in the introduction of a trans double bond between C2 (α) and C3 (β) of the acyl-CoA thioester substrate (Thorpe and Kim, 1995). Acyl-CoA dehydrogenases have been identified in animals (nine major eukaryotic classes) with five of these nine classes involved in FA β-oxidation (ACADS, ACADM, ACADL, ACADVL, and ACADVL2), and the other four involved in branched-chain amino acid metabolism (iso(3)valeryl-CoA dehydrogenase (i3VD), iso(2)valeryl-CoA dehydrogenase (i2VD), glutaryl-CoA dehydrogenase (GD), and isobutyryl-CoA dehydrogenase (iBD) (Wipperman et al., 2013). They can be categorized into three distinct groups based on their specificity for short-, medium-, or long-chain FA acyl-CoA substrates (Kim et al., 1993).

Inside the mitochondrion, acyl-CoAs are degraded via β-oxidation, a cyclic process consisting of four enzymatic steps. Each cycle shortens the acyl-CoA by releasing the two carboxy-terminal carbon atoms as acetyl-CoA. The cycle is initiated by dehydrogenation of the acyl-CoA to *trans*-2-enoyl-CoA by an acyl-CoA dehydrogenase. This step is followed by hydration catalyzed by an enoyl-CoA hydratase, generating (*S*)−3-hydroxy acyl-CoA, which is subsequently dehydrogenated to 3-ketoacyl-CoA in a reaction performed by (*S*)−3-hydroxy acyl-CoA dehydrogenase. Finally, a thiolase cleaves the 3-ketoacyl-CoA into a two-carbon chain–shortened acyl-CoA and an acetyl-CoA (van Houten et al., 2016) (Figure 4).

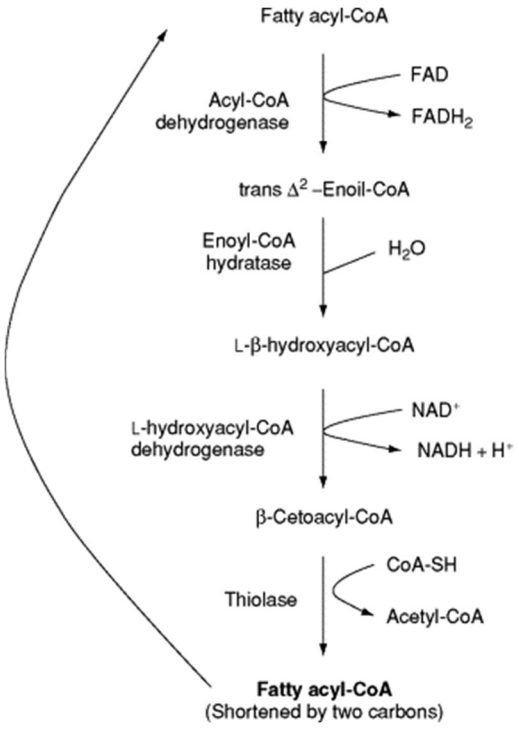

Figure 4. Fatty acid β-oxidation stages (R indicates the alkyl group; the FA has been activated by binding CoA-SH). The four stages render acetyl-CoA and acyl-CoA that are 2C residues shorter than the starting compound. The process is repeated as many times as required until the acyl chain is degraded in 2C segments. On the last step, a 4-carbon acyl substrate undergoes the stages of β-oxidation, producing 2 acetyl-CoA (Blanco and Blanco, 2017).

Based on the various substrate specificities of the individual FA oxidation enzymes, it is assumed that the long-chain acyl-CoAs first undergo two to three β-oxidation cycles by the membrane-bound enzymes VLCAD and mitochondrial trifunctional protein (MTP). The resulting medium-chain acyl-CoAs are then handled by the matrix-localized enzymes ACADM, crotonase, short-chain 3-hydroxy acyl-CoA dehydrogenase (SCHAD), and medium-chain 3-ketoacyl-CoA thiolase (MCKAT). In the end, the short-chain acyl-CoAs are metabolized by ACADS, crotonase, SCHAD, and MCKAT (van Houten et al., 2016). ACADS is a mitochondrial enzyme that catalyzes the dehydrogenation of short-chain FA (SCFA, up to six carbons in length (den Besten et al., 2013)) thereby initiating the cycle of β-oxidation. This process creates acetyl-CoA, the key substrate for hepatic ketogenesis, or ATP production by the TCA acid cycle (Turpin and Tobias, 2005). MTP harbors enoyl-CoA hydratase, (*S*)−3-hydroxy acyl-CoA dehydrogenase, and 3-ketothiolase activities that are specific for long-chain intermediates (van Houten et al., 2016).

Facilitation of β-oxidation of NEFA, by 'sparing' glucose for oxaloacetate formation in the major peripheral tissues, increases the diversion of pyruvate to oxaloacetate formation which facilitates the entry of acetyl-CoA derived from FA β-oxidation into the TCA cycle

through citrate formation (Eaton et al., 1996; Sugden et al., 2001). However, if the TCA cycle gets overloaded (e.g. by capacious drainage of oxaloacetate for gluconeogenesis), the acetyl-CoA is shunted off to produce ketone bodies (acetoacetic acid, acetone, and BHB) to prevent cessation of the TCA cycle and accumulation of acetyl-CoA (Sato et al., 1999; Sugden et al., 2001).

When FA mobilization from adipocytes is accelerated, hepatic cells convert excess acetyl CoA generated from β-oxidation into ketone bodies (Herdt, 2000). Rate of ketone body formation is directly proportional to FA oxidation rates, and although acetyl-CoA conversion to ketone bodies, rather than complete β-oxidation, is less energetically efficient (Stipanuk, 2000), ketosis is an important energy-providing mechanism for dairy cows in early lactation. The reason behind this is due to lactation, the majority (more than 80%) of available glucose is partitioned to the mammary gland (Bell, 1995), and vital organs that cannot metabolize FA as an energy source (e.g., the brain cells and erythrocytes) rely on ketone oxidation for survival (van Wijk and van Solinge, 2005; Stipanuk, 2000).

1.1.4.3.2 Peroxisomal β-oxidation

An alternative pathway to hepatic mitochondrial NEFA oxidation is via peroxisomes, subcellular organelles present in most organs of the body (Singh, 1997). However, compared with mitochondrial β-oxidation which generates energy in the form of reduced NADH in addition to acetyl CoA, peroxisomal β-oxidation produces hydrogen peroxide and heat; peroxisomes do not contain a respiratory chain linked to ATP formation. It is, therefore, proposed that the less energy efficient peroxisomal β-oxidation may play a role as an overflow pathway to oxidize FA only during extensive NEFA mobilization (Figure 3; Drackley, 1999b).

Peroxisomes are subcellular organelles that are present in virtually every eukaryotic cell and catalyse many metabolic functions. These metabolic functions include (1) FA β-oxidation; (2) ether phospholipid biosynthesis; (3) FA α-oxidation (occurs in those fatty acids that have a methyl group (CH3) at the beta-carbon, which blocks β-oxidation), and (4) glyoxylate detoxification. Since peroxisomes lack a TCA cycle and a respiratory chain, peroxisomes are relatively helpless organelles that rely heavily on their cross-talk with other subcellular organelles to metabolize the end products of metabolism as generated in peroxisomes (Wanders, 2013, 2014; Hunt et al., 2014). Many of the metabolites which require peroxisomes for their homeostasic regulation are involved in signal transduction pathways (Wanders, 2013).

It has been asserted that peroxisomal β-oxidation in the liver of dairy cows may be a part of the hepatic adaptations to negative energy balance (Grum et al., 2002). As an illustration in a study, peroxisomal β-oxidation capacity and the ratio of peroxisomal to total β-oxidation in Holstein cows declined from week 3 to 12 after parturition when the mammals were in the positive energy balance and then increased at week 42 postpartum (Grum et al., 2002). When hepatic peroxisomal β-oxidation rates were compared in liver homogenates from cows and rats during different nutritional and physiological states, peroxisomal oxidation in liver homogenates from cows represented 50% and 77% of the total capacity for the initial cycle of β-oxidation of palmitate (16:0) and octanoate (8:0), respectively, but only 26% and 65% for rats, whereas lactation or food deprivation did not alter rates of hepatic peroxisomal β-oxidation of palmitate or octanoate in cows (Grum et al., 1994).

LCFA regulate energy metabolism as ligands of PPARs. The PPAR-α that is expressed primarily in the liver is essential for metabolic adaptation to starvation by inducing genes for β-oxidation and ketogenesis and by downregulating energy expenditure through fibroblast growth factor 21 (FGF21) (Inagaki et al., 2007). PPAR-δ is highly expressed in skeletal muscle and induces genes for LCFA oxidation during fasting and endurance exercise. PPAR-δ also regulates glucose metabolism and mitochondrial biogenesis by inducing forkhead box protein O1 (FOXO1) and peroxisome proliferator-activated receptor-gamma coactivator 1-alpha (PGC1-α) (Furuyama et al., 2003; Tanaka et al., 2003). Genes targeted by PPAR-γ in adipocytes suggest that PPAR-γ senses incoming non-esterified LCFA and induces the pathways to store LCFA as triglycerides (Rosen and MacDougald, 2006). Adiponectin, another important target of PPAR-γ may act as a spacer between adipocytes to maintain their metabolic activity and insulin sensitivity (Nakamura et al., 2014).

NEFA that do not undergo hepatic β-oxidation are re-esterified to triglyceride and released into the circulation as very low-density lipoproteins (VLDL; Figure 3). During periods of negative energy balance, hepatic capacity for FA re-esterification increases (White, 2015). However, the VLDL export rate from the liver remains low (Bauchart, 1993), possibly because of the reduced capacity to generate apoprotein B in cattle; Apoprotein A is the key component believed to control the overall rate of VLDL synthesis and secretion (Avramoglu and Adeli, 2004; Drackley, 1999a). Thus, during periods of negative energy balance, increased hepatic NEFA uptake and re-esterification combined with inefficient VLDL release can result in hepatocyte triglyceride accumulation, a phenomenon often referred to as “fatty liver” (Roche et al., 2009).

1.1.5 Strategies for improving mitochondrial function

To perform their key roles in cellular energy production, mitochondria use an intricate system that encompasses the breakdown of FA and glucose, which is coupled to oxidative phosphorylation. Mitochondria are highly dynamic structures that undergo rapid remodeling through fusion and fission to adapt to changes in the cellular context (Westermann, 2010). When mitochondria are damaged, mitophagy (a specific autophagic response confined to mitochondria) regulates their controlled degradation (Youle and Narendra, 2011); furthermore, following extensive damage or specific triggers, mitochondria are central to the initiation of apoptosis (Nunnari and Suomalainen, 2012).

Given the complex balance between the nuclear and mitochondrial genome, and the fact that mitochondria are the site of metabolic transformation and hence a hotspot of metabolic stress, it is not surprising that mitochondrial dysfunction is involved in a broad spectrum of diseases, both inherited and acquired. Prototypical inherited mitochondrial diseases can be caused by mutations in either mitochondrial DNA (mtDNA) or nuclear DNA (nDNA), and typically result in very severe multisystem disease from birth. Conversely, mitochondrial dysfunction is important, or at least implicated, in a diverse range of acquired diseases, including cancer, metabolic diseases, and neurodegenerative disorders, which are often associated with aging (Andreux et al., 2013).

Mitochondrial dysfunction results from a combination of factors, including the quantitative contribution of several genes and environmental factors such as exercise, stress and diet (Andreux et al., 2012). Deregulation of various signalling pathways, such as the insulin–IGF1 (insulin-like growth factor 1) pathway (Kenyon, 2010), the mammalian target of rapamycin (mTOR) pathway (Laplante and Sabatini, 2012), the AMP-activated protein kinase (AMPK) pathway (Hardie et al., 2012) and the sirtuin pathways, can induce mitochondrial dysfunction (Houtkooper et al., 2012; Houtkooper, et al., 2010). The treatment of mitochondrial dysfunction typically involves general measures, such as the optimization of nutrition and administration of vitamins and food supplements (Andreux et al., 2013).

With the growing understanding of mitochondrial function, it has become clear that several aspects could be targeted to improve it. There are main pathways that have been demonstrated to maintain and/or restore proper mitochondrial function, such as mitochondrial biogenesis and metabolic flexibility; mitochondrial dynamics, including fusion and fission; and

mitochondrial quality control through proteostasis, mitophagy, and apoptosis (Fulda et al., 2010; Green et al., 2011).

The following section focuses at mitochondrial biogenesis and metabolic flexibility in restoring proper mitochondrial function in 3 sections including:

Upstream sensors:

- Caloric restriction, AMPK, mTOR, NAD^+ boosters, and sirtuins

Downstream effectors:

- Nuclear receptors, NRF1 and TFAM
- Co-factors

Mitochondrial biogenesis is a complex process, driven by a set of nuclear-encoded transcription factors and assisted by transcriptional co-factors, through which the cell equilibrates its energy-harvesting capacity to meet its energy demands. Considering this transcriptional network, one can distinguish two approaches to induce mitochondrial biogenesis: targeting the upstream regulators (for example, sensors), or targeting their downstream effector pathways, for example, transcription factors and co-factors (Andreux et al., 2013).

- Upstream sensors; caloric restriction, AMPK, mTOR, NAD^+ boosters, and sirtuins: Caloric restriction does improve metabolic health and prevent pathological decline associated with aging (Colman et al., 2009; Mattison et al., 2012). The molecular network underlying the effects of caloric restriction comprises the key nutrient-sensing pathways, such as those involving insulin–IGF1, mTOR, AMPK, and the sirtuins (Houtkooper et al., 2010b). The sirtuin family of histone deacetylases has emerged as a prime target to mimic caloric restriction (Houtkooper et al., 2012). This was based on the critical dependence of sirtuins on the metabolic cofactor NAD^+ (Imai et al., 2000), and on the fact that sirtuin 1 (SIRT1) controls the activity of various transcription factors and co-factors which are known to govern mitochondrial biogenesis and function. The best-characterized sirtuin-activating compound is resveratrol. Resveratrol is a polyphenol compound that has long been used as a SIRT1 agonist. Resveratrol increases lifespan in a number of lower eukaryotes (Cantó and Auwerx, 2009). In higher eukaryotes, resveratrol increases muscle mitochondrial content

and enhances endurance performance (Baur et al., 2006). This increased ability to oxidize lipids confers the mice with protection against metabolic disease upon high-fat feeding (Baur et al., 2006; Lagouge et al., 2006). Resveratrol, however, does not directly activate SIRT1; rather, it acts indirectly via the activation of AMPK and the subsequent induction of NAD^+ levels, which stimulate the activity of SIRT1 (Canto et al., 2010; Um et al., 2010). Regardless of its mechanism of action, resveratrol enhances mitochondrial biogenesis and oxidative capacity in rodent models of diet-induced obesity, which translates into improved muscle function and protection against obesity and insulin resistance (Baur et al., 2006; Laguna et al., 2017).

Considering the crucial dependence of sirtuins on the enzymatic co-factor NAD^+ (Houtkooper et al., 2010a), modulation of NAD^+ levels should activate SIRT1 signaling and promote mitochondrial biogenesis and function. NAD^+ levels can be increased by directly stimulating NAD^+ synthesis or by inhibiting NAD^+-consuming enzymes (Houtkooper and Auwerx, 2012). Indeed, dietary supplementation with the NAD^+ precursors' nicotinamide mononucleotide (NMN) or nicotinamide riboside increased NAD^+ levels in several tissues in mice (Yoshino et al., 2011; Canto et al., 2012). In dairy cows, Niacin is a precursor for NAD^+ is involved in intermediary metabolism (including oxidative stress and inflammatory processes) and because of its potential to exert anti-lipolytic effects, it is a supplementation to examine in dairy cows especially during the transition period (Bühler et al., 2018; Ringseis et al., 2019).

The activation of AMPK, which enhances mitochondrial energy production following an increase in the AMP/ATP ratio (Canto and Auwerx, 2010), also mimics caloric restriction (Hardie et al., 2012). In healthy animals, the AMPK agonist 5-aminoimidazole4-carboxamide riboside (AICAR) increases exercise endurance by activating a gene program that is normally induced after exercise (Narkar et al., 2008). The activation of AMPK by AICAR also rescued mitochondrial dysfunction and the limited exercise capacity of mice deficient in cytochrome C oxidase (Viscomi et al., 2011). Alternatively, inhibition of mTOR, a conserved kinase that promotes cell growth and anabolism in the presence of nutrients and growth factors (Zoncu et al., 2011), simulates a state of the energy crisis and thereby activates AMPK and boosts mitochondrial activity (Harrison et al., 2009).

- Downstream effectors; nuclear receptors, NRF1, and TFAM: Nuclear receptors are popular targets for drug discovery as many nuclear receptors can be activated by small-molecule ligands. Ligand binding changes the conformation of nuclear receptors, facilitating the

exchange of transcriptional co-repressors for co-activators and inducing the transcription of their target genes (Andreux et al., 2013). The PPAR constitutes a small subfamily of the large nuclear receptor gene family (Michalik et al., 2006). The FA are natural PPAR ligands; PPARα has a crucial role in the adaptive response to fasting, by inducing the expression of genes that are involved in FA oxidation (Kersten et al., 1999). Nuclear respiratory factor 1 (NRF1) and mitochondrial transcription factor A (TFAM) are two nDNA-encoded transcription factors that have a crucial impact on mitochondrial function. NRF1 promotes, among others, the transcription of electron transport chain (ETC) subunits and nDNA-encoded mitochondrial transcription factors, including TFAM (Kelly and Scarpulla, 2004). A recombinant form of human TFAM was designed, in which an exogenous amino-terminal domain allows rapid translocation across cell membranes, whereas its mitochondrial targeting signal stimulates mitochondrial uptake. Treatment of aged mice with recombinant human TFAM stimulated oxidative metabolism. A mitochondrial targeting signal of TFAM in a study in mice could stimulate mitochondrial uptake (Kelly and Scarpulla, 2004) and treatment of aged mice with TFAM stimulated oxidative metabolism and in another study in human, it restored mitochondrial biogenesis and respiration (Iyer et al., 2012). These studies indicate that one of the strategies to amend mitochondrial dysfunctionality could be the activation of TFAM.

- Downstream effectors; co-factors: The induction of PGC1α levels has been explored as a strategy to boost mitochondrial biogenesis in mice. It was shown in the mouse that irisin (a hormone that is secreted by muscle tissue) stimulated a broad PGC1α-mediated gene expression program leading to the browning of white fat (Boström et al., 2012). Bile acids can also stimulate oxidative metabolism in adipose tissue and skeletal muscle through subsequent induction of PGC1α (Andreux et al., 2013).

1.1.5.1 Carnitine

L-carnitine (4-N-trimethylammonium-3-hydroxybutyric acid, Figure 5) occurs naturally as an essential cofactor of FA metabolism which is synthesized endogenously or obtained from dietary sources. L-Carnitine is a cofactor of several enzymes (carnitine translocase, acylcarnitine transferases I and II) necessary for the transformation of free LCFA to acylcarnitines, and their transport into the mitochondrial matrix. β-Oxidation of these compounds precedes their entry into the Krebs cycle, where energy production occurs. In the absence of L-carnitine, the accumulation of free FA in the cytoplasm produces a toxic effect on

the cell, and an energy deficit arises from the unavailability of FA within the mitochondria (Longo et al., 2016; Nelson et al., 2017).

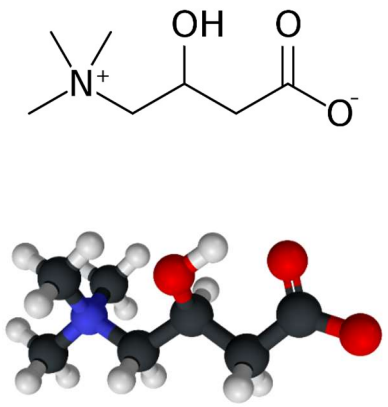

Figure 5. Chemical structure of L-carnitine (Virmani and Diedenhofen, 2015)

It has been shown that *PPARα* has a central role in the inflammatory response and oxidative stress and also in FA oxidation, lipid, and lipoprotein metabolism (Burri et al., 2010). The L-carnitine treatment can elevate PPARα activation in renal tubular cells and plays a crucial role in the L-carnitine anti-apoptosis effect. Therefore, *PPARα* may mediate the hepatoprotective effect of L-carnitine (Li et al., 2012). In rodents and pigs, it has been shown that carnitine synthesis and uptake of carnitine into cells are also regulated by PPARα, a transcription factor that is physiologically activated during fasting or energy deprivation (Schlegel et al., 2012). Feed restriction downregulated gamma-butyrobetaine hydroxylase 1 (BBOX), a key enzyme involved in L-carnitine biosynthesis in cows (Akbar et al., 2013). Schlegel et al. (2012) showed that the expression of hepatic genes of carnitine synthesis and cellular uptake of carnitine is enhanced in dairy cows during early lactation. These changes might explain increased hepatic carnitine concentrations observed in the first postpartum period and might be regarded as a physiologic means to provide liver cells with sufficient carnitine required for transport of excessive amounts of NEFA during a negative energy balance (Schlegel et al., 2012).

L-carnitine is synthesized endogenously from lysine (carbon backbone) and methionine (methyl group donor) in four enzymatic steps, namely hydroxylation at carbon 3, aldol cleavage, oxidation of the aldehyde to 4-butyrobetaine and hydroxylation of 4-butyrobetaine at carbon 3 (Adeva-Andany et al., 2017). The last enzymatic step is catalyzed by the enzyme 4-butyrobetaine dioxygenase to yield carnitine. It is generally recognized that the first three reactions of carnitine synthesis are widely distributed in the body but the final reaction is only

present in the liver, kidney, and brain (Flanagan et al., 2010). Thus, other tissues depend on carnitine uptake from the circulation (Gnoni et al., 2020). L-carnitine is taken up by the cells through the action of a carnitine transporter (Solute Carrier Family 22 Member 5 [*SLC22A5*]) located on the cell membrane, and has an important role in energy metabolism in mitochondria since the mitochondrial membrane is impermeable to acyl-CoA on its own so carnitine is a required cofactor for carnitine palmitoyltransferase-1 (*CPT-1*; present in the mitochondrial outer membrane) and 2 (*CPT-2*; located on the matrix side of the inner membrane), which condense carnitine with activated LCFA for transport from the cytosol into mitochondria (Goselinket al., 2013; Yang et al., 2019); closely related to mitochondrial membrane carrier proteins, *SLC25A20* mediates both imports of carnitine-FA complexes and export of carnitine across the inner mitochondrial membrane (Longo et al., 2016). Therefore, carnitine is essential for the normal function of all tissues containing mitochondria because the primary function of carnitine is to facilitate the shuttling of activated LCFA from the cytosol into the mitochondrial matrix, where fatty acid β-oxidation takes place (Ringseis et al., 2018). Hepatic β-oxidation of LCFA is stimulated by exogenous carnitine in several species (Drackley et al., 1991a, 1991b; Owen et al., 2001; Spaniol et al., 2003). Additionally, carnitine supports β-oxidation by transporting short- and medium-chain FA (MCFA) from peroxisomes to mitochondria and by altering the intramitochondrial ratio of acetyl-coenzyme A (CoA): CoA (Carlson et al., 2007).

Carnitine also regulates CoA concentration and removal of the produced acyl groups. Acyl-CoA acts as a restraining factor for several enzymes participating in intermediary metabolism. Transformation of acyl-CoA into acylcarnitine is an important system also for removing the toxic acyl groups (Evangeliou and Vlassopoulos, 2003; Hoppel, 1982).

1.1.6 Experimental models for inducing inflammation

Inflammatory condition is associated with the activated immune system, including activated immune cells and bio-molecules (Kulkarni et al., 2006). Inflammation is a defensive response of an organism against invasion by foreign bodies like bacteria, parasites, and viruses. An acute inflammatory response is manifested as redness, heat, swelling, pain, and the loss of function. Increased vascular permeability, accelerated blood flow, and nerve fiber sensitization is associated with swelling, redness, and pain respectively (Calixto et al., 2003). The protective effects of the inflammatory cascade and the potential for tissue destruction are usually balanced in a normal state. Whereas, chronic inflammation is usually characterized by substantial destruction and recovery of injured tissues from an inflammatory response (Chung et al., 2010).

If uncontrolled, inflammation may give rise to numerous diseased states. Furthermore, chronic inflammation is also linked with various steps of tumorigenesis (Patil et al., 2019).

To mimic the course of sepsis, for the development of new therapeutic options and identification of the biological mechanism of inflammations and the effect of potential drugs and supplements on them, various models have been evolved. These models can be classified into three major types: exogenous administration of pathogens [inoculation with *Escherichia coli*], disruption of the endogenous protective barrier [caecal ligation and puncture model (CLP)], and exogenous administration of endotoxin [lipopolysaccharide (LPS) treatment], (Seemann et al., 2017). All three models have advantages and disadvantages and it is still controversial as to which of these animal models is most suitable.

The LPS animal model has several essential advantages, including technical ease and high reproducibility, particularly in the inflammatory response elicited. Shortly after LPS administration, high levels of pro-inflammatory cytokines are released and can be measured in the circulation (Remick and Ward, 2005) that leads to the rapid development of systemic inflammatory response syndrome (SIRS) (Recknagel et al., 2013; Stortz et al., 2017). In this method, the inflammatory response to gram-negative bacteria invasion is caused by the host reaction to the LPS which is a component in the cell wall of gram-negative bacteria (Lüderitz et al., 1984). As mentioned earlier, purified LPS administered to animals mimics the clinical symptoms caused by a bacterial infection (Memon et al., 1992; Steiger et al., 1999). It has been shown that LPS administration in dairy cows decreases milk yield as a result of decreased DMI and the increased energy demands of the immune system (Zhao et al., 2018). The immune system is an energy-demanding process preferentially obtains most of its energy supply quantitatively from glucose and glutamine. Besides, other fuels were reported to be utilized by lymphocytes, such as ketone bodies and fatty acids. The activation of the immune system necessitates a reallocation of nutrients and energy from dispensable functions such as growth and production (Calder et al., 2007).

1.2 From DNA to protein

Genes in DNA encode protein molecules involved in all the functions necessary for life. For example, enzymes like DNA polymerases and other enzymes that make copies of DNA during cell division, as well as hormones, receptors, etc. Expressing a gene is a process in which the corresponding protein is manufactured. This multi-layered process has two major steps. The first step is transcription, a process in which the information in DNA is transferred to a

messenger RNA (mRNA) molecule. During transcription, the DNA of a gene serves as a template for complementary base-pairing, and RNA polymerase II catalyzes the formation of a pre-mRNA molecule, which is then processed to form mature mRNA. The resulting mRNA is a single-stranded copy of the gene, which next must be translated into a protein molecule (Clancy et al., 2009). The translation of the nucleotide sequence of an mRNA molecule into protein which is the second major step in gene expression takes place in the cytoplasm on a large ribonucleoprotein assembly called a ribosome. The transfer RNA (tRNA) molecules get attached to the amino acids that are used for protein synthesis. Each amino acid is recognized by specific tRNA based on complementary base-pair interactions, particular sets of three nucleotides in the mRNA (codons). The sequence of nucleotides in the mRNA is then read from one end to the other in sets of three according to the genetic code. The process of gene expression is not finished by creating the sequence of amino acids that constitutes a protein so this new polypeptide chain must fold up into its unique three-dimensional conformation, bind to small-molecule cofactors required for its activity, get appropriately modified by protein kinases and finally be assembled correctly with the other protein subunits with which it functions. Many of these proteins are involved in the functions necessary for life, for example, enzymes, including those that metabolize nutrients in different parts of metabolism or those that form the membrane channels (Alberts et al., 2002).

Metabolism refers to the chemical reactions that occur within an organism to sustain life and studying about it, involves investigating different levels of measurements from mRNA, proteins, or metabolites. As mRNA is eventually translated into protein, we might assume that there should be some sort of correlation between the level of mRNA and that of a related protein, but we need to consider that there are many processes between transcription and translation.

Even with the significant developments in the technologies used to quantify protein abundance during the past years, protein identification and quantification is still behind the high-throughput experimental techniques used to determine mRNA expression levels. Yet, while mRNA expression values have shown their usefulness in a broad range of applications, these results are only correlative, rather than causative. It is probably the concentration of proteins and their interactions that are the true causative forces in the cell, and we ought to be studying the corresponding protein quantities but researchers have widely used mRNA abundance data in cell metabolism studies because of a more limited ability to measure protein abundances, in compare with more repeatable and technically easier mRNA experiments. Anyways, measurements taken from mRNA and protein levels are complementary and both are

necessary for a complete understanding of how the cell works (Hatzimanikatis et al., 1999, Greenbaum et al., 2003).

1.3 Assessment of mRNA abundance via microfluidics technology

To analyse the mRNA abundance in a biological experiment, reverse-transcription quantitative PCR (RT-qPCR) is a technique commonly used (Bustin, 2002). The abundance of mRNA can inform us about changes in protein expression and enables us to infer changes in cell function (Vandesompele et al., 2002). A platform available for RT-qPCR analysis is the BioMark HD (Fluidigm, San Francisco, CA), which utilizes microfluidics technology. In contrast to standard RT-qPCR using 96-well plates, the integrated fluidic circuits (IFC) used in the current study (96.96 Dynamic Array IFC; Fluidigm) generate 96 times the number of data points. Furthermore, the 96.96 IFCs allow quantification of 96 genes and 96 samples per chip using fewer reagents and starting material than standard RT-qPCR reactions. This platform was used in this study to investigate the abundance of genes of interest and in the following chapters will be discussed in detail.

1.4 Reference genes

Quantitative PCR (qPCR) is an excellent method for measuring mRNA abundance but relies on the use of a suitable uniformly expressed reference gene or genes to control for the amount of RNA in each sample. Many researchers select commonly used reference genes that may not be suitable for their system. It is necessary to test whether differences in organisms, conditions, or treatments affect the uniform expression of potential reference genes.

1.4.1 Why we use reference genes?

As mentioned above, qPCR is an excellent method for measuring mRNA abundance but has some complicating factors like quality of RNA, the efficiency of reverse transcription, the efficiency of PCR reaction, variation in extractions and purifications, and also amount of RNA per sample. To be able to differentiate actual differences in gene expression from simple variation in starting material is the reason why we would use a reference gene. So, we normalize the target gene to a reference gene that is expressed at a uniform level in all samples in a given experiment. This method is called a normalized gene expression or $\Delta\Delta$Ct analysis method.

1.4.2 Selection of good reference genes

To find a gene that is expressed uniformly is difficult because of individual differences between organisms, differences due to culture conditions, differences due to experimental treatments, etc. So, it is not always enough to use reference genes that other studies have used, and reference genes should be verified for the specific experimental conditions.

2 Objectives

Although a plethora of studies has outlined potential causes and consequences of systemic oxidative stress in dairy cattle (Sordillo and Aitken, 2009), few have addressed the effect of systemic inflammatory stress on mitochondrial function. Since there is a growing interest in the use of additives as effective sources of nutrients or supplements that complement the diet, and considering the role of L-carnitine in the transport of FA for β-oxidation and production of ATP and as an antioxidant that reduces metabolic stress in the cell (Citil et al., 2009), we hypothesized that L-carnitine supplementation could improve the FA metabolism and relieve inflammatory stress in mid-lactating dairy cows challenged by an experimentally intravenous LPS administration. Thus, we aimed to compare L-carnitine supplementation with control fat supplementation to address potential changes in capacity for hepatic FA metabolism in the liver in the context of a systemic inflammatory challenge by LPS using liver biopsies to determine changes in abundance of 41 key genes and selected proteins involved in hepatic FA metabolism. In this study, by investigating the expression of key genes and selected proteins involved in FA uptake, activation, translocation, β-oxidation, synthesis and ketogenesis in mitochondria, presented in Figure 6 (e.g., *PPARα*, *SREBF1*, *CPT1, CPT2, SLC25A20, SLC22A5, FABP1, ACACA, COX4I1, MUT*) we tried to extend our understanding about the molecular mechanisms of lipid metabolism and development of nutritional and management approaches to prevent metabolic disorders. Concerning the aforementioned factors, the objectives of this study were:

1. To characterize the changes of either mRNA or protein abundance of the aforementioned factors in mid-lactation period of dairy cows challenged by LPS.
2. To investigate the effects of dietary supplementation with L-carnitine during mid-lactation on mRNA and protein abundance of some genes involved in hepatic metabolism of FA.
3. To relate the findings to the metabolic profiles and performance data.

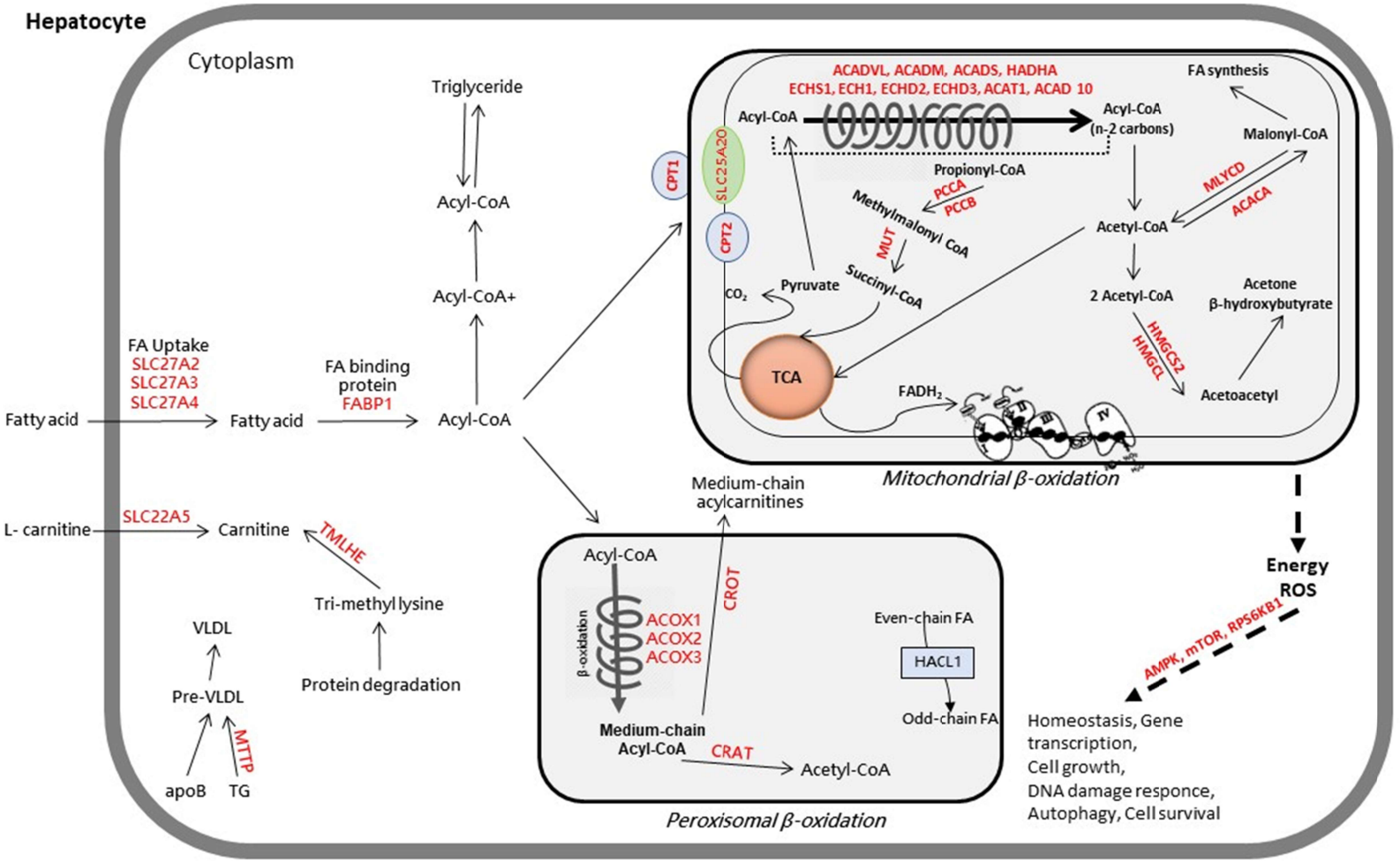

Figure 6. An overview of fatty acid uptake and oxidation in a hepatocyte. Fatty acids are transported into the cell by the action of fatty acid transport proteins (FATP), and plasma membrane fatty acid binding proteins (FABP). Inside the cell, FAs are activated to acyl-CoA by acyl-CoA synthases (ACS), that traps them in the cytoplasm. Longer chain fatty acids (C17–C26) are preferentially oxidized in the peroxisomes rather than in mitochondria. Acyl-CoA is then transported into the mitochondria by CPT1 and 2 and subject to β-oxidation. Acetyl-CoA then enters the TCA cycle followed by the electron transport chain to produce ATP or it can go through ketogenesis or will be used for resynthesise of FA.

3 MATERIALS AND METHODS

The animal experiment was carried out at the experimental station of the Institute of Animal Nutrition, Friedrich-Loeffler-Institute (FLI) in Braunschweig, Germany. The experiment was conducted according to the European Community regulations concerning the protection of experimental animals and was approved by the LAVES (Lower Saxony State Office for Consumer Protection and Food Safety, Germany) (AZ33.19-42502-04-16/2378).

3.1 Animals, treatment, and experimental design

A detailed description of the animals, treatment, and experimental design comprising the peripartal phase has already been reported (Meyer et al., 2020). Briefly, 59 multiparous Holstein cows at day 42 *ante partum (ap)* were assigned to two groups: control (CON, n = 30) and carnitine (CAR, n = 29), balanced for numbers of lactation (2-5 lactations), body weight (568-1008 kg), body condition score (2.5 - 4.75) and fat-corrected milk yield of the previous lactation. Both groups were fed a partial mixed ration (PMR) from late gestation to mid-lactation. The composition of roughage remained unchanged during the whole trial composed of 70% maize silage and 30% grass silage (dry matter (DM) based). Following the recommendation of nutrient and energy supply of the Society of Nutrition Physiology (GfE, 2009) the proportion of roughage to concentrate was variable. During the dry period until day 1 *ap*, diets of 80% roughage and 20% concentrate were fed. The concentrate portion was then increased from 30% to 50% over 14 days *pp.* From then on, 50% concentrate was continuously fed until the end of the study on day 126 *pp*. The PMR was offered *ad libitum* in feed weighing troughs (RIC, System Insentec B.V., Marknesse, The Netherlands) and the supplementary, restricted, pelleted concentrate was provided by concentrate feeding stations (System Insentec B.V.).

In the CAR group, 25 g L-carnitine (per cow and day) from a rumen-protected L-carnitine product (Carneon 20 Rumen-Pro, Lohmann Animal Nutrition GmbH, Cuxhaven, Germany) were included in the concentrate. Since fat was used for the rumen protection of the L-carnitine, to balance the fat content of the L-carnitine product, the concentrate for the CON group was supplemented with an equivalent amount of fat product (Berga Fat F-100 HP, Berg+Schmidt GmbH and Co. KG, Hamburg, Germany). All animals were kept in a free-stall barn, with free access to water. At day111 *pp*, the cows of both groups were challenged with a single intravenous injection of 0.5 µg/kg body weight LPS (*Escherichia coli* O111: B4, Sigma-Aldrich, St. Louis, Missouri, USA) (Figure 7). Before calving, the body weight (BW) was

recorded once a week, and during the lactation period, twice a day with a scale situated between the milking parlor and barn. Each cow was equipped with an ear transponder to enable the recording of feed and water intake individually. Cows were housed in free stall barns. From day 110 *pp* until day 126 *pp* each cow was housed in a calving pen to be supervised closely during the LPS challenge.

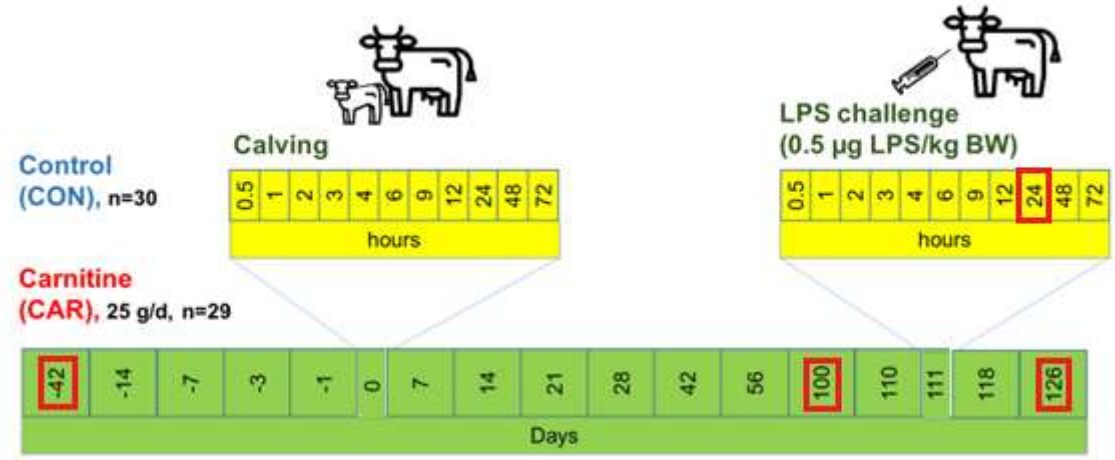

Figure 7. Experimental design and blood sampling and liver biopsy plan of the study. Days are shown relative to calving and hours are shown relative to calving and LPS challenge respectively and each one represents a blood sampling timepoint. The liver biopsies were taken at day 42 *ap* and days 100 *pp*, 112 *pp* (24 h LPS), and 126 *pp,* shown in red squares.

3.2 Sample collection

Blood samples were collected from *Vena jugularis externa* by needle puncture or for frequent sampling, after calving and after LPS challenge, by indwelling catheters (from 0.5 h until 12 h after calving and after LPS challenge). Before blood collection, 20 mL of blood was aspirated and discarded from a catheter which was flushed with 20 mL of 0.9% saline solution after the collection. Blood samples were taken at the following time points: day 42, 14, 7, 3 and 1 *ap*, 0.5, 1, 2, 3, 4, 6, 9, 12, 24, 48, 72 h *pp*, day 7, 14, 21, 28, 42, 56, 100 and 110 *pp*, and then 0.5, 1, 2, 3, 4, 6, 9, 12, 24, 48, 72 h after LPS challenge and day 118 and 126 *pp* (Figure 7).

The liver biopsies were taken at day 42 *ap* and days 100, 112 and 126 *pp* (to avoid increasing the stress at the time when there are immunological and metabolic stresses after calving, no liver biopsy was collected during the short period after calving) under local anesthesia (Isocain ad us. vet.; Selectavet, Weyarn/Holzolling, Germany) with a Bard Magnum Biopsy instrument (Bard Magnum, Covington, GA, USA). The liver tissues were obtained by performing a small incision through the skin at the intercostal space, 20 cm laterally from the backline. Tissue

samples were immediately snap-frozen in liquid nitrogen and stored at -80 °C until further processed.

The cows were milked twice a day at 5:30 am and 3:30 pm. The milk yield was recorded by a milk counter (Lemmer Fullwood GmbH, Lohmar, Germany). To analyse milk ingredients, milk samples were taken two times per week during morning and evening milking.

3.3 Parameters for performance, health status, and energy metabolism

The methods for the analysis of dry matter intake (DMI), net energy balance (net EB), NEFA, BHB, rectal temperature (RT), free carnitine in plasma and glucose concentrations in blood of the cows in this study have been reported before elsewhere (Meyer et al., 2020) and will be mentioned below:

3.3.1 Analyses

Samples from the PMR were taken daily, and the concentrate part was sampled once a week. The feed samples were pooled over four-week periods. Following the methods of the Association of German Agricultural Analytic and Research Institutes (VDLUFA, 2007), the pooled feed samples were analysed for dry matter (method number 3.1). For NEFA and BHB in serum, analyses were performed by a photometric method using the Eurolyser CCA 180 (Eurolyser Diagnostica GmbH, Salzburg, Austria). The concentrations of free carnitine (CA) were analysed in ethylenediaminetetraacetic acid (EDTA) plasma by a tandem mass spectrometry method according to Hirche et al. (2009). Automated blood gas and electrolyte analyser (GEM Premier 4000, Werfen, Kirchheim, Germany) were used for the determination of glucose concentration in fresh whole blood samples.

3.3.2 Clinical checks

For rectal temperature, each cow was clinically examined right before LPS administration and from 0.5 up to 72 h after LPS according to the methods of Dirksen et al. (1990).

3.3.3 Calculations

To calculate energy balance (EB) we used this equation:

EB (MJ NEL/d) = NEI (MJ NEL/d) – ΔNE (MJ NEL/d) – NEL (MJ NEL/d) – NEM (MJ NEL/d)

Where NEI is daily net energy intake, ΔNE is an adjustment of daily net energy intake for the proportion of concentrates in the diet, NEL is daily net energy requirements for lactation and NEM is daily net energy for maintenance.

So net energy balance (net EB) was calculated by using the following equation:

$$\text{net EB (MJ NEL/d)} = \text{total NEL intake (MJ NEL/d)} - (\text{NEM (MJ NEL/d)} + \text{NEL (MJ NEL/d)})$$

Milk energy, NEM, and NEL were calculated according to the Society of Nutrition Physiology (GfE, 2001):

$$\text{Milk energy (MJ NEL/kg)} = 0.38 \times \text{milk fat (\%)} + 0.21 \times \text{milk protein (\%)} + 0.95$$

$$\text{NEM (MJ NEL/d)} = 0.293 \times \text{body weight}^{0.75}\ \text{(kg)}$$

$$\text{NEL (MJ NEL/d)} = (\text{milk energy (MJ NEL/kg)} + 0.086) \times \text{milk yield (kg/d)}$$

3.4 Laboratory analyses

3.4.1 Quantification of the mRNA abundance of target genes related to fatty acid metabolism in liver tissue

3.4.1.1 RNA extraction

43 cows that could continue the trial to the end of the study were selected from both groups (CON, n = 21 and CAR, n = 22) and the liver homogenates were made for them from liver biopsies using the Qiagen reagent (Qiagen N.V., Hilden, Germany) and homogenization tubes with ceramic beads (1.4 mm) and a Precellys 24 homogenizer (PEQLAB Biotechnology GmbH, Darmstadt, Germany) from 20 mg of the liver samples according to the manufacturer's instructions. The total RNA extraction and purification were done using the miRNeasy Mini Kit (Qiagen) including the On-Column DNase I treatment to remove residual genomic DNA from the RNA samples. The quantity and purity of RNA were evaluated by measuring the absorbance at 260 and 280 nm by the NanoDrop 1000 spectrophotometer (VWR/Peqlab Biotechnologie, Erlangen, Germany) and only samples with a 260/280 ratio of ≥ 1.8 were used for downstream applications. The extraction was repeated for the samples with a ratio of less than 1.8. The RNA quality was assessed by checking the 18S and 28S ribosomal RNA bands (28S:18S rRNA ratio of 2:1) on gel electrophoresis. The RNA integrity number (RIN) was evaluated in 10 randomly selected samples (CON, n = 5 and CAR, n = 5) for each time point using RNA 6000 nano kit (part number 5067-1511, Agilent Technologies, Santa Clara, CA, USA) on a Bioanalyzer 2100 (Agilent Technologies). In a scale ranges from 1 to 10 when 1 is

the most degraded profile and 10 indicating maximum RNA integrity, the average RIN ± SD (7.73 ± 0.34) was around 8 and passed the commonly accepted threshold of 7 which is recommended for qPCR analysis (Brenaut et al., 2012). Complementary DNA (cDNA) was generated by reverse transcribing 250 ng of total RNA/20 µL. The abundance of mRNA from the target and reference genes was assayed by RT-qPCR on a 96.96 gene expression (GE) chip for use in the BioMark HD instruments (Fluidigm, San Francisco, USA).

3.4.1.2 Microfluidics Fluidigm arrays

In contrast to the classical RT-qPCR, the use of microfluidic-based qPCR chips, utilizing regular qPCR primers with a DNA-binding dye, is highly cost-effective, and enables parallel analysis of a large number of samples across many probes, with relatively low effort.

The 96.96 Dynamic Array™ IFC for Gene Expression (Figure 8) used in the current study allowed for the quantitative analysis of the mRNA abundance of 41 key genes involved in FA metabolism (Table 1, the rest of the genes is related to other pathways and will not be presented in this thesis) by the BioMark HD real-time PCR system at the Leibniz-Institute for Farm Animal Biology, Institute for Genome Biology, Dummerstorf, Germany. The analysis involved sequence-specific preamplification and quantitation of gene expression using real-time PCR on the BioMark HD system (Fluidigm).

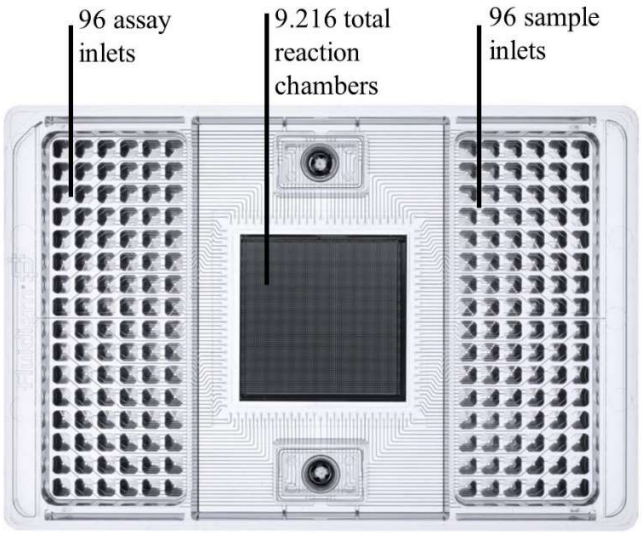

Figure 8. 96.96 Dynamic Array™ IFC for Gene Expression. Each assay is pipetted into one of the inlets on the left side and each sample mixture is pipetted into one of the inlets on the right side of the chip. Then the IFCs are placed into an IFC controller HX device where the precise pneumatic pressure is used to load the reaction chambers in the middle by assays and samples.

The primer design for 41 target genes was undertaken using publicly online available bovine gene sequences from the National Center for Biotechnology Information gene database (NCBI, http://www.ncbi.nlm.nih.gov) and its online specific primer design tool

(https://www.ncbi.nlm.nih.gov/tools/primer-blast/) according to conditions suggested by Biomark for designing primers:

- GC% primer range of 30-70% (50% optimal)
- Last 5 bases better to have 2 to 4 Gs or Cs
- Last base better to be G or C (3' end)
- Span a lengthy intron (greater than 1000 bp) or design a primer to overlap an exon-exon boundary
- Primer melting temperature (Tm) within 56 – 62 °C (optimal 59 °C)
- Primer length within 18 - 21 base pairs
- Blast the primers against the appropriate species genome to look for any significant off-target products
- Ideal amplicon length within 60-150 base pairs (optimal 80 base pair)
- Standard desalted oligos are sufficient. No need for further purification like high-performance liquid chromatography (HPLC)

The designed primers had been tested using the conditions of a BioMark HD real-time PCR system in an Mx3000P cycler, (Agilent, Santa Clara, CA, USA) with pooled samples [95 °C for 10 min (95 °C for 30 s, 59 °C for 60 s, and 72 °C for 60 s) × 40 cycles]. Cycle threshold values (Ct) were checked to be at 29 at the highest (indicating high amounts of the target sequence) and the melting curves were checked to be without any pre or post peaks. Non-working primers were taken out according to their Ct and melting curve and were replaced with repeatedly designed primers. Primer sequences and the real-time PCR conditions are provided in Table 1.

The reverse transcription was performed in triplicate for each sample following by the original *Minimum Information for Publication of qPCR Experiments* (MIQE) guidelines (Bustin et al., 2009). A preamplification of cDNA was done to create specific target amplified reactions by multiplexing forward and reverse primers (500 nM) of the assays with 2x concentration PreAmp Master Mix (Fluidigm): preamp master mix 1.0 µL, pooled delta gene assay mix (500 nM) 0.5 µL, DNase free water 2.25 µL and cDNA 1.25 µL. Thermal cycling conditions for the reaction using this master mix were 95 °C for 2 min, and 10 cycles of 95 °C for 15 s, 60 °C for 4 min and keeping the products in 4 °C for later use.

Assay mixtures, including combined forward and reverse primers (100 µM) 0.25 µL, 1x DNA suspension buffer (10 mM Tris, pH 8.0, 0.1 mM EDTA) 2.25 µL, and 2x assay loading reagent (Fluidigm) 2.5 µL, made the final concentration of each primer as 5 µM in the IFC inlet and 500 nM in the final chamber reaction. Sample mixtures involved 2X SsoFast EvaGreen Supermix (BioRad) 2.5 µL, 20X DNA binding dye (Fluidigm) 0.25 µL, and 2.25 µL of

preamplified and exonuclease treated samples. Samples were exonuclease treated by DNase-free water 1.4 µL, exonuclease I reaction buffer (New England BioLabs, PN M0293S) 0.2 µL, exonuclease I, 20 U/µL (Fluidigm) and the thermal cycle condition was 37 °C for 30 min, 80 °C for 15 min and 4 °C for later use.

On a 96.96 gene expression chip (Fluidigm, Figure 8) 5.0 µL of each assay and 5.0 µL of each sample mixture were pipetted into the IFC inlets. To load the chambers by assays and samples, the IFCs were placed into an IFC controller HX (Fluidigm, Figure 9). The IFC controller is a compact single-bay instrument that employs pneumatic pressure to precisely meter samples and reagents and to control valves within IFCs. The IFCs were transferred to Biomark™ HD System (Fluidigm, Figure 9) for real-time fluorescence detection afterward.

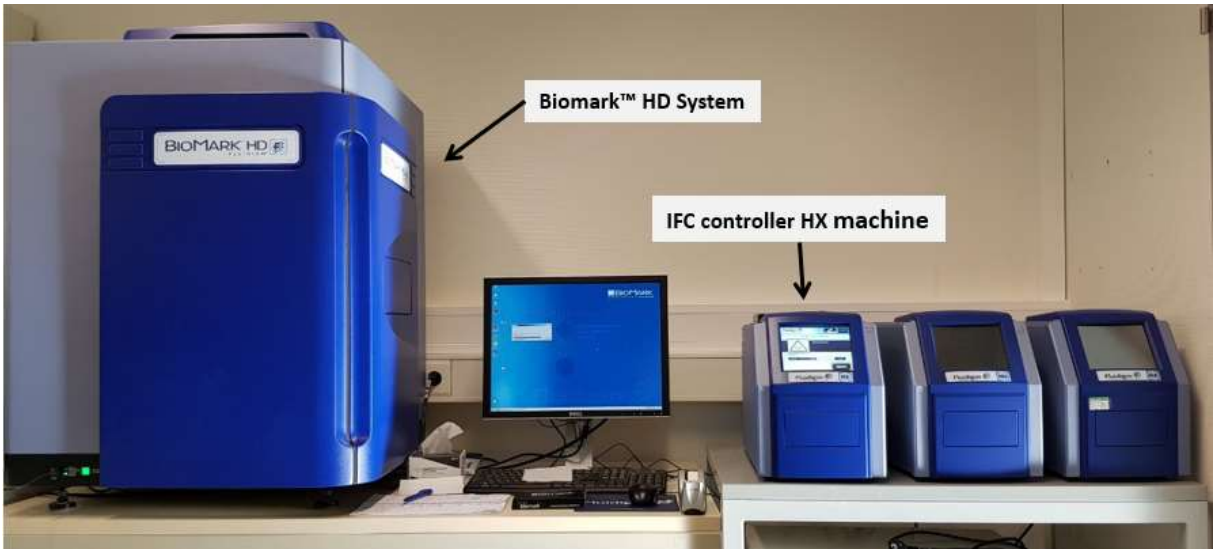

Figure 9. Fluidigm IFC controller HX machine and Biomark™ HD System

The gene expression thermal cycling protocol "GE Fast 96X96 PCR+Melt v2.pcl" (Biomark HD Data Collection software v3.0.2), 70 °C for 40 min, 60 °C for 30 s, 95 °C for 1 min, followed by 30 cycles of 96 °C for 5 s, and 60 °C for 20 s, was used to generate crossing point (Ct) values[1]. Then, 60 °C for 3 s followed by increasing temperature gradually up to 95 as 1 cycle in each 3 s to create the melting curve. To correct run-to-run variation, 3 inter-run calibrators

[1]Ct values were calculated from the system's software (BioMark Real-time PCR Analysis; Fluidigm)

from pooled samples were used for each IFC. All the reactions were performed in triplicates (Figure 10).

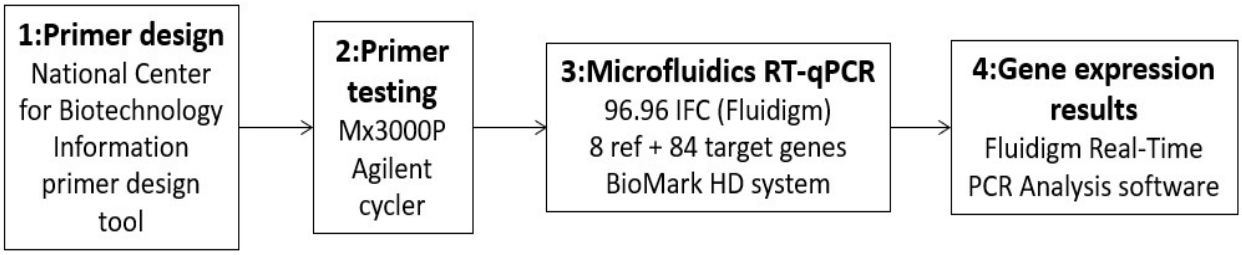

Figure 10. Diagram depicting the Microfluidics Fluidigm gene expression workflow that was employed for reverse-transcription quantitative PCR (RT-qPCR) analysis including primer design through to gene expression results.

The analysis software (Fluidigm Real-Time PCR Analysis Software, v4.5.2) gave cycle threshold (Ct) values and calculated ΔCt values, as well as the quality score for each amplification. Out of these ΔCt values calculated from the Ct value of the gene of interest minus the average Ct value of the reference genes (a set of 3 most stable reference genes selected for this study out of 8 reference genes suggested by previous studies. Look at section 3.5.1.3, under the title of evaluating reference genes) for every single sample. The relative abundance (ΔΔCt) was calculated out of the ΔCt values for target genes for each unknown sample minus the average ΔCt values for reference genes. The fold change of ΔΔCt was calculated as shown in equation:

$$\Delta\Delta Ct = \Delta Ct \text{ reagent of test gene for unknown sample - (average } \Delta Ct \text{ reagent of a reference gene for reference sample)}$$

$$\text{Fold change} = 2^{-(\Delta\Delta Ct)}$$

The quality threshold in the Biomark system analysis software (Fluidigm) is a qualitative tool to measure the quality of each amplification curve. In this method, each amplification curve is compared to an ideal exponential curve and is given a quality score between 0 and 1, where 0 is a flat line and 1 is a perfect sigmoid. To build this quality scores, factors include the linearity of the baseline, the delta normalized reporter value (Rn) of the final product or signal that is produced, the slope of the amplification plot, and the return to linearity after exponential growth are taken into account. A default arbitrary cut-off value of 0.65 for the quality threshold in the Real-Time PCR Analysis software was used for this study. The amplification with quality scores less than the threshold was automatically removed by the software from two next calculations including the Ct threshold calculation and a reference normalization calculation. For example, if the reference gene Ct has a failed quality score, it was not used in a ΔCt

calculation. The means of quality scores reported by the Fluidigm Real-Time PCR Analysis Software are presented in Table 1.

Data mining on the list of 41 genes significantly changed by group, time, and their interaction was performed using the Kyoto Encyclopedia of Genes and Genomes pathways (KEGG; http://www.genome.jp/kegg/) with the Database for Annotation, Visualization and the Integrated Discovery tool (DAVID; http://david.abcc.ncifcrf.gov; Hosack et al., 2003).

Table 1. Characteristics of the primers and the real-time PCR conditions

Gene[1]	Sequence (5′–3′)		NCBI accession no.	Product length (bp)	Melting temp. (°C)	GC content %	Mean quality score
MTTP	Forward	TGGAGCTGAAAACCACGGAA	NM_001101834.1	138	60	50	0.99
	Reverse	GGCATCCTTTGCACTTGCTC			60	55	
SLC27A3	Forward	CTTCACCTGTGGACTGTGGG	XM_024989955.1	134	60	60	0.99
	Reverse	AGGCATGTGTCCGTCATGTT			60	50	
SLC27A4	Forward	TTCCCTACTCTGCTACAGCC	XM_024998569.1	147	59	55	0.85
	Reverse	CTTGGGTCCAGGGCAGTTT			60	58	
MLYCD	Forward	GAACGGGGTGCTGAAAAACA	NM_001098946.1	142	59	50	0.99
	Reverse	CATCCAGGTTTTCACGGGGT			60	55	
ACOX3	Forward	GACCACCCGAATGGCATAGT	XM_024993139.1	105	60	55	0.98
	Reverse	CCTTTGGAAACACTTCTTTGATGGA			60	40	
ECH1	Forward	GGAGGTGGACGTAGGTTTGG	XM_024979072.1	110	60	60	0.99
	Reverse	TCATCTTGCGGGCAGTGTAG			60	55	
ECHDC2	Forward	CCCATGTCTTCCGGTTTCCTA	XM_015465413.2	71	59	52	0.99
	Reverse	CAAACTGCTCCTCCTACGGG			60	60	
ALDH3A1	Forward	CAGCATCCGGTAGGGTGATAG	NM_001046423.1	82	60	57	0.99
	Reverse	GCAGCCTTTGCATCCTGAAC			60	55	
TMLHE	Forward	GGGGTTGGGCCAGTCTTAAA	NM_001076064.1	81	60	55	0.99
	Reverse	GACAGCCCGGTCATAGTTGT			60	55	
CRAT	Forward	CGACCTGCCTCTGTCAACAT	XM_024998525.1	108	60	55	0.99
	Reverse	AGGCGTCCACAAACTGTAGG			60	55	
CROT	Forward	CCGTGGTGGTGCTTCGTTA	NM_177494.2	71	60	58	0.99
	Reverse	AAAGCAAAGGTAGCTCCGCA			60	50	
ACACA	Forward	ACGGCTGACTGGAGTTGAAG	NM_174224.2	186	60	55	0.99
	Reverse	AACGTCTGCTTGTCCGTCTT			60	50	
COX4I1	Forward	AAACACCCGGGACGACTAAG	NM_001001439.3	196	60	55	0.80
	Reverse	CGTCCTGGCTAGAAGGTCAG			60	60	
SLC27A2	Forward	ATGGCGTGCCTCAACTACAA	NM_001192863.1	188	60	50	0.99
	Reverse	GAGTTGACCCCATCCGTGTT			60	55	
SLC25A20	Forward	GTTCCTTAACTGGGCTGTGC	NM_001077936.2	172	59	55	0.99
	Reverse	ACAATGGTCTCGACAGGTCC			59	55	
ACADS	Forward	GTTCAAGTTGGCGGACATGG	NM_001034401.2	199	60	55	0.93
	Reverse	TGGCATCTCCTTCACGTAGC			60	55	

PCCB	Forward	CCTGTATCGGTTAACGAACGC	NM_001038548.2	155	59	52	0.99
	Reverse	TCGCTCTCAACAAAACTGCC			59	50	
MUT	Forward	CCTTTGCACTTGCTTGGTCC	NM_173939.2	134	60	55	0.99
	Reverse	AGGTGCACGGTCTTACTCAC			60	55	
ACOX1	Forward	AGGAAGTTTGGCATCGCAGA	NM_001035289.3	89	60	50	0.99
	Reverse	TAATTGAGGCCCACAGGTTCC			60	52	
SLC22A5	Forward	GTGCTGTTTGTGACGATGGG	NM_001046502.2	143	60	55	0.99
	Reverse	GTTCCCAGGACAAATGCTGC			60	55	
HMGCL	Forward	GCTTTGGAAGCTGGGCG	NM_001075132.1	99	59	65	0.99
	Reverse	CCACAGATGAGGTGCTGACA			60	55	
HMGCS2	Forward	GGAAGCGTGTGTCTCCTGA	XM_010803104.3	183	59	58	0.98
	Reverse	CCACATATCTTTAAACGGGACGC			60	48	
ACAT1	Forward	CGGAGAGAGAGGTCGGAGAT	NM_001046075.1	103	60	60	0.99
	Reverse	AACTTCGCTCCGCATACCTT			60	50	
FGF21	Forward	GATGTTTCGGGGCGTGAATG	XM_005219486.4	208	60	55	0.99
	Reverse	TGGCTAACTGAGGCAGATCG			60	55	
RPS6KB1	Forward	ATTTGCCTCCCTACCTCACG	NM_205816.1	80	59	55	0.99
	Reverse	TCCAAGACGAGAAGCAGCAT			59	50	
ACOX2	Forward	TGCTGCACACAGGTTCTCA	XM_024982656.1	205	59	53	0.99
	Reverse	TGTTGGTGAGTTCCTCCACG			60	55	
PCCA	Forward	ACCGCAGAAGCTGCTACATA	NM_001083509.1	199	59	50	0.99
	Reverse	GAGGATACGCACCTTGTACACT			60	50	
CPT1	Forward	AGCTCAGAGACAAATGCCCA	NM_001034349.2	90	59	50	0.99
	Reverse	ATCAGCCTTGGGAACTTGGAA			60	48	
CPT2	Forward	CGGCCTGATCTCCATACACC	NM_001045889.2	205	60	60	0.99
	Reverse	CTGGTAGTGCATAGTGGGCA			59	55	
mTOR	Forward	TTCCGACCTTCTGCCTTCAC	XM_002694043.6	128	60	55	0.99
	Reverse	ACAGCCACAGAAAGTAGCCC			60	55	
APOB	Forward	TTGGGCTTACCGACAATGCT	XM_024999521.1	216	60	50	0.94
	Reverse	GTGCCTTTGCTTTCTGTGGG			60	55	
PRKAG1	Forward	GATGAGAAAGGGCGTGTGGT	NM_174586.2	70	60	55	0.99
	Reverse	AGGTCTTTTCTGCTGCCAGG			60	55	
ECHDC3	Forward	TGGCAAGTGACAAGTCCTCC	NM_001193156.1	109	60	55	0.99
	Reverse	TCTAAGGCCACCTTTCTCGG			59	55	
FABP1	Forward	AGTCCAGACCCAGGAGAACT	NM_175817.3	178	60	55	0.91

	Reverse	CTCCCCCAAGGTGAACTCAT			59	55	
HADHA	Forward	TTCTACCAATGAGCAGGCCC	NM_174335.2	185	60	55	0.99
	Reverse	ACTTGCTGGGAGGGAGAGAT			60	55	
ACADVL	Forward	CTGGAAAGTGACAGATGAGTGC	NM_174494.2	117	59	50	0.98
	Reverse	TTTGTCCCCTCGAAGATCCG			59	55	
ACADM	Forward	CGTGAGCCAGGATCAGGATT	NM_001075235.1	164	60	55	0.97
	Reverse	CCAAGCTCCCAGGCTCTTTTA			60	52	
ECHS1	Forward	CCTGGCTCTTCTGCCCG	NM_001025206.2	109	60	71	0.99
	Reverse	TTCAGCTGGATCAACCCCAC			60	55	
ACAD10	Forward	GTTTGCTTGGAGGTGAACCC	NM_001192292.1	113	59	55	0.99
	Reverse	GCCAAGGCGATCCTCCTAAA			60	55	
PPARGC1A	Forward	TGCAGTACACATCAGCCTCA	NM_177945.3	95	59	50	0.99
	Reverse	TGCCAGGAGTTTGGTTGTGATA			59	45	
YWHAZ	Forward	CCTACTCCGGACACAGAACAT	NM_174814.2	198	59	52	0.99
	Reverse	TGACCTACGGGCTCCTACAA			60	55	
EIF3K	Forward	CCAGGCCCACCAAGAAGAA	NM_001034489	125	59	55	0.99
	Reverse	TTATACCTTCCAGGAGGTCCATGT			60	57	
HPCAL1	Forward	CCATCGACTTCAGGGAGTTC	NM001098964	99	60	58	0.98
	Reverse	CGTCGAGGTCATACATGCTG			60	55	
POLR2A	Forward	CTATCGCAGAACCCACTCACC	NM_001206313.2	91	60	57	0.99
	Reverse	CACAGCGGGAAGGATGTCTG			61	60	
GAPDH	Forward	CCGCATCCCTGAGACAAGAT	NM_001034034.2	218	60	55	0.99
	Reverse	ATGACGAGCTTCCCGTTCTC			60	55	
MARVELD1	Forward	TCGGTGCTTTGATGTCTTGC	NM_001101262.1	71	59	50	0.99
	Reverse	CAATCCACGGGCACTTCCTA			60	55	
LRP10	Forward	TTTTCCCGAATCCTGCCTGT	NM_001100371.1	73	60	50	0.99
	Reverse	ACAGGCCTCTGTAAGGTGC			59	58	
EMD	Forward	GACTTAGATTCGGCGTCCGT	NM_203361.1	140	60	55	0.99
	Reverse	TCAGGTTCCCCGTAAGTCCT			60	55	

[1]Target genes: *MTTP* = microsomal triglyceride transfer protein; *SLC27A3* = solute carrier family 27 member 3; *SLC27A4* = solute carrier family 27 member 4; *MLYCD* = malonyl-CoA decarboxylase; *ACOX3* = acyl-CoA oxidase 3, pristanoyl; *ECH1* = enoyl-CoA hydratase 1; *ECHDC2* = enoyl-CoA hydratase domain containing 2; *ALDH3A1* = aldehyde dehydrogenase 9 family member A1; *TMLHE* = trimethyllysine hydroxylase; *CRAT* = carnitine O-acetyltransferase; *CROT* = carnitine O-octanoyltransferase; *ACACA* = acetyl-CoA carboxylase alpha; *COX4I1* = cytochrome c oxidase subunit 4I1; *SLC27A2* = solute carrier family 27 member 2; *SLC25A20* = solute carrier family 25 member 20; *ACADS* = acyl-CoA dehydrogenase short-chain; *PCCB* = propionyl-CoA carboxylase subunit beta; *MUT* = methylmalonyl-CoA mutase; *ACOX1* = acyl-CoA oxidase 1; *SLC22A5* = solute carrier family

22 member 5; *HMGCL* = 3-hydroxy-3-methylglutaryl-CoA lyase; *HMGCS2* = 3-hydroxy-3-methylglutaryl-CoA synthase 2; *ACAT1* = acetyl-CoA acetyltransferase 1; *FGF21* = fibroblast growth factor 21; *RPS6KB1* = ribosomal protein S6 kinase B1; *ACOX2* = acyl-CoA oxidase 2; *PCCA* = propionyl-CoA carboxylase subunit alpha; *CPT1* = carnitine palmitoyltransferase 1; *CPT2* = carnitine palmitoyltransferase 2; *MTOR* = mechanistic target of rapamycin kinase; *APOB* = apolipoprotein B; *PRKAG1* = protein kinase AMP-activated non-catalytic subunit gamma 1; *ECHDC3* = enoyl-CoA hydratase domain containing 3; *FABP1* = FA binding protein 1; *HADHA* = hydroxyacyl-CoA dehydrogenase trifunctional multienzyme complex subunit alpha; *ACADVL* = acyl-CoA dehydrogenase very long-chain; *ACADM* = acyl-CoA dehydrogenase medium-chain; *ECHS1* = enoyl-CoA hydratase, short-chain 1; *ACAD10* = acyl-CoA dehydrogenase family, member 10;*PPARGC1A* = peroxisome proliferator-activated receptor gamma coactivator.
Reference genes: *YWHAZ* = tyrosine 3-monooxygenase/tryptophan 5-monooxygenase activation protein zeta; *EIF3K* = Eukaryotic Translation Initiation Factor 3 Subunit K; *HPCAL1* = Hippocalcin like 1; *POLR2A* = RNA polymerase II subunit A; *GAPDH* = glyceraldehyde-3-phosphate dehydrogenase; *MARVELD1* = MARVEL domain containing 1; *LRP10* = LDL receptor related protein 10, *EMD* = emerin.

3.4.2 Quantification of target proteins

3.4.2.1 ELISA for bovine haptoglobin (bHp)

Haptoglobin was measured in serum samples from 14-time points starting at 110 days after calving until 114 days after calving (1 day before LPS, 0.5, 1, 2, 3, 4, 6, 9, 12 h after LPS and 1, 2 and 3 days after LPS) in 30 cows from CON and 29 cows from CAR using an in-house developed ELISA according to Hiss et al. (2004). In brief, microtiter plates (EIA plate 9018, Corning Costar, Cambridge, MA, USA) were coated with serum sample (dilution 1/3,000) at 4 °C for an overnight period. After blocking with 200 µL of 2.5% casein in 0.05 *M* NaCl, pH 7.4, at room temperature for 2 h, the plates were washed 5 times and then stored in storage buffer at +4 °C. Before use, the storage buffer was decanted, and the plates were tapped against a tissue paper to remove the remaining buffer. To each well, 50 µL of test or control (dilution at least 1/100) were added in duplicate. Calibration curves were created using serum samples at dilutions from 9 µg/mL to 0.012 µg/mL in duplicate. Fifty µL of the rabbit anti-bovine Hp (lab production, code 49, dilution 1/50,000) were then added and incubated on a shaker for 2 h at room temperature. After 3 washes, 100 µL of the second antibody (mouse anti-rabbit IgG peroxidase, #A1949, Sigma-Aldrich, St. Louis, MO, USA, 1/800,000 dilution) were added and incubated for 30 min. After 5 washes, the wells were filled with 140 µL of a freshly prepared substrate solution containing 0.05 *M* citric acid, 0.055 *M* Na_2HPO_4, 0.05% urea hydrogen peroxide, 2% ProClin 150, and 2% of a tetramethylbenzidine solution (12.5 mg/mL in dimethylsulfoxide). The reaction was stopped after 30 min with 50 µL of 1 *M* oxalic acid, and the optical density (OD) was determined at 450 nm with a microtiter plate reader (SynergyH1, Bio-Tec Instruments, Inc., Winooski, VT). The Hp concentrations in unknown samples were then calculated from the calibration curve. Outlier detection was done for the results with producing a box-plot by SPSS (version 26; SPSS Inc., Chicago, IL, USA). Values more than three interquartile ranges (IQR) from the end of a box were labeled as outliers and removed from the analysis (Hoaglin and Iglewicz, 1986).

3.4.2.2 Capillary Western Blotting for target proteins related to fatty acid metabolism

20 mg of liver samples from 2-time points (100 days after calving (11 days before LPS) and 112 days after calving (24 h after LPS)) from 22 cows (11 from CON and 11 from CAR, randomly selected from the animals with the most complete set of liver biopsy samples) were homogenized in ice-cold Tris/HCl lysis buffer (pH 7.4) containing protease inhibitors cOmplete™, Mini Protease Inhibitor Cocktail, 1 tablet per 10 mL; Roche Diagnostics, Mannheim, Germany; Pefabloc SC [4-(2-aminoethyl) benzenesulfonyl fluoride hydrochloride,

1 m*M*, Sigma Aldrich, St. Louis, MO] for inhibiting serine protease, cysteine protease, and metalloproteases in a tissue-to-buffer ratio of 1:8 using the Precellys 24 system (VWR/Peqlab Biotechnologie, Erlangen, Germany). Total protein concentration was measured via Bradford assay (Roti Nanoquant K880, Carl Roth, Karlsruhe, Germany) by generating a standard curve using bovine serum albumin.

Protein quantification was performed by Simple Western size-based protein assay (WES, ProteinSimple, San Jose, CA), an automated capillary-based electrophoretic immunoassay, as per the manufacturer's instructions (https://www.proteinsimple.com/technical_library.html). In brief, samples were first diluted with 0.1× sample buffer to adjust the protein concentration to dilution within the linear range (between 0.3125 and 0.9375 µg/µL) and then diluted 4:1 by adding 3 µL of the 5× master mix. The final samples were heated for 5 min at 95 °C, placed on ice for 5 min, briefly centrifuged twice (2,500 × *g*, 5 s, 20 °C) with short vortex spins in between, and applied to the wells in duplicate. A control sample was also loaded on every plate to correct for inter-run variations (accepted interassay CV <20%, intra-assay CV <15%). Primary antibodies against total AMPK (#2532; Cell signaling technology, Danvers, MA, USA), total ACACA (#3662S; Cell signaling technology) and total SLC25A20 (#PA5-42411; ThermoFisher Scientific, Waltham, MA USA) were diluted 1:150, 1:100 and 1:30, respectively. All other reagents (antibody diluent, secondary antibodies, streptavidin-HRP, luminol-S, hydrogen peroxide) loaded on the plate were obtained from ProteinSimple and used according to the recommendations. Simple Western analysis was performed with multi-image exposures and otherwise instrument default settings at room temperature (RT). Using Compass Software (ProteinSimple), the area under the curve, which represents the signal intensity of the chemiluminescent immunoreaction, and which directly correlates with the abundance of the target protein, was assessed for each sample and normalized to the control. To normalize the data, first the sample and control mean ($Mean_x$) were corrected ($Mean_{Px}$) based on the amount of protein loaded (Px):

$$Mean_{PX} = Mean_X / P_X$$

Subsequently, the sample mean value ($Mean_{Px}$) corrected for the protein amount was divided into the control mean value corrected for the protein amount of the respective plate ($Mean_{IRC\ plate}$) and to the mean of the controls across all plates ($Mean_{IRC\ \Sigma\ plates}$) related:

$$\text{Corrected protein} = Mean_{Px} / [(Mean_{IRC\ plate} + Mean_{IRC\ \Sigma\ plates}) \times 0.5]$$

3.5 Statistical analyses

3.5.1.1 Evaluating reference genes

In this study, we examine the use of 8 reference genes commonly used in many other studies namely *YWHAZ*, *EIF3K*, *HPCAL1*, *POLR2A*, *GAPDH*, *MARVELD1*, *LRP10* and *EMD* versus a selection of 3 most stable reference genes to normalize the mRNA data of the study. To determine the most stably expressed genes for mRNA data normalization, a set of 8 genes (Crookenden et al., 2017; Saremi et al., 2012) was tested using the conditions of a BioMark HD real-time PCR system (mentioned above) and their stability was evaluated using qBase^{PLUS} 2.0 software (Biogazelle, Ghent, Belgium, Figure 17) to determine average expression stability (M) value for each gene to rank the stable level of the candidate reference genes based on their expression stability (Vandesompele et al., 2002). It has been shown that M value and gene stability have a negative correlation (Hu et al., 2016). Genes with the highest M value are considered to be the least stable ones, while those with the lowest M value have the most stable expression.

3.5.2 Target genes and proteins

Outlier detection was done for the results by producing a box-plot by SPSS (version 26; SPSS Inc.). Values more than three interquartile ranges (IQR) from the end of a box were labeled as outliers and removed from the analysis (Hoaglin and Iglewicz, 1986). The data from target mRNA and protein in liver and Hp in serum were analysed using the MIXED procedure of SAS (version 9.2; SAS Institute Inc., Cary, NC, USA). Before analysis, the data were screened for normality using the UNIVARIATE procedure of SAS, and any parameter that was not normally distributed was transformed using a $\log_{10}$ transformation before analysis. The model included the random effect of cow and the fixed effects of group, time, and their interaction (group × time). Data from initial mRNA abundance (at day 42 *ap*) were considered as covariates. The Tukey-Kramer adjustment was applied to account for multiple comparisons. The threshold of significance was set at $P \leq 0.05$; trends were declared at $0.05 < P \leq 0.10$.

3.5.3 Correlations

The relationships between the abundance of different mRNA were tested with the Spearman correlation test using the statistics program JMP Pro (version 15, SAS Institute Inc., Cary, NC, USA). A Spearman's rank correlation coefficient (R_S) of $R_S \geq 0.9$ was rated as very high, R_S = 0.68 to 1.0 as strong or high, R_S = 0.36 to 0.67 as modest or moderate, and $R_S \leq 0.35$ as low or weak correlation (Taylor, 1990).

4 RESULTS

4.1 Performance and treatment responses

The measurements of dry matter intake, energy balance, milk yield, milk composition, clinical findings and concentrations of carnitine, NEFA, BHB, and glucose were performed by the project partners of the MitoCow consortium at the FLI in Braunschweig and the respective manuscript is published elsewhere (Meyer et al., 2021).

4.1.1 Dry matter intake

As reported by Meyer et al. (2021), dry matter intake (DMI) was similar in both CAR and CON ($P_{Group} = 0.80$) and was not affected by L-carnitine supplementation over time ($P_{Group \times Time} = 0.19$). For DMI, a time-dependent variation was found ($P_{Time} < 0.001$). The DMI dropped by 35% from day 3 before LPS and reached a nadir on the day of LPS in both CAR and CON. Afterward, there was a continuous increase until the second day after LPS when it almost reached the starting levels (Figure 11).

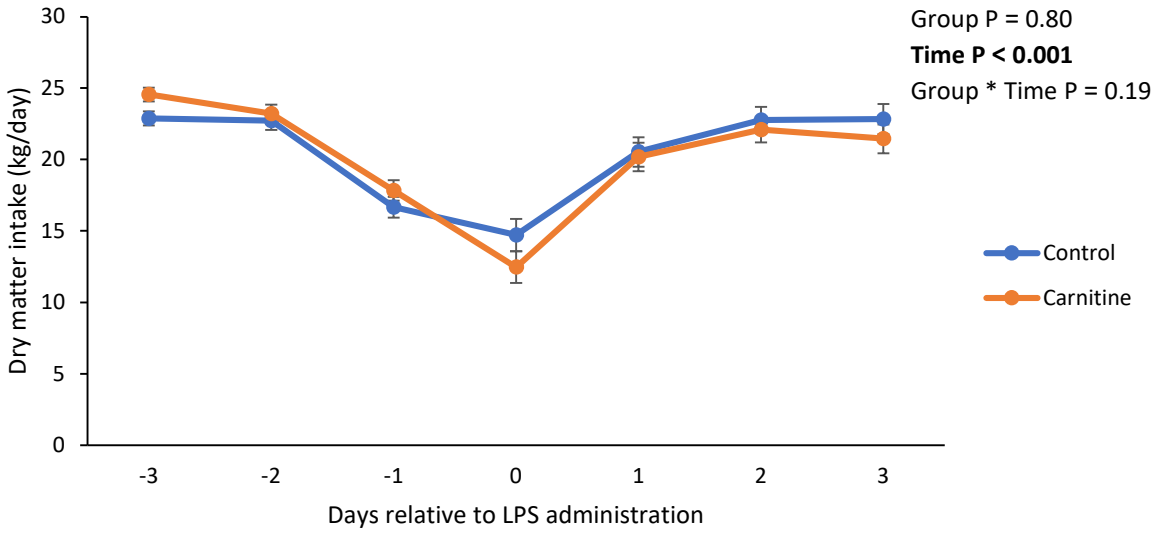

Figure 11. Dry matter intake of cows fed a non-supplemented (CON) or an L-carnitine-supplemented diet (CAR). Data are given as LS-Means ± SE (Meyer et al., 2021).

4.1.2 Milk

Milk production per day was similar in CAR and CON ($P_{Group} = 0.66$) from 3 days before until 3 days after LPS with a slight trend of difference over time ($P_{Group \times Time} = 0.09$). Daily milk yield changed with time ($P_{Time} < 0.001$) as there was a sudden decrease to 13% less milk yield on the day of LPS which continued to decrease in CAR the following day. Milk yield

started to increase in CON from the day after LPS and in CAR from day 2 after LPS till the last sampling time point (3 days after LPS) (Figure 12).

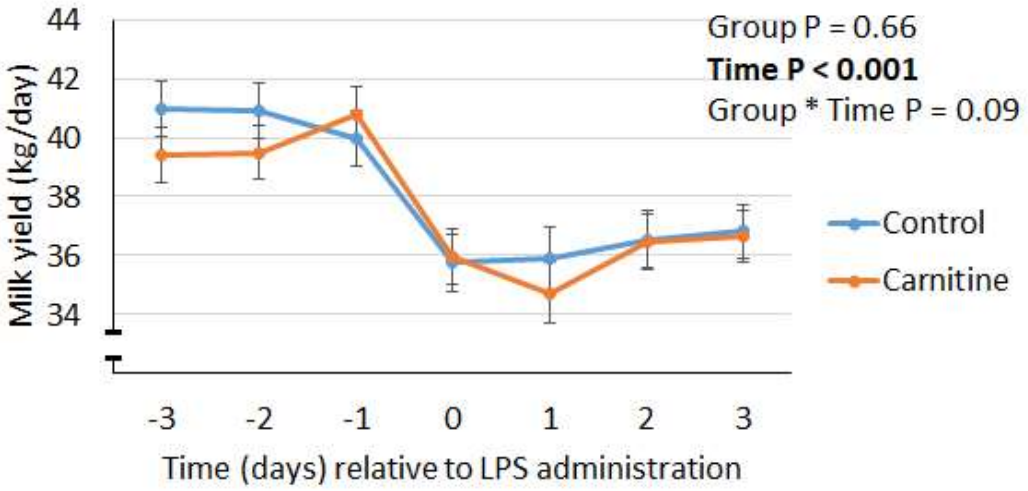

Figure 12. Milk yield of cows fed a non-supplemented (CON) or an L-carnitine-supplemented diet (CAR). Data are given as LS-Means ± SE (Meyer et al., 2021).

4.1.3 Clinical findings

The rectal temperature (Figure 13) was alike in CAR and CON ($P_{Group} = 0.25$) but it was affected by time ($P_{Time} < 0.001$). The rectal temperature increased continuously in both groups by 3.7% until 4 h to a maximum level of 39.4 ± 0.1 °C after LPS administration, and it decreased afterward to the initial level at 24 h after LPS and then observed unchanged till the end of the trial.

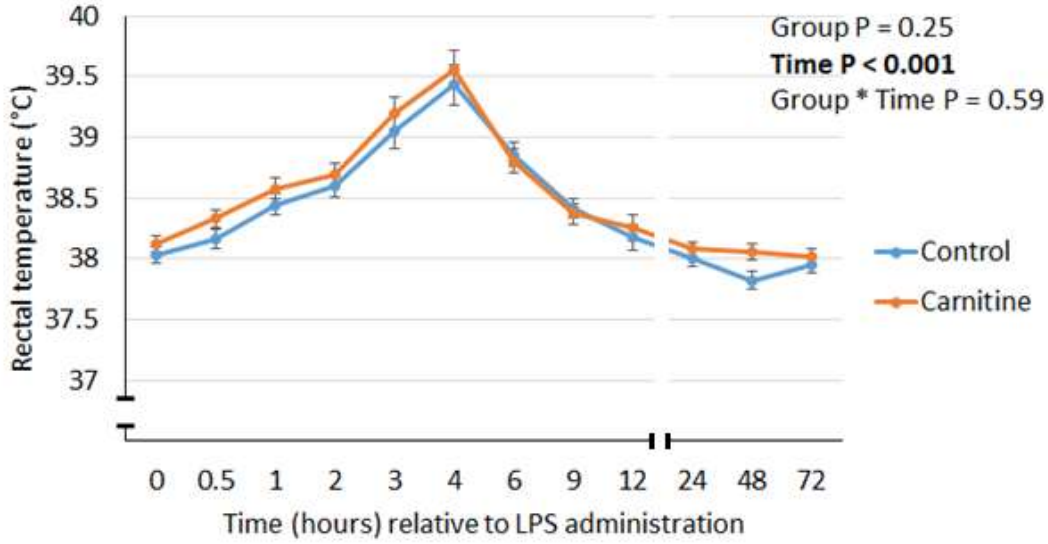

Figure 13. Rectal temperature of cows fed a non-supplemented (CON) or an L-carnitine-supplemented diet (CAR). Data are given as LS-means ± SE (Meyer et al., 2021).

4.1.4 Blood parameters

4.1.4.1 Carnitine

The concentration of free carnitine in the blood (Figure 14) was different between CAR and CON ($P_{Group} < 0.001$) and was differently affected by L-carnitine supplementation over time ($P_{Group \times Time} < 0.001$). The initial level of the mean of carnitine concentration in CAR was on average 9 times higher than CON. The concentration of the carnitine level in CON was almost unchanged over the whole experiment. In CAR, carnitine concentration dropped by about 50% until 12 h after LPS to increase afterward by about 50% until 48 h after LPS. Thereafter, it was unchanged until the end of the experiment.

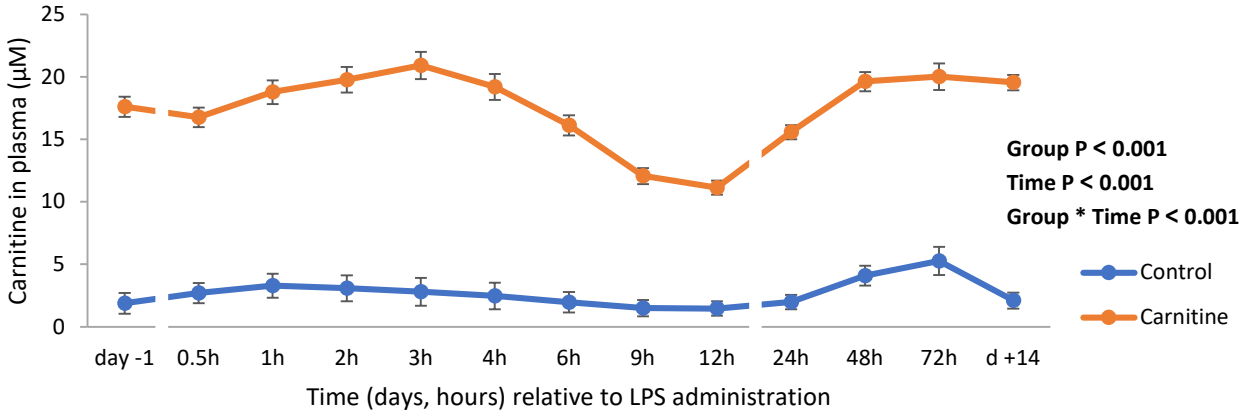

Figure 14. L-carnitine in plasma of cows fed a non-supplemented (CON) or an L-carnitine-supplemented diet (CAR). Data are given as LS-means ± SE (Meyer et al., 2021).

4.1.4.2 Haptoglobin

Jugular injection of LPS led to an increase of Hp concentrations both in CAR and CON (Figure 15). The difference in Hp levels in the serum of the CON and CAR groups was not significant ($P_{Group} = 0.94$) but the effect of time was ($P_{Time} < 0.001$). The first increase was observed 2 h after injection of LPS ($P = 0.004$) when compared with the initial basal concentration. Maximal Hp concentrations of more than 8-fold above basal concentrations were maintained until 48 h after LPS injection in both CAR and CON.

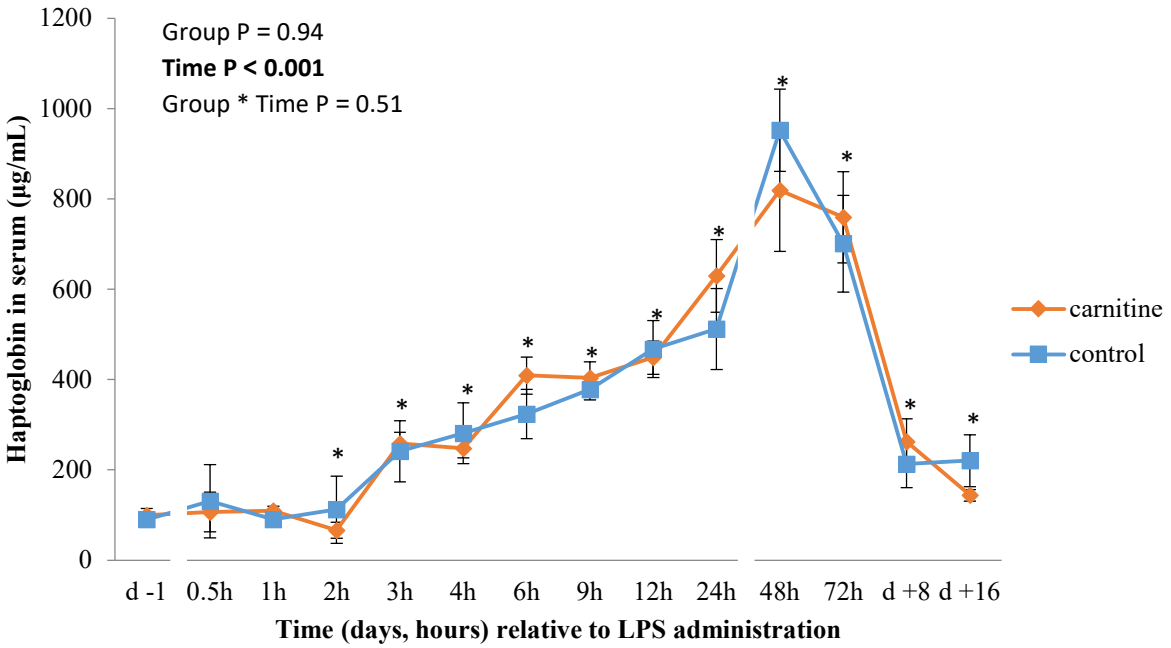

Figure 15. Haptoglobin concentration (mean ± SE) in serum before and after jugular LPS application. Asterisks indicate differences (*$P < 0.05$) between each time point compared with -24 h.

4.1.4.3 Serum Parameters with Relevance for Energy Metabolism

The results from net EB, NEFA, BHB, and glucose are summarized in Figure 16. As presented, the net EB was similar in CAR and CON ($P_{Group} = 0.13$) but it was affected by time ($P_{Time} < 0.001$) reaching a negative value in both the CAR and CON at the week of LPS challenge and the amounts of it were higher for the CAR. Net EB started changing from a negative to a positive from the week 1 after LPS. In a shorter period from a day before till 14 days after the LPS challenge, the NEFA concentration in plasma was lower in the CAR compared with CON ($P_{Group} = 0.04$) and the effect of time was significant ($P_{Time} < 0.001$). Also, irrespective of treatment ($P_{Group} = 0.25$), there was an increase in BHB concentration at the first time point after LPS and then decreased till 3 hours after LPS. After that, there was a steady increase of BHB concentration till 48 hours post LPS administration when the BHB reached its maximum concentration in the serum in CON followed by another decrease which went on till 7 days after LPS and then increased slightly at the last sampling time point ($P_{Time} < 0.001$). For glucose concentration, a time-dependent variation was found ($P_{Time} < 0.001$), its level increased at the first time point after LPS and then decreased to its starting value and remained almost unchanged during the rest of the time points.

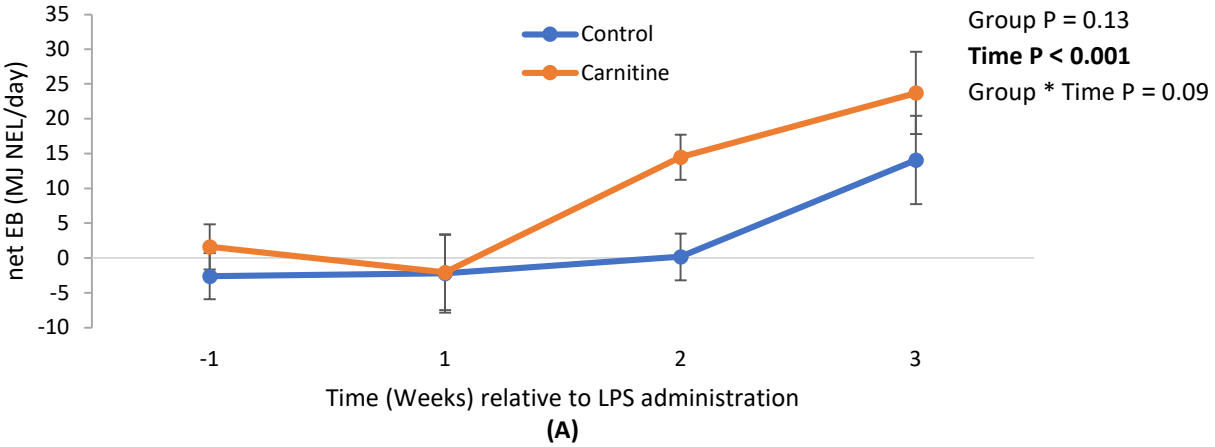
net EB (MJ NEL/day)
35
30
25
20
15
10
5
0
-5
-10
Control
Carnitine
Group P = 0.13
Time P < 0.001
Group * Time P = 0.09
-1
1
2
3
Time (Weeks) relative to LPS administration

(A)

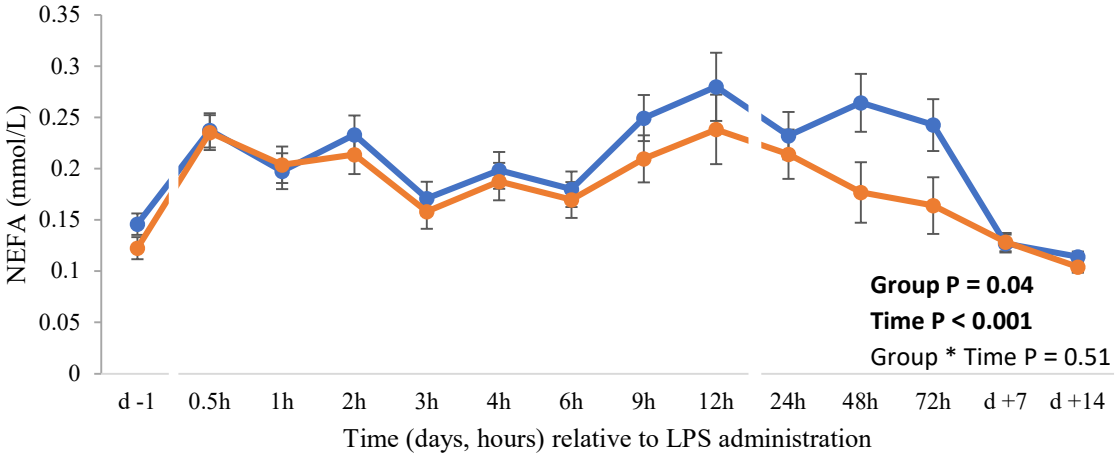
NEFA (mmol/L)
0.35
0.3
0.25
0.2
0.15
0.1
0.05
0
Group P = 0.04
Time P < 0.001
Group * Time P = 0.51
d -1
0.5h
1h
2h
3h
4h
6h
9h
12h
24h
48h
72h
d +7
d +14
Time (days, hours) relative to LPS administration

(B)

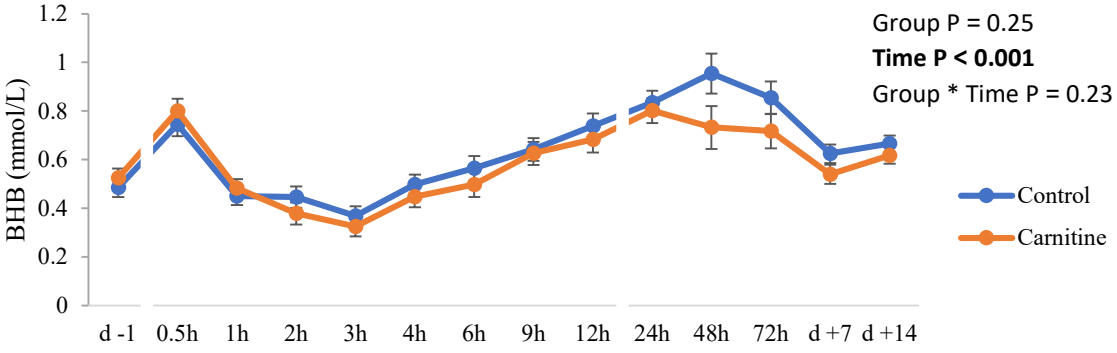
BHB (mmol/L)
1.2
1
0.8
0.6
0.4
0.2
0
Group P = 0.25
Time P < 0.001
Group * Time P = 0.23
Control
Carnitine
d -1
0.5h
1h
2h
3h
4h
6h
9h
12h
24h
48h
72h
d +7
d +14
Time (days, hours) relative to LPS administration

(C)

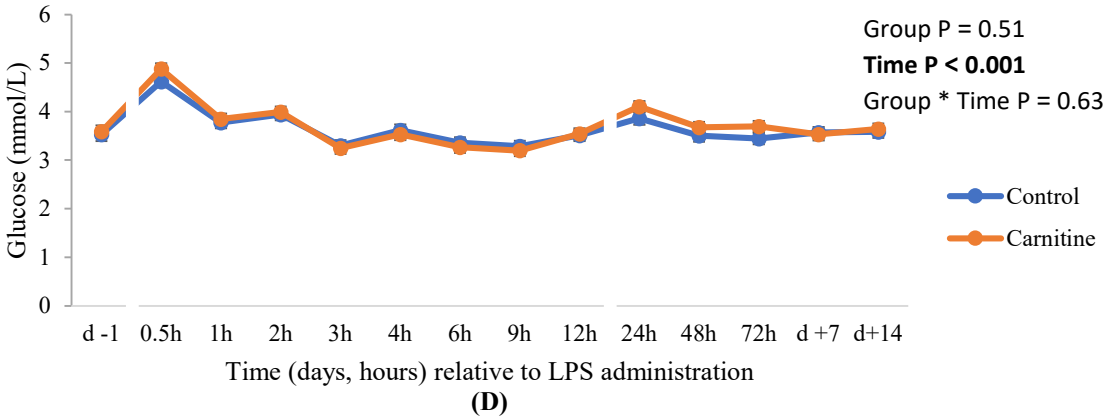

Figure 16. (**A**) Net energy balance (EB), (**B**) Serum concentrations of non-esterified fatty acids (NEFA), and (**C**) ß-hydroxybutyrate (BHB), and (**D**) whole blood concentrations of Glucose in cows fed a non-supplemented (CON) or an L-carnitine-supplemented diet (CAR). Data are given as LS-means ± SE (Meyer et al., 2021).

4.2 Most stable reference genes

In this study, the stability of the mRNA abundance of the candidate reference genes were evaluated by qbase+ software and the three most stable genes were *HPCAL*, *EIF3K*, and *LRP10*. To compare the results of analysis by 8 vs. 3 reference genes, target genes were normalized using the Fluidigm real-time PCR Analysis Software 4.5.2 (Fluidigm) once with 8 and once with the 3 most stable reference genes identified by qbase+ software and then compared (Figure 17).

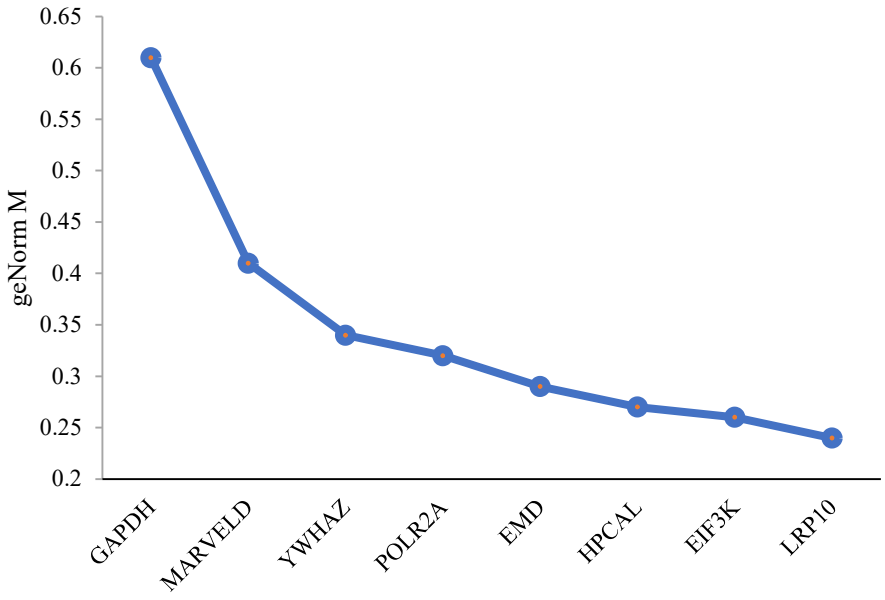

Figure 17. Ranking of the reference genes in hepatocytes. The transcriptional stability of the candidate reference genes was evaluated by qbase+ software. A total of three genes were identified to have high transcriptional stability (*HPCAL, EIF3K*, and *LRP10*). X-axes, internal reference genes.

The results from the mRNA abundance of 41 targeted genes in this study normalized by 8 versus 3 most stable reference genes are presented in table 2. As shown, the large difference between these 2 sets of data is considerable that shows selecting 8 genes for normalization of the mRNA results was not optimal and emphasizes the selection of proper stable endogenous control genes as an important step of any RT-qPCR study.

Table 2. Comparison of results for fixed effects of group, time, and their interaction (group × time) for mRNA abundance of 41 targeted genes normalized by 8 or 3 most stable reference genes.

		P-value with 8 references genes[1]			*P*-value with 3 references genes[1]		
Pathway	**Gene name**	Group	Time	G × T	Group	Time	G × T
AMPK/mTOR	*PRKAG1 (AMPK)*	0.36	0.33	0.85	0.51	**0.01**	**<.0001**
	mTOR	0.39	0.09	0.15	0.52	**<.0001**	0.89
	RPS6KB1	0.59	0.28	0.10	0.91	**<.0001**	**<.0001**
	PPARGC1A	**0.05**	0.79	0.25	0.65	**<.0001**	**<.0001**
	SREBF1	0.37	0.16	0.74	0.98	**<.0001**	0.19
Carnitine metabolism	*SLC22A5*	0.48	0.84	0.37	0.16	**<.0001**	**<.0001**
	TMLHE	0.42	0.53	0.44	0.56	**<.0001**	**<.0001**
	CRAT	0.09	0.82	0.06	0.9	**0.02**	**0.03**
	CROT	0.11	0.28	0.16	0.43	0.47	**0.03**
FA uptake	*SLC25A20*	0.17	0.28	**0.01**	0.36	0.39	0.07
	SLC27A2	0.10	0.79	0.83	**0.04**	**<.0001**	0.43
	SLC27A3	0.22	0.41	0.39	0.37	0.08	0.31
	SLC27A4	0.16	0.63	0.43	0.29	**<.0001**	0.91
Ketogenesis	*HMGCL*	0.46	0.74	0.39	0.53	0.45	0.18
	ACAT1	**0.02**	0.71	0.10	0.27	**0.04**	0.08
	FGF21	0.76	0.81	**0.05**	0.45	**<.0001**	0.55
	HMGCS2	0.16	0.25	0.84	0.51	0.09	**0.03**
Lipoprotein synthesis	*APOB*	0.20	0.48	**0.02**	0.25	**0.02**	0.83
	MTTP	**0.03**	0.09	0.08	0.50	**<.0001**	**<.0001**
Mitochondrial FA oxidation	*FABP1*	0.14	0.92	0.86	0.52	**<.0001**	**<.0001**
	ACACA	0.92	0.06	0.68	0.95	**<.0001**	**<.0001**
	COX4I1	0.98	0.92	0.81	0.73	**0.03**	**0.03**
	ACAD10	0.14	0.92	0.86	0.15	**0.05**	**0.03**
	ACADM	0.15	0.22	0.71	0.98	0.53	**<.0001**
	ACADVL	0.22	0.45	0.35	0.94	0.15	**<.0001**
	HADHA	0.32	0.55	0.45	0.95	**<.0001**	**<.0001**
	CPT2	0.19	0.84	0.29	0.53	0.16	**0.01**
	CPT1	0.48	0.27	0.30	**<.0001**	**<.0001**	**<.0001**
	PCCA	0.88	0.87	0.38	0.25	**<.0001**	**0.01**
	PCCB	**0.01**	**0.05**	0.07	0.70	**<.0001**	**0.04**
	MUT	0.27	0.64	0.97	0.50	**<.0001**	**<.0001**
	ACADS	0.39	0.35	0.52	0.24	**<.0001**	**0.01**
	MLYCD	0.43	0.75	0.19	0.06	**<.0001**	**<.0001**

Peroxisomal FA oxidation	*ECH1*	0.72	0.58	0.44	0.42	**<.0001**	**<.0001**
	ECHDC2	0.14	0.63	**0.05**	0.12	**<.0001**	**<.0001**
	ECHS1	0.14	0.92	0.86	0.25	**<.0001**	0.11
	ECHDC3	**0.02**	0.88	0.42	0.81	**<.0001**	0.77
	ACOX2	0.46	0.19	**0.05**	0.29	**<.0001**	0.89
	ACOX3	0.60	0.55	0.16	0.20	**<.0001**	0.16
	ALDH3A1	0.10	0.56	0.09	0.45	**<.0001**	0.25
	ACOX1	0.80	0.95	**0.04**	0.17	**<.0001**	**<.0001**

[1]Significant P values (≤ 0.05) are highlighted by **bold numbers**.

4.3 Hepatic mRNA abundance of the target genes related to fatty acid metabolism

The mRNA abundance of 41 genes involved in FA metabolism in liver tissue is presented in Table 3. From the 5 genes involved in the *AMPK-mTOR* signaling pathway, i.e., *PRKAG1*, *mTOR*, *RPS6KB1*, *PPARGC1A,* and *SREBF1* changes in abundance of genes over time were observed. Interaction between group and time was observed for *PRKAG1*, *RPS6KB1,* and *PPARGC1A*. The comparison between groups within time points yielded higher mRNA abundances in the CAR group at d 112 *pp* for *PRKAG1, RPS6KB1,* and *PPARGC1A* and higher mRNA abundance in the CON group at d 100 *pp* for *RPS6KB1*.

Out of the 4 genes associated with L-carnitine metabolism, *SLC22A5*, *TMLHE,* and *CRAT* were affected by time. For *SLC22A5* and *TMLHE* an interaction of group and time was observed that the mRNA abundance was higher in the CON at d112 and 100 pp respectively.

Concerning the genes related to FA uptake, the mRNA abundance of gene *SLC27A2* was lower in the CAR group than in the CON group. Except for the *SLC25A20*, time was significant for 3 other genes in this pathway including *SLC27A2* and *A4* and a trend of that for *SLC27A3*. Besides, there was no interaction between group and time.

From the genes associated with ketogenesis, 2 were affected by time including *ACAT1* and *FGF21*. The mRNA abundance of *HMGCL* was neither affected by group nor by time, and there was no group × time interaction. A trend for a time effect was observed for *HMGCS2*.

Both genes of the lipoprotein synthesis pathways including *APOB* and *MTTP* changed over time; for *MTTP* there was also a group x time interaction, whereby the mRNA abundance in the CAR group was lower at d 100 *pp* and higher at d 112 *pp* when compared to the CON group.

Regarding genes from the mitochondrial FA oxidation pathway, the hepatic mRNA abundance of gene *CPT1* was different between the 2 groups. Changes with time were found

for *FABP1*, *ACACA*, *COX4I1*, *ACAD10*, *HADHA*, *PCCA*, *PCCB*, *MUT*, *ACADS*, *MLYCD* and *CPT1* and the effect of the interaction of supplement and time was observed for *ACADM*, *ACADVL*, *CPT2*, *PCCA*, *MUT*, *ACADS*, *MLYCD*, *FABP1*, *ACACA*, *ACAD10*, *HADHA,* and *CPT1*. The mRNA abundance in the CON was higher at d 100 *pp* for *FABP1*, *HADHA, ACADM,* and *PCCA* and at the same time point, the mRNA abundance of *ACADVL* was higher in CAR. At d 112 *pp*, the mRNA values were higher in the CON for *CPT1* and *2*, *ACADS* and *MLYCD,* and higher in the CAR for *ACACA, ACADM,* and *MUT*. Values for mRNA abundance at d 126 *pp* was lower in the CAR for *ACAD10*.

The mRNA abundance of all genes from the peroxisomal FA oxidation pathway was affected by time including *ECH1*, *ECHS1*, *ECHDC2*, *ECHDC3*, *ACOX1*, *ACOX2*, *ACOX3,* and *ALDH3A1*. From these 8 genes, a time x group interaction was observed for *ECH1, ECHDC2,* and *ACOX1*). The mRNA abundance was lower in the CAR than in the CON at d 100 *pp* for *ECH,* at d 112 *pp* and d 126 *pp* for *ECHDC2* and d 112 *pp* for *ACOX1*.

Table 3. mRNA abundance of genes involved in hepatic FA oxidation

Pathway	Gene name	Days relative to calving (LSM)						SEM[3]	*P*-value		
		100		112		126			Group	Time	G × T
		CAR[2]	CON[2]	CAR	CON	CAR	CON				
AMPK/mTOR	*PRKAG1 (AMPK)*	0.90	1.11	1.36[a]	0.93[b]	1.06	1.11	0.018	0.51	0.01	<.0001
	mTOR	0.98	0.97	0.87	0.87	1.03	1.01	0.008	0.52	<.0001	0.89
	RPS6KB1	1.02[b]	1.12[a]	1.06[a]	0.94[b]	1.13	1.15	0.010	0.91	<.0001	<.0001
	PPARGC1A	0.80	0.79	1.36[a]	1.01[b]	0.83	0.80	0.035	0.65	<.0001	<.0001
	SREBF1	2.10	2.22	2.38	2.00	2.62	3.12	0.075	0.98	<.0001	0.19
Carnitine metabolism	*SLC22A5*	0.85	0.81	0.81[b]	1.08[a]	0.79	0.82	0.034	0.16	<.0001	<.0001
	TMLHE	0.91[b]	1.09[a]	0.97	0.81	1.07	1.12	0.014	0.56	<.0001	<.0001
	CRAT	1.14	1.10	1.07	1.16	1.09	1.01	0.013	0.90	0.02	0.03
	CROT	0.88	0.99	0.93	0.92	0.93	0.91	0.014	0.43	0.47	0.03
FA uptake	*SLC25A20*	0.85	0.93	0.86	0.95	0.97	0.91	0.012	0.36	0.39	0.07
	SLC27A2	0.76	0.97	1.05	1.29	0.76	0.88	0.016	0.04	<.0001	0.43
	SLC27A3	1.61	0.97	1.40	1.03	1.29	1.02	0.087	0.37	0.08	0.31
	SLC27A4	2.03	2.19	3.11	4.26	2.56	3.26	0.137	0.29	<.0001	0.91
Ketogenesis	*HMGCL*	1.37	1.25	1.19	1.37	1.36	1.28	0.028	0.53	0.45	0.18
	ACAT1	0.90	0.97	0.88	0.93	0.95	0.95	0.008	0.27	0.04	0.08
	FGF21	1.56	1.96	0.95	1.08	1.72	1.79	0.054	0.45	<.0001	0.55
	HMGCS2	1.14	1.45	0.96	1.11	1.26	1.52	0.075	0.51	0.09	0.03
Lipoprotein synthesis	*APOB*	1.04	1.16	1.04	1.26	0.98	1.14	0.015	0.25	0.02	0.83
	MTTP	0.83[b]	1.09[a]	1.52[a]	1.20[b]	0.83	0.85	0.023	0.50	<.0001	<.0001
Mitochondrial FA oxidation	*FABP1*	1.01[b]	1.49[a]	0.93	0.74	1.57	1.62	0.038	0.52	<.0001	<.0001
	ACACA	1.30	1.58	1.18[a]	0.62[b]	2.73	2.87	0.069	0.95	<.0001	<.0001
	COX4I1	1.26	0.79	0.74	1.14	0.99	1.45	0.062	0.73	0.03	0.03
	ACAD10	1.09	1.15	1.10	1.09	1.10[b]	1.27[a]	0.014	0.15	0.05	0.03
	ACADM	2.29[b]	3.52[a]	3.17[a]	2.15[b]	3.10	2.82	0.074	0.98	0.53	<.0001
	ACADVL	1.90[a]	0.32[b]	0.51	1.03	0.95	0.92	0.072	0.94	0.15	<.0001
	HADHA	0.82[b]	1.09[a]	1.27	1.02	0.96	0.94	0.018	0.95	<.0001	<.0001
	CPT2	2.01	1.53	1.63[b]	2.86[a]	1.78	1.70	0.068	0.53	0.16	0.01
	CPT1	0.43	0.59	0.71[b]	1.05[a]	0.44	0.49	0.019	<.0001	<.0001	<.0001
	PCCA	0.67[b]	0.87[a]	0.88	0.91	0.86	0.92	0.015	0.25	<.0001	0.01
	PCCB	0.98	0.94	0.62	0.70	1.06	1.04	0.015	0.70	<.0001	0.04
	MUT	0.84	0.95	1.18[a]	0.95[b]	0.90	0.90	0.012	0.50	<.0001	<.0001
	ACADS	1.86	1.56	0.93[b]	1.65[a]	1.65	2.00	0.048	0.24	<.0001	0.01
	MLYCD	0.88	0.90	0.94[b]	1.25[a]	0.93	1.00	0.014	0.06	<.0001	<.0001
Peroxisomal FA oxidation	*ECH1*	0.83[b]	1.00[a]	1.17	1.05	0.84	0.91	0.014	0.42	<.0001	<.0001
	ECHDC2	1.11	1.03	0.88[b]	1.16[a]	1.07[b]	1.32[a]	0.020	0.12	<.0001	<.0001
	ECHS1	0.83	0.83	0.61	0.71	0.89	0.96	0.012	0.25	<.0001	0.11
	ECHDC3	0.97	0.97	0.88	0.87	1.02	1.03	0.013	0.81	<.0001	0.77
	ACOX2	0.86	0.99	0.99	1.16	0.88	0.96	0.025	0.29	<.0001	0.89
	ACOX3	0.95	1.10	0.76	0.78	1.04	1.11	0.014	0.20	<.0001	0.16
	ALDH3A1	0.92	0.99	0.83	0.81	0.99	1.02	0.012	0.45	<.0001	0.25
	ACOX1	0.97[b]	1.28[a]	1.19	1.08	1.19	1.32	0.017	0.17	<.0001	<.0001

[a–b] Different superscripts indicate differences between the LS mean values of treatment groups for the same gene at each time point ($P < 0.05$).

[1]Abundance is presented as Least square means over time in arbitrary units normalized to 3 endogenous control genes (*LPR10, EIF3K*, and *HPCAL*; ΔCp).

[2]CAR = L-carnitine group; CON = control group

[3]SEM = standard error of the mean

4.4 The abundance of selected proteins related to fatty acid metabolism in the liver tissue

No differences related to the L-carnitine supplementation were observed for the protein abundance of the ACACA ($P_{Group} = 0.83$). Total ACACA protein abundance was affected by time ($P_{Time} = 0.002$), but not by the interaction of time × treatment (P Group × Time = 0.45; Figure 18, A).

Differences related to the L-carnitine supplementation were not significant for the protein abundance of the AMPK nor SLC25A20 ($P_{Group} = 0.13$ and $P_{Group} = 0.15$ respectively). Total AMPK protein abundance nor total SLC25A20 protein abundance were not affected by time ($P_{Time} = 0.77$ for AMPK and $P_{Time} = 0.61$ for SLC25A20). The interaction of time × treatment was not significant for AMPK or SLC25A20 ($P_{Group \times Time}$ for AMPK= 0.49, $P_{Group \times Time}$ for SLC25A20= 0.59; Figure 18, B and C).

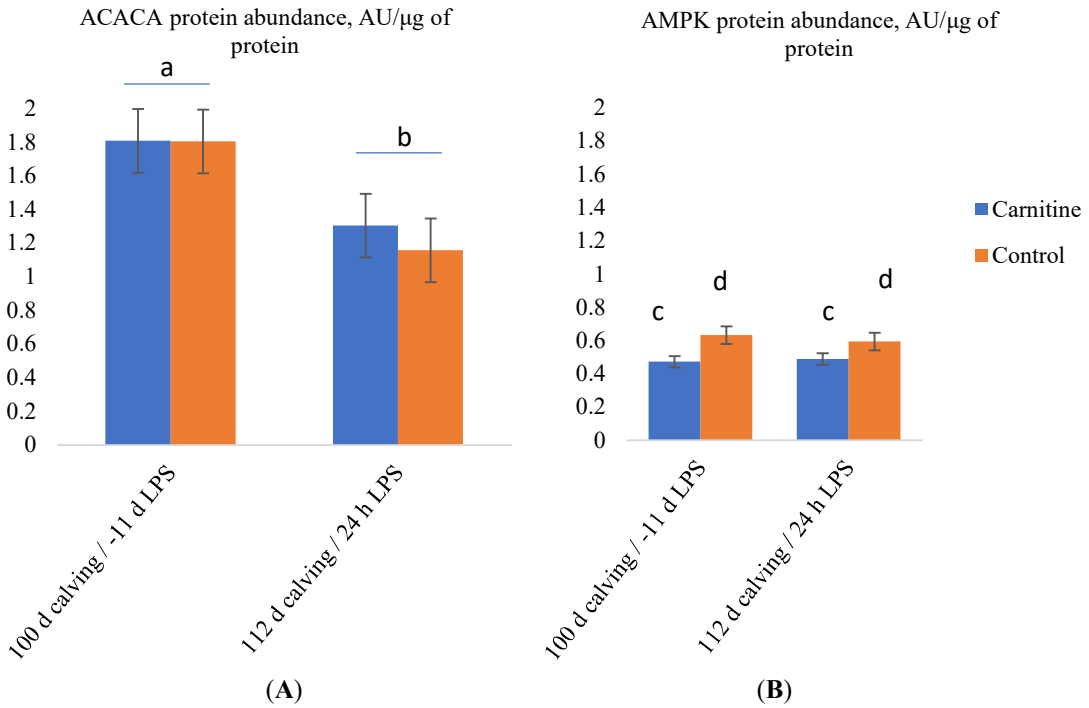

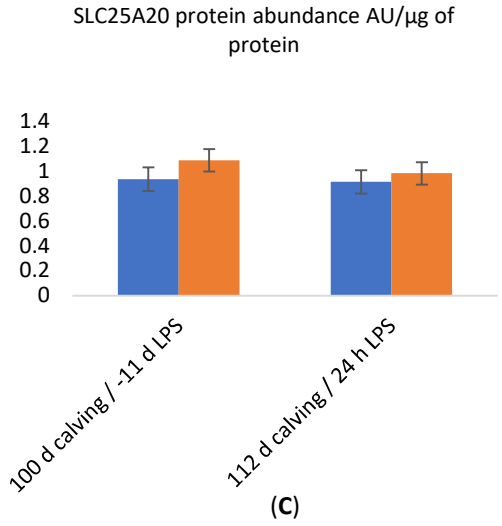

	P-Value		
	Group	Time	Group × Time
ACACA	0.83	**0.002**	0.45
AMPK	0.13	0.33	0.25
SLC25A20	0.15	0.61	0.59

(D)

Figure 18. Protein abundance [arbitrary units (AU)/µg of protein] of the ACACA (**A**), AMPK (**B**) and SLC25A20 (**C**) in the liver of dairy cows on 100 days after calving (11 days before LPS administration), and 112 days after calving (24 hours after LPS administration). (**D**) Data statistics. Data are given as means ± SE. Different lowercase letters indicate differences ($P < 0.05$) between time points (a and b) or between treatments (c and d).

4.5 Genes function and correlation

4.5.1 KEGG pathway analysis

The most relevant KEGG pathways in hepatic FA metabolism and their related genes in this study are shown in Figure 19.

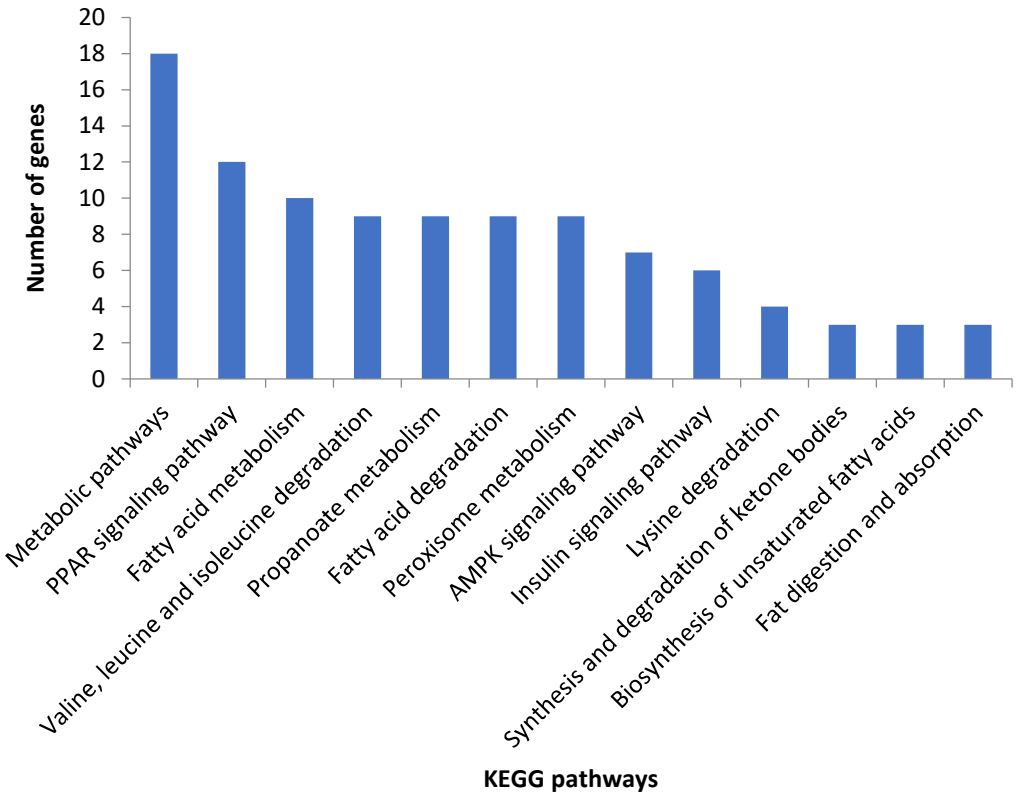

Figure 19. Presented pathways of target genes. Metabolic pathways = *ACOX2, ACOX1, ACADM, ACADS, ACACA, ECHS1, COX4I1, ACAT1, HADHA, ACOX3, ALDH3A1, ACADVL, MUT, HMGCS2, MLYCD, PCCB, PCCA, HMGCL; PPAR* signaling pathway = *ACOX2, ACOX1, ACADM, CPT2, FABP1, SLC27A2, ACOX3, SLC27A4*; FA metabolism = *ACADVL, ACOX1, ACADM, CPT2, ACADS, ACACA, ECHS1, ACAT1, HADHA, ACOX3*; Valine, leucine and isoleucine degradation = *MUT, ACADM, HMGCS2, ACADS, ECHS1, ACAT1, PCCB, HADHA, PCCA;* Propanoate metabolism = *MUT, ACADM, MLYCD, ACACA, ECHS1, ACAT1, PCCB, HADHA, PCCA*; FA degradation = *ACADVL, ACOX1, ACADM, CPT2, ACADS, ECHS1, ACAT1, HADHA, ACOX3*; Peroxisome metabolism = *ACOX2, ACOX1, ECH1, MLYCD, CRAT, SLC27A2, HMGCL, CROT, ACOX3*; AMPK signaling pathway = *SREBF1, MLYCD, PRKAG1, ACACA, RPS6KB1, mTOR, PPARGC1A*; Insulin signaling pathway = *SREBF1, PRKAG1, ACACA, RPS6KB1, mTOR, PPARGC1A*; Lysine degradation = *TMLHE, ECHS1, ACAT1, HADHA*; Synthesis and degradation of ketone bodies = *HMGCS2, ACAT1, HMGCL*; Biosynthesis of unsaturated FA = *ACOX1, HADHA, ACOX3*; Fat digestion and absorption = *APOB, FABP1, MTTP*

The DAVID software and KEGG functional enrichment analysis indicated that the abundance of mRNAs modified by group, time, and their interaction was mainly related to metabolic pathways (KEGG ID: bta01100) and also *PPAR* signaling pathway (KEGG ID: bta03320), propanoate metabolism (KEGG ID: bta00640), FA metabolism (KEGG ID: bta01212), valine, leucine and isoleucine degradation (KEGG ID: bta00280), FA degradation

(KEGG ID: bta00071), peroxisome metabolism (KEGG ID: bta04146), *AMPK* signaling pathway (KEGG ID: bta04152), insulin signaling pathway (KEGG ID: bta04910), lysine degradation (KEGG ID: bta00310), synthesis and degradation of ketone bodies (KEGG ID: bta00072), biosynthesis of unsaturated FA (KEGG ID: bta01040), and fat digestion and absorption (KEGG ID: bta04975). Notably, the *PPAR* signaling pathway was particularly affected. The pathways are summarized in Table 4.

Table 4. The most relevant Kyoto Encyclopedia of Genes and Genomes (KEGG) terms in the metabolism of FA from the list of 41 genes [DESeq2 (Love et al., 2014; P. BH < 0.05[1])] in the liver samples

KEGG pathways	No.[2]	*P*-value
Metabolic pathways	18	<0.001
ACOX2, ACOX1, ACADM, ACADS, ACACA, ECHS1, COX4I1, ACAT1, HADHA, ACOX3, ALDH3A1, ACADVL, MUT, HMGCS2, MLYCD, PCCB, PCCA, HMGCL		
Valine, leucine and isoleucine degradation	10	<0.001
MUT, ACADM, HMGCS2, ACADS, ECHS1, ACAT1, PCCB, HMGCL, HADHA, PCCA		
FA metabolism	10	<0.001
ACADVL, ACOX1, ACADM, CPT2, ACADS, ACACA, ECHS1, ACAT1, HADHA, ACOX3		
PPAR signaling pathway	8	<0.001
ACOX2, ACOX1, ACADM, CPT2, FABP1, SLC27A2, ACOX3, SLC27A4		
Propanoate metabolism	9	<0.001
MUT, ACADM, MLYCD, ACACA, ECHS1, ACAT1, PCCB, HADHA, PCCA		
FA degradation	9	<0.001
ACADVL, ACOX1, ACADM, CPT2, ACADS, ECHS1, ACAT1, HADHA, ACOX3		
Peroxisome metabolism	9	<0.001
ACOX2, ACOX1, ECH1, MLYCD, CRAT, SLC27A2, HMGCL, CROT, ACOX3		
AMPK signaling pathway	7	<0.001
SREBF1, MLYCD, PRKAG1, ACACA, RPS6KB1, mTOR, PPARGC1A		
Insulin signaling pathway	6	0.003
SREBF1, PRKAG1, ACACA, RPS6KB1, mTOR, PPARGC1A		
Lysine degradation	4	0.012
TMLHE, ECHS1, ACAT1, HADHA		
Synthesis and degradation of ketone bodies	3	0.006
HMGCS2, ACAT1, HMGCL		
Biosynthesis of unsaturated FA	3	0.027
ACOX1, HADHA, ACOX3		
Fat digestion and absorption	3	0.085
APOB, FABP1, MTTP		

[1]*P*. BH < 0.05 = *P*-value, adjusted for multiple testing using the Benjamini and Hochberg method (false discovery rate), was less than 0.05 (Benjamini and Hochberg, 1995).
[2]Number of differentially expressed genes involved in the KEGG term.

According to the different functions of each gene in the different pathways, the related genes were classified in 7 bigger functional pathways which are presented in Table 5.

Table 5. Classification of the 41 genes of interest in relevant KEGG pathway

Gene name	KEGG pathway[1]	Classification
PRKAG1	*AMPK* signaling pathway	AMPK /mTOR
mTOR	*AMPK* signaling pathway	
RPS6KB1	*AMPK* signaling pathway	
PPARGC1A	*AMPK* signaling pathway	
SLC22A5	nkpr[2]	Carnitine metabolism
TMLHE	Lysine degradation	
CRAT	Peroxisome	
CROT	Peroxisome	
SLC25A20	Nkpr	FA uptake
SLC27A2	*PPAR* signaling pathway	
SLC27A3	Insulin resistance	
SLC27A4	*PPAR* signaling pathway	
HMGCL	Synthesis and degradation of ketone bodies	Ketogenesis
ACAT1	Synthesis and degradation of ketone bodies	
FGF21	Nkpr	
HMGCS2	Synthesis and degradation of ketone bodies	
APOB	Fat digestion and absorption	Lipoprotein synthesis
MTTP	Fat digestion and absorption	
FABP1	Fat digestion and absorption	Mitochondrial FA oxidation
ACACA	FA metabolism	
COX4I1	Metabolic pathways	
ACAD10	Nkpr	
ACADM	FA metabolism	
ACADVL	FA metabolism	
HADHA	FA metabolism	
CPT2	FA metabolism	
CPT1	Nkpr	
PCCA	Propanoate metabolism	
PCCB	Propanoate metabolism	
MUT	Propanoate metabolism	
ACADS	FA metabolism	
MLYCD	Propanoate metabolism	
ECH1	Peroxisome	Peroxisomal FA oxidation
ECHDC2	Nkpr	
ECHS1	Metabolic pathways	
ECHDC3	Nkpr	
ACOX2	Peroxisome	
ACOX3	Peroxisome	
ALDH3A1	Metabolic pathways	
ACOX1	Peroxisome	

[1]The most relevant pathway is mentioned.

[2]No KEGG pathway was reported.

4.5.2 Correlations results

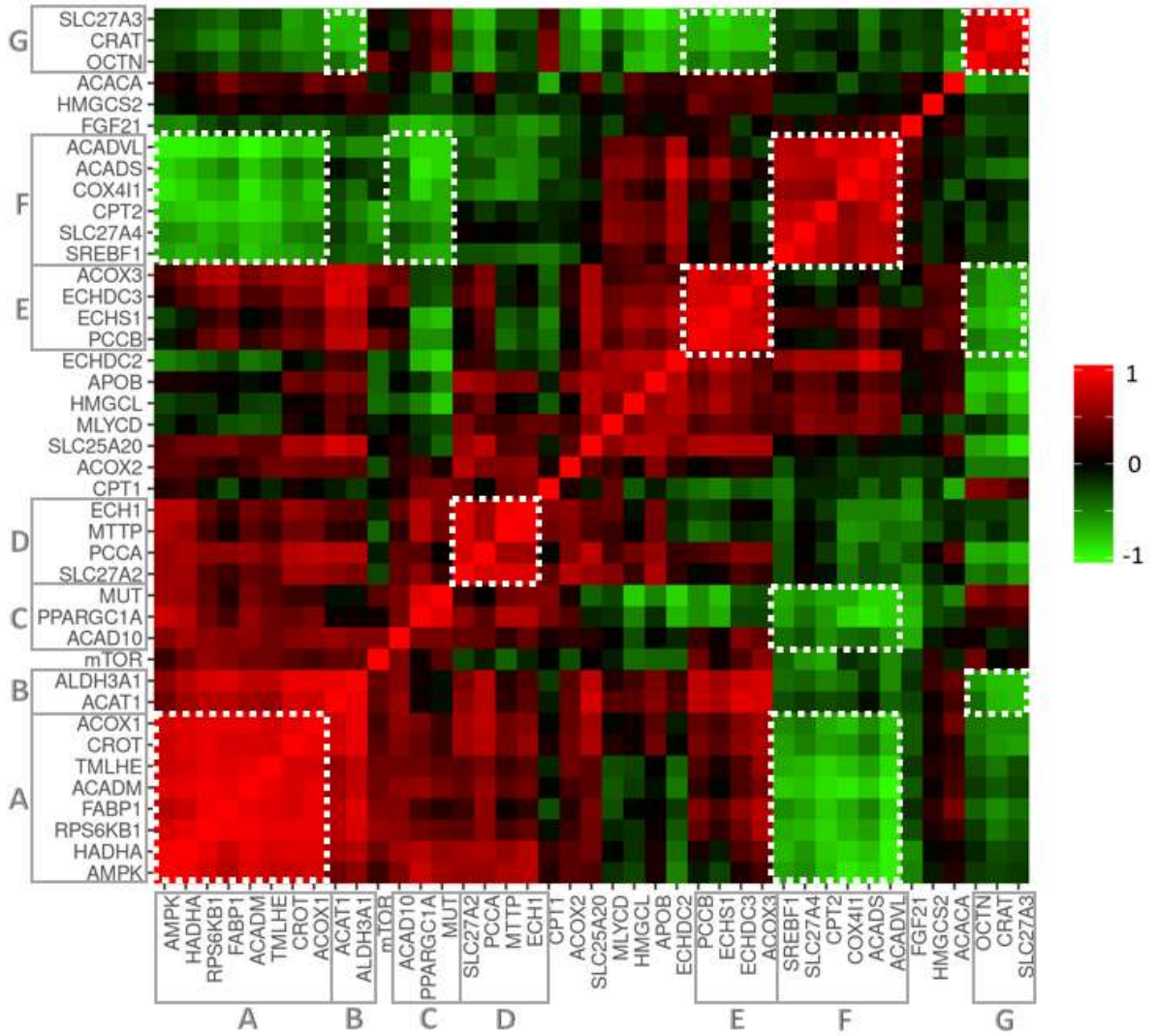

Figure 20. Heat map visualizing the correlation coefficients between levels of hepatic mRNA abundance from 41 genes related to hepatic FA metabolism. Red-colored cells represent positive correlations, and green-colored cells represent negative correlations. Gene names are provided at Table 1. Clusters of genes are put into 7 blocks of A, B, C, D, E, F and G for the ease of understanding.

Correlation coefficients between mRNA abundance of 41 target genes regarding treatment and across time were calculated (Figure 20). The figure shows clusters of genes with correlated expression. For the ease of understanding, these clusters were numbered from block A to block G. In block A, the transcript abundance of 8 genes belonging to the carnitine metabolism pathway (*TMLHE* and *CROT*), mitochondrial FA oxidation pathway (*HADHA*, *FABP1,* and *ACADM*) *AMPK/mTOR* pathway (*PRKAG1* and *RPS6KB1*) and peroxisomal FA oxidation pathway (*ACOX1*) were positively correlated with the genes from the same block and negatively correlated with block F with 6 genes, four from the mitochondrial FA oxidation pathway (*CPT2*, *COX4I1*, *ACADS,* and *ACADVL*), one from *AMPK/mTOR* pathway (*SREBF1*) and one from FA uptake pathway (*SLC27A4*) (for a detailed list of specific r and *P*-value,

see Supplemental File S1). The small-block B consisted of two genes that belong to the Ketogenesis pathway (*ACAT1*) and peroxisomal FA oxidation pathway (*ALDH3A1*) which were in a negative correlation with genes from block G (*SLC22A5* and *CRAT* from carnitine metabolism pathway and *SLC27A3* from FA uptake pathway). In block C, the mitochondrial FA oxidation pathway genes (*ACAD10 and MUT), and* the *AMPK/mTOR* pathway gene (*PPARGC1A*) were negatively correlated with genes from block F. Block D is a group of genes from mitochondrial FA oxidation pathway (*PCCA*), FA uptake pathway (*SLC27A2*), lipoprotein synthesis pathway (MTTP) and peroxisomal FA oxidation pathway (*ECH1*) with positive correlations to genes from the same block. The block E contains four genes from two different functional pathways, with positive correlations between genes from the same block: the peroxisomal FA oxidation pathway (*ECHS1, ECHDC3,* and *ACOX3*) and mitochondrial FA oxidation pathway (*PCCB*). In addition to the negative correlation of genes from block F with the genes from blocks A and C, the genes in this block were in positive correlation with the genes from the same Block. As mentioned, we observed a negative correlation between genes from block G with genes from block B and C, meanwhile the genes from block G positively correlated with themselves. As several blocks contain co-regulated genes that belong to different functional pathways, there is clear evidence for crosstalk between these pathways.

5 DISCUSSION

L-carnitine is required for mitochondrial FA oxidation. In one study, abomasal infusion of L-carnitine could elevate *in vitro* hepatic FA oxidation and reduce lipid accumulation in the liver of dairy cows. It also induced higher fat-corrected milk yield in feed-restricted lactating Holstein cows (Carlson et al., 2006; Akbar et al., 2013), whereas, in another study, infusion of up to 12 g/day of carnitine into the abomasum did not improve milk yield or digestibility of nutrient (LaCount et al., 1996). More specifically, abomasal infusion of L-carnitine (from day -25 relative to expected calving date until 56 days in milk at 6, 50, or 100 g/day) decreased total lipid in liver and triacylglycerol accumulation on day 10 after calving (Carlson, et al., 2007). Also, carnitine-supplemented cows had higher liver glycogen during early lactation. In general, carnitine supplementation increased *in vitro* palmitate (C16:0) β-oxidation by liver slices, with medium and high treatments affecting *in vitro* palmitate metabolism more potently than did the lower treatment, whereas the concentration of NEFA in serum was not affected by carnitine and as a result of greater hepatic FA β-oxidation, plasma BHB was higher for the medium and high treatments (Carlson, et al., 2007). By reduction in the accumulation of lipid in the liver and stimulating hepatic glucose output, supplementation of carnitine might improve glucose status and decline the risk of metabolic disorders during early lactation (Carlson, et al., 2007). Similarly, in liver slices obtained from cows during early lactation, carnitine increased oxidation and total utilization of palmitate and decreased palmitate esterification (Drackley et al., 1991b). Abomasal L-carnitine infusion (at 20 g/day during nine days in mid-lactation) showed to increase total carnitine in plasma, liver, muscle, and milk during feed restriction, whereas feed restriction alone could increase concentrations of carnitine in muscle and milk but not in the liver (Carlson, et al., 2007). Carnitine infusion raised the concentration of carnitine fraction in milk as well as milk carnitine output on days five to six after the start of the infusion. In the same study, on the last two days of the nine-day infusion period, all carnitine fractions were increased in carnitine-infused, feed-restricted cows, whereas all acylcarnitine except short-chain acylcarnitines were increased in milk from water-infused, feed-restricted cows. Therefore, it has been concluded that liver carnitine concentrations might limit hepatic FA oxidation capacity in dairy cows during the periparturient period. Therefore, L-carnitine supplementation has been used to decrease lipid accumulation in the liver of periparturient cows (Carlson, et al., 2007).

The present study aimed at investigating the effect of L-carnitine supplementation on hepatic metabolism of FA in lactating dairy cows during LPS triggered inflammatory stress.

We herein characterized the changes in mRNA abundance of 41 key genes and 3 selected proteins involved in different pathways from the hepatic metabolism of FA in dairy cows. Cows were assigned in 2 groups of L-carnitine dietary supplemented and control-fat supplemented and they were studied before and after an LPS administration using the Fluidigm integrated fluidic circuit arrays (IFC, Fluidigm) that have been previously used successfully for large-scale gene expression analysis studies like Citri et al., 2012; Crookenden et al., 2017; Guo et al., 2010; Viturro et al., 2014; and Wehner et al., 2016.

5.1 Interaction between metabolism and inflammation

It has been shown that FA concentration in blood is a good indicator of the magnitude of fat mobilization from adipose tissue (Bauman et al., 1988). A negative energy balance is compensated by the mobilization of FA from adipose tissue. FA are transported by binding with serum albumin and are taken up by FA transporters into tissues, mainly the liver (Meyer et al., 2020; Schlegel et al., 2012; Zhao et al., 2018). In the present study, the administration of LPS increased concentrations of FA in plasma, which was associated with a slightly negative energy balance that was confirmed by the net EB observed in both the CON and CAR, similar to previous experiments that negative EB in dairy cows was associated with metabolic disorders and reproductive failures (Schlegel et al., 2012). High NEFA in the blood is reflecting adipose tissue mobilization during the period of negative energy balance (Dänicke et al., 2014). In several studies, increased levels of NEFA were reported at inflammation (Contreras et al., 2012; Gessner et al., 2013; Grum et al., 1996; Locher et al., 2015; Nightingale et al., 2015; Sordillo and Mavangira, 2014), that is due to the increased energy demands of the immune system (Bradford et al., 2015b) and decreased DMI at inflammation (Locher et al., 2015). In phases of energy deficit, NEFA is only incompletely oxidized to acetyl-CoA and serve ketogenesis including the production of BHB. However, NEFA as well as ketone bodies provide energy for tissues, (Drackley et al., 2001). Even though the production of BHB as an indicator of ketogenesis increased after LPS in both CAR and CON, hyperketonaemia (BHB > 1.2 mmol/L, Schuh et al., 2019) was not observed in any of the treatment groups during the study. These observations seem to be in line with the less DMI after LPS as the BHB concentration started to decrease at 48 hours after LPS when the DMI had reached its pre-LPS challenge values (decreased DMI observed from one day before LPS challenge might be due to the rehousing of the cows to the calving pen the day before LPS). In the present experiment, the maximum NEFA concentration was reached from 12 h till 72 h after LPS, at the same weekly period when the net EB was most negative. From day 7 to 14 after LPS, the initial NEFA concentration was

reached again, which coincided with increased levels of DMI to the levels before the LPS administration and when the net EB was changing from negative to positive that according to the results from aforementioned studies shows the animals in this study could meet their energy demands again since it is probable that increased hepatic fatty acid oxidation, as a consequence of plasma NEFA and hepatic fatty acid uptake, created a satiety signal in these cows (Allen et al., 2009).

Carlson et al. (2007) found lower milk yields in the first 6 weeks of lactation (when cows are more prone for oxidative stress) for cows dietary supplemented with 100 g L-carnitine per day, which might be due to the lower DMI as discussed above, whereas supplementation with 6 or 50 g per day had no impact on milk yield. The results for milk yield in the present study are in support of the previous one when we observed no effect of supplementation with L-carnitine on milk production but reduced milk yield in the cows under the immune stressed state concurrent with the decline in DMI.

The intravenous infusion of LPS rapidly induces an inflammatory response in the body characterized by activation of the immune system (Bradford et al., 2015). Systemic consequences are observed as the acute phase response (APR) phenomena such as altered plasma concentration of acute-phase proteins (APP) such as serum amyloid A, C-reactive protein, and Hp (Jiang et al., 2008). Haptoglobin is a major acute-phase protein in cattle with serum concentrations < 20 μg/mL in healthy animals and 100 to 1000-fold increases in response to immune stimulation (Godson et al., 1996). In this study the serum concentrations of Hp in CAR and CON was not significantly different but systemic LPS challenge could rise up its concentration from 2 hours after systemic LPS and reached its maximum level at 48 hours after LPS which is similar to the results of Eckersall et al. (2006) that hypothesizes induced systemic cytokine followed by APP production in the liver after inflammation.

Glucose is the primary fuel of immune cells (Kvidera et al., 2017b). Reduction in milk synthesis is one of the signs of infection or inflammation in dairy cows, and this can be a strategy to save glucose for the immune system (Kvidera et al., 2017b). To ensure further that the adequate supply of fuel is available for the immune system, the body increases glucose output from the liver via both glycogenolysis and gluconeogenesis (Waldron et al., 2003). At the same time, peripheral insulin resistance may also occur which leads to a reduction in uptake of glucose by skeletal muscle and adipose tissue (Song et al., 2006). In this study, greater (~32%) circulating concentrations of glucose were observed after LPS ($P < 0.001$) which is in line with our observation that with the administration of LPS the production of milk dropped

significantly which means less demand on glucose for lactose production (Bell, 1995) suggesting that less glucose was used for milk production.

In this study, rations were designed on an isoenergetic basis and DMI remained unaffected by the L-carnitine supplementation. Carlson et al. (2007) reported that DMI did not differ between non-supplemented cows and cows receiving 6 or 50 g of non-rumen-protected L-carnitine per day, whereas, at a dosage of 100 g dietary L-carnitine per day, DMI was lower during the first two weeks of lactation. Based on these findings and the present results, we conclude that a moderate L-carnitine supplementation neither stimulates nor depressed feed intake of the cows but the LPS challenge could significantly decrease the DMI in both CAR and CON at the day of administration. In previous studies, the increase in rectal temperature of cows reported being detectable 2 to 4 h after the challenge (Hoeben et al., 2000; Lehtolainen et al., 2003). In this study, we observed that the LPS injection could raise the rectal temperature above the normal range till 4 h after the administration reflecting the response of the body to an immune stressed state.

According to these observations, we concluded that after LPS the cows were experiencing a negative energy balance due to increased activity of the immune system and reduction in DMI which could not be compensated by a reduction in milk yield. Consequently, the lipolysis escalated and a load of FA to hepatocytes increased for the generation of energy. From day 7 to 14 after LPS, the initial NEFA concentration was reached again, which coincided with increased levels of DMI to the levels before the LPS administration and when the net EB was changing from negative to positive. According to the results from aforementioned studies this observation shows the animals in this study could meet their energy demands again since it is probable that increased hepatic fatty acid oxidation, as a consequence of plasma NEFA and hepatic fatty acid uptake, created a satiety signal in these cows.

5.2 Characterization of hepatic mitochondrial metabolism of fatty acids at inflammation

In contrast to our hypothesis, the mRNA abundance of the selected genes (except *SLC27A2* and *CPT1*) for characterizing carnitine's metabolic effect, was not altered with L-carnitine treatment. However, the abundance of these genes indicates changes to the inflammatory response as expected. The reasons for the lack of the L-carnitine response in the abundance of the examined genes are not known but are likely related to the availability of the L-carnitine in

the intermediary metabolisms or the moderate dosage of supplementation which was used in this study.

5.3 AMPK/mTOR pathway

Cellular energy homeostasis depends on the availability of nutrients and it is regulated by hormones and intracellular regulatory pathways. A major player promoting fat oxidation is AMPK. At the period of energy deficiency, phosphorylated AMPK signals the inhibition of acetyl-CoA carboxylase and suppressing malonyl-CoA synthesis. Malonyl CoA inhibits CPT1, which is a rate-limiting step for the entry of FA into mitochondria for oxidation and thus its suppression enables FA transport via CPT1 (Kahn et al., 2005). AMPK is the principal regulator of cellular energy, which senses the ratio of AMP: ATP in the cytosol (Zoncu et al., 2011; Hardie et al., 2012). In addition to the metabolic energy that the animal needs for lactation, the requirement for cellular energy to defeat infections and repair tissues elevates the ratio of AMP: ATP that leads to AMPK activation by phosphorylation (Hardie et al., 2012). With this background, we hypothesized that the alteration in this pathway could serve as a possible link between energy status and inflammation so we investigated the response of the liver cells to LPS induced inflammation and inconsistent with the above-mentioned studies we observed higher mRNA abundance of *PRKAG1* (coding gene for AMPK) in hepatic cells at 24 h post LPS in comparison with results from 2 other time points in the CAR that reinforces the fact that these cells are undergoing a period of high energy demand. However, albeit the pattern of changes from the time point before to the time point after LPS were similar in mRNA and protein abundance of AMPK in both CAR and CON, we found no differences in AMPK abundance between the time points at the protein level (levels of Phosphorylated AMP-activated protein kinase (pAMPK) was not investigated in this study), suggesting that during this time, the liver is sufficiently supplied with ATP, either via glycolysis or FA oxidation (FAO). The switch in fuel selection of the liver indicates the great metabolic flexibility of the liver that integrates this organ into homeorhesis, which has been defined as the orchestrated and coordinated control of body tissue metabolism aligned to partition nutrients and energy to the dominant process of inflammatory challenge (Bauman and Currie, 1980).

Activated AMPK helps energy balance by inhibiting anabolic pathways that use ATP while stimulating glycolysis, mitochondrial biogenesis, and increasing the expression of glucose and glutamine transporters. The mammalian target of rapamycin (*mTOR*) is a less specific sensor of cellular energy status than AMPK (Hotamisligil and Erbay, 2008). The *mTOR* integrates multiple signals of satiety from amino acid abundance, growth factors, hormones, and AMPK

(Saxton and Sabatini, 2017; Zoncu et al., 2011). When nutrients are abundant, activation of mTOR stimulates anabolic pathways and cell growth; but, when cellular energy is limited, phosphorylated AMPK inhibits mTOR to save energy and reduce protein synthesis (Sheldon et al., 2018). The inhibition of mTOR boosts FA oxidation and ketogenesis and constricts lipogenesis (Li et al., 2014; Liu et al., 2016; Musso et al., 2016). In this study, we confirmed that the downregulation of mRNA abundance of *mTOR* by LPS can be associated with the increase in expression of *AMPK* at the time when energy demand is high.

Among the key features of mTOR signaling is the activation of RPS6KB1 which constitutes a well-known mechanism for controlling protein synthesis and initiation of mRNA translation (Cant et al., 2018; Laplante and Sabatini, 2009). In non-ruminants, the upregulation of the mTOR/RPS6KB1 pathway at higher uptakes of AA and glucose decreases the phosphorylation of insulin receptor substrate 1 (IRS-1), and consequently the action of insulin on nutrient uptake by cells (Bell and Bauman, 1997; Um et al., 2006). In this study, the reduction of expression of *RPS6KB1* after LPS in the CON seems to indicate the existence of a similar feedback system to increase the availability of glucose, AA, and FA to the hepatocytes at the state of high energy demand which is confirmed by the positive correlation of this gene observed with *PRKAG1* in the CON group.

Peroxisome proliferator-activated receptor-gamma coactivator 1 alpha (PPARGC1A) has been defined as an important regulator of mitochondrial biogenesis (see Cantó and Auwerx, 2009 for review). PPARGC1A increases mitochondrial biogenesis and respiration rates, and the uptake and utilization of substrates for the production of energy (Liang and Ward, 2006). AMPK has been described to directly affect PPARGC1A activity through phosphorylation (Cantó et al., 2009). We speculated that the upregulation of *PPARGC1A* after LPS in this study might promote ATP production in the liver cells. This observation is in support of Cantó et al., (2009) and of the increased abundance of gene *PRKAG1* after LPS which could show higher mitochondrial biogenesis and respiration rate in this period.

SREBF1 is a key lipogenic transcription factor that regulates the lipogenic process by activating genes involved in FA and triglyceride synthesis in the liver (Brown and Goldstein, 2008; Horton et al., 2002). Previous studies have shown an inverse correlation between AMPK and SREBF1 activities in hepatocytes of mice (Foretz et al., 2005; Yang et al., 2009; You et al., 2004; Zhou et al., 2001). AMPK interacts with SREBF1 and directly phosphorylates it. The phosphorylation of SREBF1 by AMPK is enough and necessary for inhibition of proteolytic

processing and transcriptional activity of SREBF1 (Li et al., 2011) which is confirmed in this study due to the negative correlation results observed between abundance of gene *SREBF1* and abundance of genes *RPS6KB1, PRKAG1* and *PPARGC1A*. However, we found that the *SREBF1* mRNA abundance measured in our study did not change according to previous findings of suppression of SREBF1 by AMPK since these genes were changing similarly at LPS. Since SREBF1 is one component of a more complex system that regulates the overall rate of lipogenesis in cells (Horton et al., 2002), it remains to be determined whether other lipogenic transcription factors cooperate with *SREBF1* to regulate lipogenesis in hepatocytes downstream of *AMPK*.

5.4 Carnitine metabolism

Carnitine is an unavoidable cofactor in β-oxidation of FA that enables the transport of FA as acylcarnitine esters across the inner mitochondrial membrane (Ramsay and Arduini, 1993). Carnitine is collected from dietary sources or endogenously synthesized from trimethyllysine (TML), which is released at protein degradation. The released TML is then oxidized to γ-butyrobetaine (BB) by trimethyllysine dioxygenase (*TMLHE*), 3-hydroxy-N-TML aldolase and 4-N-trimethylaminobutyraldehyde dehydrogenase (*ALDH9A1*). In the final biosynthetic step, BB is hydroxylated by γ-butyrobetaine dioxygenase (BBOX1) to form carnitine. In cows, the last step occurs in the kidney and liver only (Vaz and Wanders, 2002). The decrease in hepatic expression of *TMLHE* after LPS observed in the CON in the present data could indicate less de novo synthesis of carnitine in this group suggesting that hepatic synthesis of carnitine is an important adaptation of the tissue to cope with the inflammatory situation in not supplied group, the adaptation which was not observed in the CAR after LPS.

Tissues which are not capable of carnitine production are depended on the uptake of carnitine by organic cation transporters (*OCTN*) from the blood, particularly SLC22A5 which is the most important carnitine transporter physiologically (Lahjouji et al., 2001; Schlegel et al., 2012; Tein, 2003). In this study, we found that *SLC22A5* mRNA abundance was higher after LPS in CON. As a plasma membrane transporter, SLC22A5 helps the uptake of carnitine and other organic cations into the hepatocyte (Koepsell et al., 2007). Choline-induced *SLC22A5* expression was shown to result in an increased intracellular carnitine concentration in cows liver (Bremer, 1983; Carter and Frenkel, 1978). Increased carnitine availability has been found to reduce the liver TAG accumulation in dairy cattle through stimulation of FA oxidation, as well as an improved gluconeogenesis (Carlson et al., 2007). The increased expression of *SLC22A5* after LPS in CON, therefore, suggests an extra need for

organic cation transport into hepatocytes in the CON which was not observed in the CAR. The decrease in *TMLHE* mRNA abundance in CON with a concomitant increase of *SLC22A5* after the LPS injection may indicate that those cows relied more on carnitine uptake rather than de novo synthesis, which is affirmed by a positive correlation between downregulation of *TMLHE* in the CON group with downregulation of *RPS6KB1* ($R_S = 0.64$, $P < 0.001$) and *PRKAG1* ($R_S = 0.46$, $P < 0.001$) in the same treatment group.

Carnitine O-octanoyl transferase (*CROT*) encodes one of the members of the carnitine/choline acetyltransferase family. The encoded protein converts 4,8-dimethylnonanoyl-CoA to its corresponding carnitine ester (Houten and Wanders, 2010). This transesterification occurs in the peroxisomes and is necessary for the transport of medium- and long-chain acyl-CoA molecules out of the peroxisome to the cytosol and uptake into the mitochondria via the carnitine acylcarnitine carrier (Wanders and Waterham, 2006). Carnitine O-acetyl transferase (*CRAT*) encodes carnitine O-acetyltransferase which is a member of the carnitine acyltransferase family, and an important metabolic pathway enzyme which is found in both the mitochondria and the peroxisome and is important in energy homeostasis and fat metabolism (Houten and Wanders, 2010). This enzyme catalyzes the reversible transfer of acyl groups from a short-chain acyl-CoA thioester to carnitine and regulates the ratio of acyl-CoA/CoA (Goldberg and Dixit, 2017; Pieklik and Guynn, 1975). In this study, the hepatic mRNA abundance of *CRAT* in the CAR was downregulated after LPS while the opposite has been found for CON. Considering that the mRNA abundance of *CROT* was not altered by LPS in both groups, CAR, and CON, the inflammatory reaction could have changed the metabolism of short-chain acylcarnitines in mitochondria which are in parallel with the observed positive correlation between the mRNA abundance of this gene with the unchanged mRNA abundance of *TMLHE* ($R_S = 0.48$, $P < 0.001$) and *RPS6KB1* ($R_S = 0.74$, $P < 0.001$) in the CAR group at LPS. The upregulation of *CRAT* in CON as opposed to downregulation in CAR could indicate the facilitated transfer of short-chain acyl-CoA to mitochondria via carnitine shuttle system that led to a higher ratio of acyl-CoA/CoA in the supplemented group.

5.5 Fatty acid uptake pathway

FA is inert chemically and they need to be activated to form acyl-CoA outside the mitochondrion before they enter a metabolic pathway (Yan et al., 2015). The uptake of LCFA from plasma into a cell is mediated by FA transport proteins (FATP) which are also called SLC27 proteins (Bonen et al., 2007; Doege and Stahl, 2006; Nafikov et al., 2013; Stahl, 2004). FATP2, FATP3, and FATP4 are highly expressed in the liver (Gimeno, 2007); they act as

hepatic transporters for LCFA, transporting them into the cytosol. Hepatic FATP2 has two other functions: activating LCFA to acyl-CoA (Kazantzis and Stahl, 2012) and a minor fraction of it is localized in the liver peroxisomes, allowing peroxisomal oxidation of branched and very-long-chain FA (VLCFA) (Falcon et al., 2010). Silencing of either FATP3 or FATP4 in mice displayed increased weight and WAT fat content as their reduced FA uptake and utilization results in incremental shunting of the unconsumed FA to WAT (Kazantzis and Stahl, 2012).

SLC25A20 encodes for carnitine-acylcarnitine translocase (*CACT*), which is responsible for transporting both carnitine–FA complexes and carnitine across the inner mitochondrial membrane into mitochondria and also in the opposite direction resulting in the transport of these acylcarnitines into the cytosol. This gene, like *CPT1*, seems to be essential for the FA oxidation pathway and utilization of FA as fuel sources (Bouvier-Muller et al., 2017; Houten and Wanders, 2010).

In this study the expression of *SLC25A20*, *SLC27A3* and *SLC27A4,* as well as protein abundance of *SLC25A20*, were not differentially regulated between the CAR and the CON group, indicating that the CAR did not affect FA uptake into the liver and FA binding and transport in the liver (Schlegel et al., 2012). The protein and mRNA abundance of *SLC25A20* were not affected by LPS challenge in this study, showing that the mitochondrial FA uptake was not affected by the inflammation. The lower abundance of *SLC27A2* in the CAR group may indicate a lower in peroxisomal FA oxidation due to supplementation. The upregulation of *SLC27A2* and *SLC27A4* after LPS infusion could be an indicator of increased transport of LCFA into hepatocytes. LCFA were then directed toward oxidation in peroxisomes rather than mitochondria in response to the inflammation. It was proved with our observation about the negative correlation of *SLC27A4* with the abundance of gene *RPS6KB1* showing a decreased protein synthesis while the cell is shifting to a higher level of FA oxidation.

5.6 Ketogenesis pathway

3-hydroxy-3-methylglutaryl-CoA synthase 2 (HMGCS2) is the rate-limiting mitochondrial enzyme that catalyzes the first reaction in the synthesis of ketone bodies when acetyl-CoA is in excess to provide lipid-derived energy (Lane et al., 2001; Grala et al., 2013). Under different nutritional and hormonal conditions, the level of *HMGCS2* mRNA is strongly correlated with the rate of ketogenesis (Hegardt, 1999) as in nonruminants and likely in ruminants, the protein concentration of HMGCS2 is strongly regulated at the transcriptional level (Nakamura et al., 2014; Akbar et al., 2015) thus, it is evident that changes in mRNA of this enzyme are important

for controlling mitochondrial ketogenesis (Naeem et al., 2012). Similar to *HMGCS2*, *HMGCL* belongs to the *HMG-CoA* lyase family. The protein encoded by this gene catalyzes the final step of mitochondrial ketogenesis so it plays a key role in ketone body formation (Zammit et al., 1984; Naeem et al., 2012). In the present study, the mRNA abundance of *HMGCS2* and *HMGCL* was not influenced by LPS administration in either group indicating that LPS did not influence the ketogenic pathway in cows.

Fibroblast growth factor 21 (*FGF21*) induces metabolic changes such as an increase of lipolysis, glucose uptake, or FA oxidation. *FGF21* is also regarded as a key regulator of ketogenesis (Badman et al., 2007). The *FGF21* gene is directly regulated by *PPARα* in the liver (Badman et al., 2007; Inagaki et al., 2007). The activity of the *HMGCS2* gene stimulates FGF21 abundance (Vilà-Brau et al., 2011) and FGF21 stimulates hepatic oxidation of LCFA and gluconeogenesis (Domouzoglou and Maratos-Flier, 2011). ACAT1 is the other enzyme in the ketogenesis pathway which catalyzes the synthesis of acetoacetyl-CoA from 2 acetyl-CoA (Harmon et al., 1991). In TMR-fed cows, Schoenberg et al. (2011) reported a positive relationship between plasma FGF21 concentration coupled with greater hepatic mRNA expression and energy deficit. The FGF21 has been described as a stress hormone that is promoted after a variety of metabolic and environmental stressors (Kim and Lee, 2015). Recent findings suggested that FGF21 has an adaptive role in keeping energy homeostasis during stressful conditions (Kim and Lee, 2014). *FGF21* is highly induced in the liver in dairy cattle during the transition period (Carriquiry et al., 2009; Schlegel et al., 2013; Schoenberg et al., 2011). It has been shown that the hepatic induction of FGF21 in dairy cattle is because of metabolic stress occurring in the peripartum period, which tries to keep energy homeostasis during this period (Kim and Lee, 2015; Schoenberg et al., 2011). For instance, it has been suggested that the energy shortage caused by fasting induces *FGF21* mRNA abundance in the liver via PPARA (Badman et al., 2007) and that protein and AA restriction elevate *FGF21* expression in liver as well (Kim and Lee, 2015). Moreover, it has been found that FGF21 is particularly induced by ER (endoplasmic reticulum) stress (Schaap et al., 2013), a condition that has been observed in the liver of cows during early lactation (Gessner et al., 2014). However, both *FGF21* and *ACAT1* mRNA abundance were decreased in both CAR and CON after LPS injection in the present study. The downregulation of *FGF21* after LPS in our study is not supporting a direct relationship with *HMGCS2* as reported in other studies (Vilà-Brau et al., 2011). Nevertheless, it is in support of the results from another mRNA from this pathway indicating that hepatic mitochondrial ketogenesis was not altered by systemic inflammation in

cows. On the other hand, the negative correlation between the mRNA from carnitine metabolism and FA uptake (*SLC22A5*, *CRAT,* and *SLC27A3*) with *ACAT1* noticed in this study, could be an indicator of the availability of FA for energy synthesis rather than ketogenesis that was in line with the results from BHB concentration in serum samples showing no hyperketonaemia in any of the treatments. However, further research is required to test for potential interactions between L-carnitine treatment, *FGF21*, and ketogenesis in dairy cows.

5.7 Lipoprotein synthesis pathway

The synthesis and secretion of VLDL in the liver are complex processes that are controlled by Apolipoprotein B (APOB), APOE, and MTTP (Katoh, 2002). APOB is one of the most important structural components of VLDL; APOB is the TG-binding protein in VLDL and is necessary for stabilizing the VLDL particles (Bernabucci et al., 2004). Marcos et al. (1990) suggested that the level of hepatic *APOB* mRNA in cows with fatty liver was lower in comparison with healthy cows. They concluded that apolipoprotein synthesis in the liver is slowed down during the fatty liver. Also, Uchida et al. (1992) reported that the concentration of APOB in plasma of dairy cows with fatty liver was lower in comparison with healthy cows (Jia et al., 2019). Shahzad et al. (2015) observed downregulation of expression of *APOB* as a net result of calving during the hot season which appeared to be an inability of the liver to oxidize the higher load of NEFA, likely making cows more susceptible to liver lipidosis. In another study, Osorio et al. (2013) observed a trend for lower plasma concentration of APOB in cows suggesting that this molecule might have limited the assembly or export of VLDL from the liver.

The MTTP appears to be involved in the first step of lipidation of the newly synthesized APOB molecule during the assembly of VLDL (Kulinski et al., 2002), resulting in the formation of nascent lipoprotein particles (Wetterau et al., 1998). The greater mRNA abundance of *MTTP* could have increased the rate of lipoprotein synthesis, thus preventing the accumulation of triglycerides in hepatocytes (Vailati-Riboni et al., 2016). In a study, Kessler et al. (2014) observed that the hepatic mRNA abundance of *MTTP* was not affected after parturition, in contrast to an earlier study (Schlegel et al., 2012) where increased mRNA abundance of *MTTP* in week 1 *p.p.* was reported. However, our results are consistent with earlier works demonstrating that the *MTTP* and *APOB* mRNA levels in the bovine liver were highest around parturition (an individual inflammatory stimulus) (Bernabucci et al., 2004; Goselink et al., 2013a). In this study, the data for the increased hepatic expression of 2 genes involved in VLDL synthesis and secretion (*MTTP* and *APOB*) after LPS injection indicate that

molecular adaptations after LPS were sufficient to initiate intracellular synthesis and secretion of VLDL and, thus, TAG export from the liver, in response to inflammation, particularly in the CON cows.

5.8 Mitochondrial fatty acid oxidation pathway

FA-binding protein 1, also known as liver-type FA binding protein, is the main intracellular FA transporters in ruminants` hepatic cells (Bionaz and Loor, 2008; Schroeder et al., 2008; Wolfrum et al., 2001). FABP has a high affinity for free LCFA but can also bind to acyl-CoAs (Frolov et al., 1997). Increased lipogenesis and adipogenesis are correlated with the enhanced expression of *FABP* (Tontonoz et al., 1994; Moseti et al., 2016). The role of *FABP1* in FA uptake into the mammary gland of lactating cows was studied using dietary conjugated linoleic acid (CLA; Gutgesell et al., 2009). It was determined that dietary CLA fed to cows decreased the concentrations of medium-chain SFA and palmitic acid (16:0) in milk. The change in milk FA concentrations was accompanied by a decrease in the mRNA abundance of *FABP1* in the mammary gland and by an increase in blood FA concentrations (Gutgesell et al., 2009). The downregulation of *FABP1* in this study could indicate the reduced lipogenesis in hepatic cells after LPS in both the CAR and CON group which might be because of the metabolic adaptations that occurred in the liver due to reduced load of substrates available for lipogenesis in challenged cows. This deduction could be asserted by the noticed positive correlation of decreased *FABP1* mRNA abundance with the decreased abundance of gene *RPS6KB1* involved in the synthesis of proteins during the LPS challenge.

Key enzymes regulating de novo FA synthesis are FA synthase (FAS) and ACACA (Torrens et al., 2014; Petrov et al., 2015). *ACACA* is highly expressed in the liver and it is a rate-limiting enzyme in FA synthesis that converts acetyl-CoA to malonyl-CoA which is the first step for FA synthesis (Savage et al., 2006). In hepatic lipid synthesis, AMPK, as a central regulator of cellular energy levels, is activated in response to the increase in the cellular AMP: ATP ratio. Activated AMPK inactivates ACACA by phosphorylation of this enzyme (Saggerson, 2008) which results in the suppression of FA biosynthesis (Zhang et al., 2017). Moreover, malonyl-CoA also suppresses FA oxidation by inhibiting CPT1; therefore, reduction of *ACACA* expression may also increase fat oxidation (Savage et al., 2006). Malonyl-CoA decarboxylase (MLYCD) is found in mitochondria, peroxisomes, and the cytoplasm (Chajès et al., 2006). This protein catalyzes the breakdown of malonyl-CoA to acetyl-CoA and carbon dioxide. Malonyl-CoA is an intermediate in FA biosynthesis and also inhibits the transport of fatty acyl CoA into mitochondria. Consequently, the encoded protein acts to increase the rate

of FA oxidation. The opposing activities of ACACA and MLYCD appear to be important determinants in dynamically setting the size of the cellular pool of malonyl-CoA. The combined activities of ACACA and MLYCD result in a rapid turnover of malonyl-CoA (Saggerson, 2008). In our study, the downregulation of *ACACA* and also the decrease in protein abundance of ACACA in liver cells at the first time point after the LPS injection along with the upregulation of the FA oxidation gene (*MLYCD*) could be due to the lower energy intake and subsequent lower substrate availability for lipogenesis after LPS. As evidenced by the significant downregulation of *SREBP1* expression after LPS in this study, the role of *SREBF1* as an intermediate molecular regulator of downstream genes involved in the lipogenic process in the liver (*ACACA* and *MLYCD*) is supported (Zhou et al., 2012).

In addition to the ATP produced via glycolysis, about 90 percent of cellular ATP in produced by mitochondria (Sunny et al., 2017). Mammalian cytochrome c oxidase (COX) is the terminal complex (complex IV) of the electron transfer chain located in the inner mitochondrial membrane (Renner et al., 2003). It catalyzes the transfer of electrons from ferrocytochrome c to molecular oxygen, converting the latter to water and has also been suggested as a major regulation site for oxidative phosphorylation (Kadenbach et al., 2000). The analysis of cell lines with suppressed COX IV expression showed loss of assembly of cytochrome c oxidase complex and decrease in cytochrome c oxidase-dependent respiration and total respiration. Besides, dysfunctional cytochrome c oxidase in the cell leads to a reduction in ATP levels. Suppression of *COX IV* expression also sensitizes the cells to apoptosis. These observations provide evidence of the essential role of the *COX IV* subunit for a functional cytochrome c oxidase complex and also demonstrate control of cytochrome c oxidase over oxidative phosphorylation (Li et al., 2006). Downregulation of hepatic *COX IV* in supplemented animals in this study could indicate that the function of the mitochondrial respiratory chain was restricted in the CAR cows after LPS. This observation is in parallel with the noted positive correlation in the mRNA abundance of this gene with the reduced abundance of some of the other genes from the mitochondrial FA oxidation pathway (*ACADVL*, *ACADS,* and *CPT2*). These results were similar to another study that showed damage in mitochondrial respiratory chain function in hepatocytes of cows with mild and moderate fatty liver displaying high levels of FA (Shi et al., 2018). Furthermore, the *COX IV* mRNA abundance in the CON group was not affected by inflammation possibly indicating a shift to glycolysis for ATP synthesis in the CAR cows compared with the control group.

In dairy cows, plasma FA mainly comprises saturated FA (SFA), including palmitic acid (C16:0), stearic acid (C18:0), and, as monounsaturated FA (MUFA) also oleic acid (C18:1n9c) (Leroy et al., 2005; Tyburczy et al., 2008). For generating energy from LCFA, they need to be transported from the cytoplasm into the mitochondrial matrix across the mitochondrial membranes through a carnitine-dependent transport shuttle. This transport system is regulated by carnitine acyltransferases [i.e., carnitine palmitoyltransferase 1 (*CPT1*; present in the mitochondrial outer membrane) and 2 (*CPT2*; located on the matrix side of the inner membrane); Flanagan et al., 2010; Schooneman et al., 2014]. Inside the mitochondria, carnitine and long-chain acyl-CoA are regenerated by *CPT2*, which can then be further oxidized via the tricarboxylic acid (TCA) cycle and respiratory chain to provide ATP (Schooneman et al., 2013). Failure in these enzymes or impaired functions, or deficiency of TCA cycle intermediates, may lead to incomplete mitochondrial FA oxidation. Previously *CPT1* was found upregulated in early lactation suggesting an increased transport of FA from the cytosol into mitochondria in early lactation (Schäff et al., 2013). The activity of CPT1 and subsequent FA β-oxidation rates were shown to be increased during negative energy balance, probably because of decreased concentrations of, and reduced sensitivity to, malonyl-CoA, a potent allosteric CPT1 inhibitor (Brindle et al., 1985; Jesse et al., 1986). In the current study, the expression of *CPT1* was increased after LPS in both the CAR and the CON group. Similarly, *CPT1* was increased in Holstein cows after 12 h of the high level of grain in their diet applied to induce a certain degree of subacute ruminal acidosis (SARA, Xu et al., 2017) and after SARA exposure on 60% concentrate (Xu et al., 2015). The elevated abundance of *CPT1* is thought to be an adaptation in the liver after increased energy demand associated with LPS-mediated inflammatory acute phase response. In this study, the mRNA abundance of *CPT2* remained unchanged after LPS which might indicate a physiological increase in the capacity of long-chain fatty acyl-CoA entry into hepatic mitochondria after inflammation. We observed that there was also a negative effect in the CAR group on the mRNA abundance of *CPT1* and *CPT2* after LPS which might be due to the limited hepatic ability to oxidize overloaded FA in this group. In one study in dairy cows, the mRNA abundance of hepatic candidate genes related to β-oxidation was reported to be proportional to the FA concentrations in blood (Graber et al., 2010). The high levels of FA might be lipotoxic and may impair the function of mitochondria and then inhibit the β-oxidation (Song et al., 2013; Finucane et al., 2015; Lei et al., 2016). Data obtained in mice demonstrated that a high concentration of long-chain acyl-CoA inhibited the activity of *CPT1* and *CPT2* (Ciapaite et al., 2011; Flamment et al., 2012). Similarly, *CPT1* activity in dairy cows with severe hepatic lipidosis was lower than that in dairy cows without hepatic

lipidosis (Mizutani et al., 1999). Accordingly, the decreased expression of *CPT1* and *CPT2* in the CAR cows after LPS in this study might be due to the inhibition effect of the high concentration of FA and long-chain acyl-CoA in this group (in this study NEFA concentrations in CAR was lower than NEFA in CON after LPS but these levels were still higher than the levels of NEFA before LPS administration).

FA oxidation in the liver occurs mainly through β-oxidation, where FA in mitochondria is either completely oxidized to acetyl-CoA or partially oxidized to ketones (Wajner and Amaral, 2016). Inside the mitochondrion, carbon chain-length specific enzymes, known as acyl-CoA dehydrogenases, catalyze the next step of β-oxidation. Specifically, members of this family are involved in β-oxidation of FA: ACADS acts on acyl-CoA with carbon chain lengths of 4 to 6 (Ikeda et al., 1985); ACADM acts on acyl-CoA with carbon chain lengths of 4 to 16, with preferred substrates that have carbon chain lengths of 6 to 12 (Zeng and Li, 2005); LCAD acts on acyl-CoA with carbon chain lengths of 6 to 16, with preferred substrates that have carbon chain lengths of 8 to 14 (Ikeda et al., 1985; Swank et al., 2013), ACADVL, has optimal chain length specificity for fatty acyl-CoAs having 16 and more carbons in length (Amaral et al., 2009) and HADHA which catalyzes the last three steps of mitochondrial β-oxidation of LCFA (Lane et al., 2001). Previous studies indicate that ACADVL catalyzes the major part of mitochondrial palmitoyl-CoA dehydrogenation in the liver, heart, skeletal muscle, and skin fibroblasts and it is a rate-limiting enzyme in the LCFA β-oxidation system (Aoyama et al., 1995; Aoyama et al., 1994; Izai et al., 1992). In the present study, major genes involved in FA β-oxidation (*ACAD10, ACADM, ACADVL, ACADS*, and *HADHA*) were similar in mRNA abundance between the CAR and CON cows. The mRNA abundance of *ACAD10*, *ACADM*, *ACADVL,* and *ACADS* was not affected by LPS except for the downregulation of *ACADS* and upregulation of *HADHA* mRNA in the CAR after LPS administration. According to these observations, we suggest that neither the L-carnitine supplementation nor LPS challenge influenced the flow of FA into the hepatic β-oxidation.

PCCA and *PCCB* are the α and β subunits of propionyl-CoA carboxylase that encode the biotin-binding region of this enzyme which is involved in the mitochondrial metabolism of propionate (Dieho et al., 2016). PCC catalyzes the conversion of propionyl CoA to methylmalonyl CoA and, as such, is involved in the use of propionate as the major substrate for gluconeogenesis in ruminants (Graber et al., 2010; Skibiel et al., 2018; Tanaka and Armitage, 1975). The *MUT* gene encodes the enzyme methylmalonyl-CoA mutase (its cofactor is vitamin B12), which is essential for metabolic reactions and energy metabolism in ruminant hepatocytes

because it catalyzes the conversion of methylmalonyl CoA to succinyl CoA, which can enter the tricarboxylic acid cycle or be used in the gluconeogenesis pathway (Laguna et al., 2017). Downregulation of *PCCB* after LPS in both the CAR and CON in the present study could, therefore, indicate insufficient production of glucose, which led to low blood glucose concentrations, likely because of a decreased supply of propionate during the inflammation period as a result of decreased DMI observed after LPS which is similar to findings from Greenfield et al. (2000) and Graber et al. (2010) in dairy cows around parturition. Zarrin et al. (2014) suggested BHB as an alternative energy source at inflammation in dairy cows during lipopolysaccharide-induced mastitis. However, our data are difficult to interpret because post LPS hepatic *PCCA* and *MUT* mRNA abundance was increased in the CAR treatment which is an indication for the liver metabolic adaptation in response to the increased glucose demand after LPS. This is paralleled by the negative correlation observed in this study between the abundance of *MUT* and *SREBF1* mRNA, the latter involved in lipogenesis. The abundance of *PCCA* mRNA was positively correlated with two mRNA coding for two proteins in peroxisomes, ECH1 and SLC27A2, pointing towards increased peroxisomal β-oxidation of FA.

5.9 Peroxisomal fatty acid oxidation pathway

The hydratase superfamily contains a diverse set of enzymes including *ECHDC2* and *3* which are associated with long-chain, very-long-chain, and branched-chain FA oxidation in both mitochondria and peroxisome (Wheeler et al., 2019). The other member of this family is Enoyl-CoA hydratase 1 (*ECHS1*). The second step in mitochondrial β-oxidation of medium- and short-chained FA and oxidation of BCAAs is catalyzed by ECHS1 which is localized in the mitochondrial matrix (Shi et al., 2019; Zhang et al., 2017). The last member of the hydratase superfamily targeted in this study was Enoyl-CoA Hydratase 1 (ECH1). This enzyme functions in the auxiliary step of the LCFA β-oxidation pathway localized in the peroxisomes (Hsu et al., 2001). In a study, it was shown that hepatic β-oxidation in the peroxisomes was not affected by feeding supplemental fat or nicotinic acid during weeks 4 to42 of lactation dairy cows (Grum et al., 2002). Similarly, we observed that none of the mRNA related to the hydratase superfamily was differentially regulated in the CAR group compared with the control group. The abundance of *ECHS1*, *ECHDC2,* and 3 mRNA was downregulated after LPS administration which is in support of the reduced abundance of other mRNA associated with mitochondrial β-oxidation of FA in this study. The positive correlation of the mRNA abundance of these 3 genes and *PCCB* from the mitochondrial FA β-oxidation pathway with each other observed in the current study further supports this notion. The abundance of *ECH1* mRNA was

increased after LPS in both the CAR and CON group, a finding that was in parallel to other results from this study, confirming the elevated peroxisomal oxidation of FA rather than mitochondrial β-oxidation in response to the inflammation which was verified by positive correlation observed between mRNA levels of this gene and of *SLC27A2*, which is involved in the uptake of long- and branched-chain FA into the peroxisome.

ACOX1 also named straight-chain acyl-CoA oxidase, encodes the first enzyme that begins the process of breakdown of the straight-chain substrates that are oxidized in peroxisomes including long and very-long-chain FA, dicarboxylic acids and poly-unsaturated FA (Morrison et al., 2018). *ACOX2* and *ACOX3* are structurally very similar and both are involved in the peroxisomal degradation of the branched-chain FA (Ferdinandusse et al., 2018). *ACOX2* is also known as branched-chain acyl-CoA oxidase (Veldhoven, 2010) and had been considered as an indicator of β-oxidation of branched-chain FA in peroxisomes in dairy cows (Khazanehei et al., 2015). In previous studies, the greater hepatic expression of *ACOX1* in dairy cows was related to an increase in hepatic LCFA oxidation and ketogenesis in response to the higher influx of FA (Bionaz et al., 2013; Akbar et al., 2015) and after LPS challenge (Graugnard et al., 2013). In this study, LPS increased *ACOX2* mRNA in both the CAR and CON group whereas the abundance of *ACOX1* in the CON was decreased. Our data indicate a greater capacity for peroxisomal β-oxidation of branched-chain FA and decreased degradation of very-long-chain FA after LPS that is confirmed by the observed negative correlation between the abundance of this gene with the abundance of genes *SLC27A4* and *ACADVL*, which are involved in uptake and β-oxidation of LCFA, respectively. Downregulation of *ACOX3* could be a sign of high efficiency of FA metabolism by *ACOX2* since it was reported that *ACOX3* is responsible for the oxidation of BCFA in the case of *ACOX2* deficiency (Ferdinandusse et al., 2018). Similarly, in this study, this mRNA was in positive correlation with *ECHDC3* and *ECHS1* from peroxisomal, and *PCCB* from mitochondrial FA β-oxidation pathways.

Aldehyde dehydrogenases (ALDHs) are a family of enzymes involved in the maintenance of cellular homeostasis (Muzio et al., 2012; Wang et al., 2009). This family is known to modulate several cell functions, including proliferation, differentiation, and survival, as well as the cellular response to oxidative stress. ALDH proteins can detoxify such cytotoxic and cytostatic aldehydes generated via the normal metabolism of several lipids, as well as the oxidation of unsaturated FA due to oxidative stress, into less reactive forms like carboxylic acids (Alnouti and Klaassen, 2007; Muzio et al., 2012; Muzio et al., 2006; Nita and

Grzybowski, 2016; Pappa et al., 2003). The ALDH3 family contains enzymes that have a specific role in FA and peroxidic aldehyde metabolism (Holmes and Hempel, 2011). The ALDH3A1 protein inhibits mitochondrial respiration (Canuto et al., 1985) and it has a fundamental role in the metabolism of toxic medium-chain saturated and unsaturated aldehydes derived from lipid peroxidation is a consequence of oxidative stress exerted on polyunsaturated FA and leads to the formation of reactive by-products such as lipid hydroperoxides and aldehydes including 4-hydroxy-2-nonenal (HNE) (Marchitti et al., 2011, Esterbauer et al., 1991). HNE is generated by the peroxidation of cellular lipids. In humans and rats, HNE is the most reactive and cytotoxic of the aldehydic by-products of lipid peroxidation (Benedetti et al., 1980). Concerning ALDHs, most studies in the literature have been limited to a few tissues and were not quantitative. These previous studies were primarily performed in rat and human tissues. In the present study, downregulation of *ALDH3A1* mRNA abundance in the CAR and CON could lead us to hypothesize that the metabolism of FA and aldehydes is decreased upon LPS which is in parallel to other results from this study showing decreased mitochondrial respiration after LPS, indicating a shift to glycolysis for ATP synthesis (the level of glucose in blood remained unchanged after LPS in this study) in response to an inflammatory challenge in hepatocytes which could be confirmed by the negative correlation between the mRNA abundance of genes from carnitine metabolism and LCFA uptake (*SLC22A5*, *CRAT,* and *SLC27A3*) with *ALDH3A1* that could be another indicator of the availability of FA or, as mentioned before, the carbohydrates, for energy generation.

6 CONCLUSIONS

This study provides a characterization of the mRNA abundance of key genes related to mitochondrial metabolism of FA in hepatocytes of dairy cows. Besides, some of these genes were also assessed at the level of the protein. Integrated microfluidic circuit chips were used for the quantification of the mRNA. Increased transport of LCFA into hepatocytes and then their direction toward oxidation in peroxisomes rather than mitochondria along with the increased abundance of mRNA coding for proteins specifically in peroxisomes in both the control and the treatment group receiving L-carnitine supplementation emphasized the rise in peroxisomal β-oxidation of FA in hepatocytes of dairy cows during systemic inflammation provoked by injecting LPS. We also observed that hepatic mitochondrial ketogenesis was not stimulated by LPS. The abundance of mRNA related to lipogenesis decreased and possibly intracellular synthesis and secretion of VLDL were stimulated during the response to LPS. At the same time, LPS could decrease the abundance of ACACA (involved in FA synthesis) at the protein level. We observed that L-carnitine supplementation at the used dosage did not induce a significant effect on the abundance of selected genes and proteins involved in hepatic FA metabolism in dairy cows except for *SLC27A2* and *CPT1* (involved in the uptake of FA into cytoplasm and mitochondria, respectively) at the mRNA level. Finally, according to these observations, we suggest that the L-carnitine supplementation did not influence the flow of FA into the hepatic β-oxidation. Moreover, LPS infusion has shifted the FA metabolism in hepatocytes towards peroxisomal rather than mitochondrial β-oxidation.

7 SUMMARY

An inflammatory challenge of the health status of an animal coincides with changes in nutrient metabolism which is related to the negative energy balance (NEB) that results from the reduced dry matter intake (DMI). Besides, inflammation requires more energy due to the increased activity of the immune system. Increased lipid mobilization due to the NEB may in turn augment the inflammatory response. L-Carnitine is a cofactor of several enzymes (carnitine translocase, acylcarnitine transferases I, and II) necessary for the transformation of free LCFA (long-chain fatty acid) to acylcarnitines, and their transport into the mitochondrial matrix. β-Oxidation of these compounds precedes their entry into the Krebs cycle, where energy production occurs. In the absence of L-carnitine, the accumulation of fatty acids (FA) in the cytoplasm produces a toxic effect on the cell, and an energy deficit arises from the unavailability of FA within the mitochondria. This dissertation aimed at characterizing the regulation of several genes that are involved in hepatic FA metabolism at both the mRNA and the protein level during lipopolysaccharide (LPS)-induced inflammation at mid-lactation. Besides, dietary supplementation with L-carnitine vs. control was tested. L-carnitine supplementation was started from day 42 ante partum (*ap*) until day 126 of lactation. At day 111 postpartum (*pp*), a jugular infusion of LPS was given to all cows. The tissue in focus was the liver. Initially, suitable reference genes were identified as a methodological prerequisite for the study. Using tissue samples obtained from 43 pluriparous cows for mRNA abundance and 22 cows for protein abundance, the hepatic abundance of 41 different target genes, 8 reference genes and 3 target proteins was characterized in liver samples biopsied at day 42 *ap* and days 100, 112 and 126 of lactation for mRNA and day 100 and 112 of lactation (equal to day -11 and 1 relative to LPS challenge) for protein abundance. Microfluidics Integrated Fluidic Circuit chips (IFC, 96.96 dynamic arrays) were used to quantify the mRNA abundance of 5 genes from the AMPK/mTOR pathway, 4 genes involved in carnitine metabolism, 4 genes involved in FA uptake, 4 genes involved in ketogenesis, 2 genes of lipoprotein synthesis, 14 and 8 genes, respectively, involved in mitochondrial and peroxisomal β-oxidation. Capillary Western blotting was used to measure the abundance of 3 target proteins, one from AMPK/mTOR, one from mitochondrial β-oxidation, and the other one from FA uptake pathways. The groups treated with L-carnitine or control differed in mRNA abundance of 2 genes, *SLC27A2* from the FA uptake pathway, and *CPT1* from the mitochondrial FA oxidation pathway but not at the protein level. Time effect which was considered as the effect of LPS on the abundance of genes and proteins was observed significant for 32 mRNA, including *PRKAG1, mTOR, RPSKKB1, PPARGC1A* and *SREBF1* from AMPK/mTOR pathway, *SLC22A5, TMLHE* and *CRAT* from

carnitine metabolism pathway, *SLC27A2* and *SLC27A4* from FA uptake pathway, *ACAT1* and *FGF21* from ketogenesis pathway, *APOB* and *MTTP* from lipoprotein synthesis pathway, *FABP1, ACACA, COX4I1, HADHA, CPT1, PCCA, PCCB, MUT, ACADS* and *MLYCD* from mitochondrial β-oxidation and *ECH1, ECHDC2, ECHS1, ECHDC3, ACOX1, ACOX2, ACOX3* and *ALDH3A1* from the peroxisomal β-oxidation pathway and protein abundance of ACACA from the mitochondrial β-oxidation pathway. The results of this study provide a characterization of the abundance of key genes and selected proteins that are related to mitochondrial metabolism of FA in hepatocytes. We observed that L-carnitine supplementation at the used dosage did not induce a significant effect on mRNA abundance related to hepatic FA metabolism except for *SLC27A2* and *CPT1* involved in hepatic and mitochondrial FA uptake, respectively, at mRNA level. We also observed that the protein abundance of ACACA involved in the FA synthesis from the mitochondrial β-oxidation pathway was reduced after LPS. On the other hand, these results indicate that jugular LPS infusion has shifted the FA metabolism in hepatocytes towards peroxisomal β-oxidation rather than mitochondrial.

8 REFERENCES

Adeva-Andany, M.M., I. Calvo-Castro, C. Fernández-Fernández, C. Donapetry-García, and A.M. Pedre-Piñeiro. 2017. Significance of L-carnitine for human health. IUBMB Life 69:578–594.

Adewuyi, A.A., E. Gruys, and F.J.C.M. van Eerdenburg. 2005. Non esterified fatty acids (NEFA) in dairy cattle. A review. Vet. Q. 27:117–126. doi:10.1080/01652176.2005.9695192.

Ahmadian, M., R.E. Duncan, K. Jaworski, E. Sarkadi-Nagy, and H.S. Sul. 2007. Triacylglycerol metabolism in adipose tissue. Future Lipidol. 2:229–237. doi:10.2217/17460875.2.2.229.

Aitken, S.L., C.M. Corl, and L.M. Sordillo. 2011. Immunopathology of Mastitis: Insights into Disease Recognition and Resolution. J. Mammary Gland Biol. Neoplasia 16:291–304. doi:10.1007/s10911-011-9230-4.

Akbar, H., M. Bionaz, D.B. Carlson, S.L. Rodriguez-Zas, R.E. Everts, H.A. Lewin, J.K. Drackley, and J.J. Loor. 2013. Feed restriction, but not L-carnitine infusion, alters the liver transcriptome by inhibiting sterol synthesis and mitochondrial oxidative phosphorylation and increasing gluconeogenesis in mid-lactation dairy cows. J. Dairy Sci. 96:2201–2213.

Akbar, H., T.M. Grala, M. Vailati Riboni, F.C. Cardoso, G. Verkerk, J. McGowan, K. Macdonald, J. Webster, K. Schutz, S. Meier, L. Matthews, J.R. Roche, and J.J. Loor. 2015. Body condition score at calving affects systemic and hepatic transcriptome indicators of inflammation and nutrient metabolism in grazing dairy cows. J. Dairy Sci. 98:1019–1032. doi:https://doi.org/10.3168/jds.2014-8584.

Allen, M.S., B.J. Bradford, and M. Oba. 2009. Board Invited Review: The hepatic oxidation theory of the control of feed intake and its application to ruminants. J. Anim. Sci. 87:3317–3334. doi:10.2527/jas.2009-1779.

Alnouti, Y., and C.D. Klaassen. 2007. Tissue Distribution, Ontogeny, and Regulation of Aldehyde Dehydrogenase (Aldh) Enzymes mRNA by Prototypical Microsomal Enzyme Inducers in Mice. Toxicol. Sci. 101:51–64. doi:10.1093/toxsci/kfm280.

Do Amaral, B.C., E.E. Connor, S. Tao, J. Hayen, J. Bubolz, and G.E. Dahl. 2009. Heat-stress abatement during the dry period: Does cooling improve transition into lactation?. J. Dairy Sci. 92:5988–5999.

Andreux, P.A., R.H. Houtkooper, and J. Auwerx. 2013. Pharmacological approaches to restore mitochondrial function. Nat. Rev. Drug Discov. 12:465–483. doi:10.1038/nrd4023.

Andreux, P.A., E.G. Williams, H. Koutnikova, R.H. Houtkooper, M.-F. Champy, H. Henry, K.

Schoonjans, R.W. Williams, and J. Auwerx. 2012. Systems genetics of metabolism: the use of the BXD murine reference panel for multiscalar integration of traits. Cell 150:1287–1299. doi:10.1016/j.cell.2012.08.012.

Aoyama, T., M. Souri, S. Ushikubo, T. Kamijo, S. Yamaguchi, R.I. Kelley, W.J. Rhead, K. Uetake, K. Tanaka, and T. Hashimoto. 1995. Purification of human very-long-chain acyl-coenzyme A dehydrogenase and characterization of its deficiency in seven patients. J. Clin. Invest. 95:2465–2473. doi:10.1172/JCI117947.

Aoyama, T., I. Ueno, T. Kamijo, and T. Hashimoto. 1994. Rat very-long-chain acyl-CoA dehydrogenase, a novel mitochondrial acyl-CoA dehydrogenase gene product, is a rate-limiting enzyme in long-chain fatty acid beta-oxidation system. cDNA and deduced amino acid sequence and distinct specificities of the cDNA-ex. J. Biol. Chem. 269:19088–19094.

Avramoglu, R.K., and K. Adeli. 2004. Hepatic regulation of apolipoprotein B. Rev. Endocr. Metab. Disord. 5:293–301.

Babior, B.M. 1999. NADPH oxidase: an update. Blood-new york- 93:1464–1476.

Badman, M.K., P. Pissios, A.R. Kennedy, G. Koukos, J.S. Flier, and E. Maratos-Flier. 2007. Hepatic Fibroblast Growth Factor 21 Is Regulated by PPARα and Is a Key Mediator of Hepatic Lipid Metabolism in Ketotic States. Cell Metab. 5:426–437. doi:10.1016/j.cmet.2007.05.002.

Bartlett, K., and S. Eaton. 2004. Mitochondrial β-oxidation. Eur. J. Biochem. 271:462–469.

Bauchart, D. 1993. Lipid absorption and transport in ruminants. J. Dairy Sci. 76:3864–3881.

Bauman, D.E., and W.B. Currie. 1980. Partitioning of nutrients during pregnancy and lactation: a review of mechanisms involving homeostasis and homeorhesis. J. Dairy Sci. 63:1514–1529.

Bauman, D.E., C.J. Peel, W.D. Steinhour, P.J. Reynolds, H.F. Tyrrell, A.C.G. Brown, and G.L. Haaland. 1988. Effect of bovine somatotropin on metabolism of lactating dairy cows: influence on rates of irreversible loss and oxidation of glucose and nonesterified fatty acids. J. Nutr. 118:1031–1040.

Baur, J.A., K.J. Pearson, N.L. Price, H.A. Jamieson, C. Lerin, A. Kalra, V. V Prabhu, J.S. Allard, G. Lopez-Lluch, K. Lewis, P.J. Pistell, S. Poosala, K.G. Becker, O. Boss, D. Gwinn, M. Wang, S. Ramaswamy, K.W. Fishbein, R.G. Spencer, E.G. Lakatta, D. Le Couteur, R.J. Shaw, P. Navas, P. Puigserver, D.K. Ingram, R. de Cabo, and D.A. Sinclair. 2006. Resveratrol improves health and survival of mice on a high-calorie diet. Nature 444:337–342. doi:10.1038/nature05354.

Bell, A.W. 1995. Regulation of organic nutrient metabolism during transition from late pregnancy to

early lactation. J. Anim. Sci. 73:2804–2819.

Bell, A.W., and D.E. Bauman. 1997. Adaptations of glucose metabolism during pregnancy and lactation. J. Mammary Gland Biol. Neoplasia 2:265–278. doi:10.1023/A:1026336505343.

Bell, A.W., W.S. Burhans, and T.R. Overton. 2000. Protein nutrition in late pregnancy, maternal protein reserves and lactation performance in dairy cows. Proc. Nutr. Soc. 59:119–126.

Benedetti, A., M. Comporti, and H. Esterbauer. 1980. Identification of 4-hydroxynonenal as a cytotoxic product originating from the peroxidation of liver microsomal lipids. Biochim. Biophys. Acta - Lipids Lipid Metab. 620:281–296. doi:https://doi.org/10.1016/0005-2760(80)90209-X.

Bernabucci, U., B. Ronchi, L. Basiricò, D. Pirazzi, F. Rueca, N. Lacetera, and A. Nardone. 2004. Abundance of mRNA of apolipoprotein B100, Apolipoprotein E, and Microsomal Triglyceride Transfer Protein in Liver from Periparturient Dairy Cows*. J. Dairy Sci. 87:2881–2888. doi:https://doi.org/10.3168/jds.S0022-0302(04)73418-9.

Bernabucci, U., B. Ronchi, N. Lacetera, and A. Nardone. 2002. Markers of oxidative status in plasma and erythrocytes of transition dairy cows during hot season. J. Dairy Sci. 85:2173–2179. doi:https://doi.org/10.3168/jds.S0022-0302(02)74296-3.

Bernabucci, U., B. Ronchi, N. Lacetera, and A. Nardone. 2005. Influence of body condition score on relationships between metabolic status and oxidative stress in periparturient dairy cows. J. Dairy Sci. 88:2017–2026. doi:https://doi.org/10.3168/jds.S0022-0302(05)72878-2.

Bertoni, G., E. Trevisi, X. Han, and M. Bionaz. 2008. Effects of inflammatory conditions on liver activity in puerperium period and consequences for performance in dairy cows. J. Dairy Sci. 91:3300–3310.

den Besten, G., K. van Eunen, A.K. Groen, K. Venema, D.-J. Reijngoud, and B.M. Bakker. 2013. The role of short-chain fatty acids in the interplay between diet, gut microbiota, and host energy metabolism. J. Lipid Res. 54:2325–2340. doi:10.1194/jlr.R036012.

Bilal, M.S., J.A. Abaker, Z. ul Aabdin, T. Xu, H. Dai, K. Zhang, X. Liu, and X. Shen. 2016. Lipopolysaccharide derived from the digestive tract triggers an inflammatory response in the uterus of mid-lactating dairy cows during SARA. BMC Vet. Res. 12:284. doi:10.1186/s12917-016-0907-1.

Bionaz, M., S. Chen, M.J. Khan, and J.J. Loor. 2013. Functional role of PPARs in ruminants: potential targets for fine-tuning metabolism during growth and lactation. PPAR Res. 2013:684159. doi:10.1155/2013/684159.

Bionaz, M., and J.J. Loor. 2008. ACSL1, AGPAT6, FABP3, LPIN1, and SLC27A6 are the most abundant isoforms in bovine mammary tissue and their expression is affected by stage of lactation. J. Nutr. 138:1019–1024. doi:10.1093/jn/138.6.1019.

Blanco, A., and G. Blanco. 2017. Chapter 15 - Lipid Metabolism. A. Blanco and G.B.T.-M.B. Blanco, ed. Academic Press.

Bolisetty, S., and E.A. Jaimes. 2013. Mitochondria and reactive oxygen species: physiology and pathophysiology. Int. J. Mol. Sci. 14:6306–6344. doi:10.3390/ijms14036306.

Bonen, A., A. Chabowski, J.J. and Luiken, and J.F. Glatz. 2007. Is membrane transport of FFA mediated by lipid, protein, or both? Mechanisms and regulation of protein-mediated cellular fatty acid uptake: molecular, biochemical, and physiological evidence. Physiology (Bethesda). 22:15.

Boström, P., J. Wu, M.P. Jedrychowski, A. Korde, L. Ye, J.C. Lo, K.A. Rasbach, E.A. Boström, J.H. Choi, J.Z. Long, S. Kajimura, M.C. Zingaretti, B.F. Vind, H. Tu, S. Cinti, K. Højlund, S.P. Gygi, and B.M. Spiegelman. 2012. A PGC1-α-dependent myokine that drives brown-fat-like development of white fat and thermogenesis. Nature 481:463–468. doi:10.1038/nature10777.

Bouvier-Muller, J., C. Allain, G. Tabouret, F. Enjalbert, D. Portes, C. Noirot, R. Rupp, and G. Foucras. 2017. Whole blood transcriptome analysis reveals potential competition in metabolic pathways between negative energy balance and response to inflammatory challenge. Sci. Rep. 7:2379. doi:10.1038/s41598-017-02391-y.

Bradford, B.J., K. Yuan, J.K. Farney, L.K. Mamedova, and A.J. Carpenter. 2015a. Invited review: Inflammation during the transition to lactation: New adventures with an old flame. J. Dairy Sci. 98:6631–6650. doi:10.3168/JDS.2015-9683.

Bremer, J. 1983. Carnitine--metabolism and functions. Physiol. Rev. 63:1420–1480. doi:10.1152/physrev.1983.63.4.1420.

Brindle, N.P., V.A. Zammit, and C.I. Pogson. 1985. Regulation of carnitine palmitoyltransferase activity by malonyl-CoA in mitochondria from sheep liver, a tissue with a low capacity for fatty acid synthesis. Biochem. J. 232:177–182.

Brown, M.S., and J.L. Goldstein. 2008. Selective versus total insulin resistance: a pathogenic paradox. Cell Metab. 7:95–96.

Bühler, S., J. Frahm, R. Tienken, S. Kersten, U. Meyer, K. Huber, and S. Dänicke. 2018. Effects of energy supply and nicotinic acid supplementation on serum anti-oxidative capacity and on expression of oxidative stress-related genes in blood leucocytes of periparturient primi- and

pluriparous dairy cows. J. Anim. Physiol. Anim. Nutr. (Berl). 102:e87–e98. doi:10.1111/jpn.12705.

Burke, C.R., S. Meier, S. McDougall, C. Compton, M. Mitchell, and J.R. Roche. 2010. Relationships between endometritis and metabolic state during the transition period in pasture-grazed dairy cows. J. Dairy Sci. 93:5363–5373. doi:10.3168/jds.2010-3356.

Burton, J.L., M.E. Kehrli Jr., S. Kapil, and R.L. Horst. 1995. Regulation of L-selectin and CD18 on bovine neutrophils by glucocorticoids: effects of cortisol and dexamethasone. J. Leukoc. Biol. 57:317–325. doi:10.1002/jlb.57.2.317.

Bustin, S.A. 2002. Quantification of mRNA using real-time reverse transcription PCR (RT-PCR): Trends and problems. J. Mol. Endocrinol. 29:23–39. doi:10.1677/jme.0.0290023.

Bustin, S.A., V. Benes, J.A. Garson, J. Hellemans, J. Huggett, M. Kubista, R. Mueller, T. Nolan, M.W. Pfaffl, and G.L. Shipley. 2009. The MIQE Guidelines: minimum information for publication of quantitative real-time pcr experiments.

Calder, P.C., G. Dimitriadis, and P. Newsholme. 2007. Glucose metabolism in lymphoid and inflammatory cells and tissues. Curr. Opin. Clin. Nutr. Metab. Care 10:531–540. doi:10.1097/MCO.0b013e3281e72ad4.

Calixto, J.B., M.F. Otuki, and A.R.S. Santos. 2003. Anti-inflammatory compounds of plant origin. Part I. Action on arachidonic acid pathway, nitric oxide and nuclear factor κ B (NF-κB). Planta Med. 69:973–983.

Cant, J.P., J.J.M. Kim, S.R.L. Cieslar, and J. Doelman. 2018. Symposium review: Amino acid uptake by the mammary glands: Where does the control lie? J. Dairy Sci. 101:5655–5666. doi:https://doi.org/10.3168/jds.2017-13844.

Canto, C., and J. Auwerx. 2010. AMP-activated protein kinase and its downstream transcriptional pathways. Cell. Mol. Life Sci. 67:3407–3423. doi:10.1007/s00018-010-0454-z.

Cantó, C., and J. Auwerx. 2009. PGC-1alpha, SIRT1 and AMPK, an energy sensing network that controls energy expenditure. Curr. Opin. Lipidol. 20:98–105. doi:10.1097/MOL.0b013e328328d0a4.

Cantó, C., Z. Gerhart-Hines, J.N. Feige, M. Lagouge, L. Noriega, J.C. Milne, P.J. Elliott, P. Puigserver, and J. Auwerx. 2009. AMPK regulates energy expenditure by modulating NAD+ metabolism and SIRT1 activity. Nature 458:1056–1060. doi:10.1038/nature07813.

Canto, C., R.H. Houtkooper, E. Pirinen, D.Y. Youn, M.H. Oosterveer, Y. Cen, P.J. Fernandez-Marcos, H. Yamamoto, P.A. Andreux, P. Cettour-Rose, K. Gademann, C. Rinsch, K. Schoonjans, A.A. Sauve, and J. Auwerx. 2012. The NAD(+) precursor nicotinamide riboside enhances oxidative metabolism and protects against high-fat diet-induced obesity. Cell Metab. 15:838–847. doi:10.1016/j.cmet.2012.04.022.

Canto, C., L.Q. Jiang, A.S. Deshmukh, C. Mataki, A. Coste, M. Lagouge, J.R. Zierath, and J. Auwerx. 2010. Interdependence of AMPK and SIRT1 for metabolic adaptation to fasting and exercise in skeletal muscle. Cell Metab. 11:213–219. doi:10.1016/j.cmet.2010.02.006.

Canuto, R.A., M.E. Biocca, G. Muzio, R. Garcea, and M.U. Dianzani. 1985. The effect of various aldehydes on the respiration of rat liver and hepatoma AH-130 cells. Cell Biochem. Funct. 3:3–8. doi:10.1002/cbf.290030103.

Carlson, D.B., N.B. Litherland, H.M. Dann, J.C. Woodworth, and J.K. Drackley. 2006. Metabolic effects of abomasal L-carnitine infusion and feed restriction in lactating Holstein cows. J. Dairy Sci. 89:4819–4834.

Carlson, D.B., J.W. McFadden, A. D'Angelo, J.C. Woodworth, and J.K. Drackley. 2007a. Dietary L-carnitine affects periparturient nutrient metabolism and lactation in multiparous cows. J. Dairy Sci. 90:3422–3441. doi:https://doi.org/10.3168/jds.2006-811.

Carlson, D.B., J.C. Woodworth, and J.K. Drackley. 2007b. Effect of L-carnitine infusion and feed restriction on carnitine status in lactating Holstein cows. J. Dairy Sci. 90:2367–2376.

Carriquiry, M., W.J. Weber, S.C. Fahrenkrug, and B.A. Crooker. 2009. Hepatic gene expression in multiparous Holstein cows treated with bovine somatotropin and fed n-3 fatty acids in early lactation. J. Dairy Sci. 92:4889–4900. doi:https://doi.org/10.3168/jds.2008-1676.

Carter, A.L., and R. Frenkel. 1978. The relationship of choline and carnitine in the choline deficient rat. J. Nutr. 108:1748–1754. doi:10.1093/jn/108.11.1748.

Castillo, C., J. Hernandez, A. Bravo, M. Lopez-Alonso, V. Pereira, and J.L. Benedito. 2005. Oxidative status during late pregnancy and early lactation in dairy cows. Vet. J. 169:286–292.

Celi, P. 2011. Biomarkers of oxidative stress in ruminant medicine. Immunopharmacol. Immunotoxicol. 33:233–240.

Chajès, V., M. Cambot, K. Moreau, G.M. Lenoir, and V. Joulin. 2006. Acetyl-CoA carboxylase α is essential to breast cancer cell survival. Cancer Res. 66:5287 LP – 5294. doi:10.1158/0008-5472.CAN-05-1489.

Chen, L., H. Deng, H. Cui, J. Fang, Z. Zuo, J. Deng, Y. Li, X. Wang, and L. Zhao. 2017. Inflammatory responses and inflammation-associated diseases in organs. Oncotarget 9:7204–7218. doi:10.18632/oncotarget.23208.

Chung, H.J., H.S. Lee, J.S. Shin, S.H. Lee, B.M. Park, Y.S. Youn, and S.K. Lee. 2010. Modulation of acute and chronic inflammatory processes by a traditional medicine preparation GCSB-5 both in vitro and in vivo animal models. J. Ethnopharmacol. 130:450–459.

Ciapaite, J., N.M. van den Broek, H. te Brinke, K. Nicolay, J.A. Jeneson, S.M. Houten, and J.J. Prompers. 2011. Differential effects of short- and long-term high-fat diet feeding on hepatic fatty acid metabolism in rats. Biochim. Biophys. Acta - Mol. Cell Biol. Lipids 1811:441–451. doi:https://doi.org/10.1016/j.bbalip.2011.05.005.

Citri, A., Z.P. Pang, T.C. Südhof, M. Wernig, and R.C. Malenka. 2012. Comprehensive qPCR profiling of gene expression in single neuronal cells. Nat. Protoc. 7:118.

Colman, R.J., R.M. Anderson, S.C. Johnson, E.K. Kastman, K.J. Kosmatka, T.M. Beasley, D.B. Allison, C. Cruzen, H.A. Simmons, J.W. Kemnitz, and R. Weindruch. 2009. Caloric restriction delays disease onset and mortality in rhesus monkeys. Science 325:201–204. doi:10.1126/science.1173635.

Contreras, G.A., W. Raphael, S.A. Mattmiller, J. Gandy, and L.M. Sordillo. 2012. Nonesterified fatty acids modify inflammatory response and eicosanoid biosynthesis in bovine endothelial cells. J. Dairy Sci. 95:5011–5023.

Contreras, G.A., and L.M. Sordillo. 2011. Lipid mobilization and inflammatory responses during the transition period of dairy cows. Comp. Immunol. Microbiol. Infect. Dis. 34:281–289. doi:https://doi.org/10.1016/j.cimid.2011.01.004.

Counotte, G.H.M., R.A. Prins, R. Janssen, and M.J.A. DeBie. 1981. Role of Megasphaera elsdenii in the fermentation of DL-[2-13C] lactate in the rumen of dairy cattle. Appl. Environ. Microbiol. 42:649–655.

Crookenden, M.A., C.G. Walker, A. Heiser, A. Murray, V.S.R. Dukkipati, J.K. Kay, S. Meier, K.M. Moyes, M.D. Mitchell, J.J. Loor, and J.R. Roche. 2017a. Effects of precalving body condition and prepartum feeding level on gene expression in circulating neutrophils. J. Dairy Sci. 100:2310–2322. doi:https://doi.org/10.3168/jds.2016-12105.

Crookenden, M.A., C.G. Walker, B. Kuhn-Sherlock, A. Murray, V.S.R. Dukkipati, A. Heiser, and J.R. Roche. 2017b. Technical note: Evaluation of endogenous control gene expression in bovine

neutrophils by reverse-transcription quantitative PCR using microfluidics gene expression arrays. J. Dairy Sci. 100:6763–6771. doi:10.3168/jds.2016-12460.

Curtis, C.R., H.N. Erb, C.J. Sniffen, R.D. Smith, P.A. Powers, M.C. Smith, M.E. White, R.B. Hillman, and E.J. Pearson. 1983. Association of parturient hypocalcemia with eight periparturient disorders in Holstein cows. J. Am. Vet. Med. Assoc. 183:559–561.

Dänicke, S., U. Meyer, S. Kersten, and J. Frahm. 2018. Animal models to study the impact of nutrition on the immune system of the transition cow. Res. Vet. Sci. 116:15–27. doi:https://doi.org/10.1016/j.rvsc.2018.01.023.

Dänicke, S., U. Meyer, J. Winkler, K. Schulz, S. Ulrich, J. Frahm, S. Kersten, J. Rehage, G. Breves, and S. Häußler. 2014. Description of a bovine model for studying digestive and metabolic effects of a positive energy balance not biased by lactation or gravidity. Arch. Anim. Nutr. 68:460–477.

Davis, C.L., and R.E. Brown. 1970. Low-fat milk syndrome. Low-fat milk Syndr.

Dieho, K., J. Dijkstra, J.T. Schonewille, and A. Bannink. 2016. Changes in ruminal volatile fatty acid production and absorption rate during the dry period and early lactation as affected by rate of increase of concentrate allowance. J. Dairy Sci. 99:5370–5384. doi:https://doi.org/10.3168/jds.2015-10819.

Dirksen, G., H.-D. Gründer, and M. Stöber. 1990. Die klinische untersuchung des rindes. Parey.

Doege, H., and A. Stahl. 2006. Protein-mediated fatty acid uptake: novel insights from in vivo models. Physiology 21:259–268. doi:10.1152/physiol.00014.2006.

Domouzoglou, E.M., and E. Maratos-Flier. 2011. Fibroblast growth factor 21 is a metabolic regulator that plays a role in the adaptation to ketosis. Am. J. Clin. Nutr. 93:901S-905S. doi:10.3945/ajcn.110.001941.

Drackley, J.K. 1999a. Biology of dairy cows during the transition period: the final frontier?. J. Dairy Sci. 82:2259–2273. doi:https://doi.org/10.3168/jds.S0022-0302(99)75474-3.

Drackley, J.K., D.C. Beitz, and J.W. Young. 1991a. Regulation of in vitro metabolism of palmitate by carnitine and propionate in liver from dairy cows. J. Dairy Sci. 74:3014–3024. doi:https://doi.org/10.3168/jds.S0022-0302(91)78487-7.

Drackley, J.K., D.C. Beitz, and J.W. Young. 1991b. Regulation of in vitro palmitate oxidation in liver from dairy cows during early lactation. J. Dairy Sci. 74:1884–1892. doi:https://doi.org/10.3168/jds.S0022-0302(91)78354-9.

Drackley, J.K., T.R. Overton, and G.N. Douglas. 2001. Adaptations of glucose and long-chain fatty acid metabolism in liver of dairy cows during the periparturient period. J. Dairy Sci. 84:E100–E112.

Eaton, S., K.B. Bartlett, and M. Pourfarzam. 1996. Mammalian mitochondrial β-oxidation. Biochem. J. 320:345–357.

Elis, S., A. Desmarchais, S. Freret, V. Maillard, V. Labas, J. Cognié, E. Briant, C. Hivelin, J. Dupont, and S. Uzbekova. 2016. Effect of a long-chain n-3 polyunsaturated fatty acid enriched diet on adipose tissue lipid profiles and gene expression in Holstein dairy cows. J. Dairy Sci. 99:10109–10127. doi:10.3168/jds.2016-11052.

Emanuelson, U.L.F., P.A. Oltenacu, and Y.T. Gröhn. 1993. Nonlinear mixed model analyses of five production disorders of dairy cattle. J. Dairy Sci. 76:2765–2772.

Esterbauer, H., R.J. Schaur, and H. Zollner. 1991. Chemistry and biochemistry of 4-hydroxynonenal, malonaldehyde and related aldehydes. Free Radic. Biol. Med. 11:81–128.

Evangeliou, A., and D. Vlassopoulos. 2003. Carnitine metabolism and deficit-when supplementation is necessary?. Curr. Pharm. Biotechnol. 4:211–219.

Falcon, A., H. Doege, A. Fluitt, B. Tsang, N. Watson, M.A. Kay, and A. Stahl. 2010. FATP2 is a hepatic fatty acid transporter and peroxisomal very long-chain acyl-CoA synthetase. Am. J. Physiol. Metab. 299:E384–E393. doi:10.1152/ajpendo.00226.2010.

Ferdinandusse, S., S. Denis, C.W.T. van Roermund, M.A. Preece, J. Koster, M.S. Ebberink, H.R. Waterham, and R.J.A. Wanders. 2018. A novel case of ACOX2 deficiency leads to recognition of a third human peroxisomal acyl-CoA oxidase. Biochim. Biophys. Acta - Mol. Basis Dis. 1864:952–958. doi:https://doi.org/10.1016/j.bbadis.2017.12.032.

Fielding, B.A., and K.N. Frayn. 1998. Lipoprotein lipase and the disposition of dietary fatty acids. Br. J. Nutr. 80:495–502. doi:DOI: 10.1017/S0007114598001585.

Finkel, T. 2011. Signal transduction by reactive oxygen species. J. Cell Biol. 194:7–15. doi:10.1083/jcb.201102095.

Finucane, O.M., C.L. Lyons, A.M. Murphy, C.M. Reynolds, R. Klinger, N.P. Healy, A.A. Cooke, R.C. Coll, L. McAllan, K.N. Nilaweera, M.E. O'Reilly, A.C. Tierney, M.J. Morine, J.F. Alcala-Diaz, J. Lopez-Miranda, D.P. O'Connor, L.A. O'Neill, F.C. McGillicuddy, and H.M. Roche. 2015. Monounsaturated fatty acid–enriched high-fat diets impede adipose NLRP3 inflammasome–mediated IL-1β secretion and insulin resistance despite obesity. Diabetes 64:2116 LP – 2128. doi:10.2337/db14-1098.

Flamment, M., J. Rieusset, H. Vidal, G. Simard, Y. Malthièry, B. Fromenty, and P.-H. Ducluzeau. 2012. Regulation of hepatic mitochondrial metabolism in response to a high fat diet: a longitudinal study in rats. J. Physiol. Biochem. 68:335–344. doi:10.1007/s13105-012-0145-3.

Flanagan, J.L., P.A. Simmons, J. Vehige, M.D.P. Willcox, and Q. Garrett. 2010. Role of carnitine in disease. Nutr. Metab. (Lond). 7:30. doi:10.1186/1743-7075-7-30.

Foretz, M., N. Ancellin, F. Andreelli, Y. Saintillan, P. Grondin, A. Kahn, B. Thorens, S. Vaulont, and B. Viollet. 2005. Short-term overexpression of a constitutively active form of AMP-activated protein kinase in the liver leads to mild hypoglycemia and fatty liver. Diabetes 54:1331 LP – 1339. doi:10.2337/diabetes.54.5.1331.

Frolov, A., T.-H. Cho, E.J. Murphy, and F. Schroeder. 1997. Isoforms of rat liver fatty acid binding protein differ in structure and affinity for fatty acids and fatty acyl CoAs. Biochemistry 36:6545–6555. doi:10.1021/bi970205t.

Fulda, S., L. Galluzzi, and G. Kroemer. 2010. Targeting mitochondria for cancer therapy. Nat. Rev. Drug Discov. 9:447–464. doi:10.1038/nrd3137.

Furuyama, T., K. Kitayama, H. Yamashita, and N. Mori. 2003. Forkhead transcription factor FOXO1 (FKHR)-dependent induction of PDK4 gene expression in skeletal muscle during energy deprivation. Biochem. J. 375:365–371. doi:10.1042/bj20030022.

Garrett, E.F., K. V Nordlund, W.J. Goodger, and G.R. Oetzel. 1997. A cross-sectional field study investigating the effect of periparturient dietary management on ruminal pH in early lactation dairy cows.

Gaynor, P.J., D.R. Waldo, A. V Capuco, R.A. Erdman, L.W. Douglass, and B.B. Teter. 1995. Milk fat depression, the glucogenic theory, and trans-C18:1 fatty acids. J. Dairy Sci. 78:2008–2015. doi:https://doi.org/10.3168/jds.S0022-0302(95)76826-6.

Gessner, D.K., G. Schlegel, J. Keller, F.J. Schwarz, R. Ringseis, and K. Eder. 2013. Expression of target genes of nuclear factor E2-related factor 2 in the liver of dairy cows in the transition period and at different stages of lactation. J. Dairy Sci. 96:1038–1043.

Gessner, D.K., G. Schlegel, R. Ringseis, F.J. Schwarz, and K. Eder. 2014. Up-regulation of endoplasmic reticulum stress induced genes of the unfolded protein response in the liver of periparturient dairy cows. BMC Vet. Res. 10:46. doi:10.1186/1746-6148-10-46.

GfE, Gs. 2001. Empfehlungen zur energie-und nährstoffversorgung der milchkühe und aufzuchtrinder [recommendations of energy and nutrient supply for dairy cows and breeding cattle].

Gimeno, R.E. 2007. Fatty acid transport proteins. Curr. Opin. Lipidol. 18:271–276. doi:10.1097/MOL.0b013e3281338558.

Gnoni, A., S. Longo, G. V Gnoni, and A.M. Giudetti. 2020. Carnitine in human muscle bioenergetics: can carnitine supplementation improve physical exercise?. Mol. 25. doi:10.3390/molecules25010182.

Goad, D.W., C.L. Goad, and T.G. Nagaraja. 1998. Ruminal microbial and fermentative changes associated with experimentally induced subacute acidosis in steers. J. Anim. Sci. 76:234–241.

Goldberg, E.L., and V.D. Dixit. 2017. Carnitine acetyltransferase (CRAT) expression in macrophages is dispensable for nutrient stress sensing and inflammation. Mol. Metab. 6:219–225. doi:https://doi.org/10.1016/j.molmet.2016.12.008.

Goselink, R.M.A., J. van Baal, H.C.A. Widjaja, R.A. Dekker, R.L.G. Zom, M.J. de Veth, and A.M. van Vuuren. 2013a. Effect of rumen-protected choline supplementation on liver and adipose gene expression during the transition period in dairy cattle. J. Dairy Sci. 96:1102–1116. doi:https://doi.org/10.3168/jds.2012-5396.

Goselink, R.M.A., J. Van Baal, H.C.A. Widjaja, R.A. Dekker, R.L.G. Zom, M.J. De Veth, and A.M. Van Vuuren. 2013b. Effect of rumen-protected choline supplementation on liver and adipose gene expression during the transition period in dairy cattle. J. Dairy Sci. 96:1102–1116.

Gozho, G.N., D.O. Krause, and J.C. Plaizier. 2006. Rumen lipopolysaccharide and inflammation during grain adaptation and subacute ruminal acidosis in steers. J. Dairy Sci. 89:4404–4413. doi:10.3168/jds.S0022-0302(06)72487-0.

Gozho, G.N., D.O. Krause, and J.C. Plaizier. 2007. Ruminal lipopolysaccharide concentration and inflammatory response during grain-induced subacute ruminal acidosis in dairy cows. J. Dairy Sci. 90:856–866.

Gozho, G.N., J.C. Plaizier, D.O. Krause, A.D. Kennedy, and K.M. Wittenberg. 2005. Subacute ruminal acidosis induces ruminal lipopolysaccharide endotoxin release and triggers an inflammatory response. J. Dairy Sci. 88:1399–1403. doi:https://doi.org/10.3168/jds.S0022-0302(05)72807-1.

Graber, M., S. Kohler, T. Kaufmann, M.G. Doherr, R.M. Bruckmaier, and H.A. van Dorland. 2010. A field study on characteristics and diversity of gene expression in the liver of dairy cows during the transition period. J. Dairy Sci. 93:5200–5215.

Grala, T.M., J.R. Roche, C.V.C. Phyn, A.G. Rius, R.H. Boyle, R.G. Snell, and J.K. Kay. 2013. Expression of key lipid metabolism genes in adipose tissue is not altered by once-daily milking

during a feed restriction of grazing dairy cows. J. Dairy Sci. 96:7753–7764. doi:https://doi.org/10.3168/jds.2013-6849.

Graugnard, D.E., K.M. Moyes, E. Trevisi, M.J. Khan, D. Keisler, J.K. Drackley, G. Bertoni, and J.J. Loor. 2013. Liver lipid content and inflammometabolic indices in peripartal dairy cows are altered in response to prepartal energy intake and postpartal intramammary inflammatory challenge1. J. Dairy Sci. 96:918–935. doi:https://doi.org/10.3168/jds.2012-5676.

Green, D.R., L. Galluzzi, and G. Kroemer. 2011. Mitochondria and the autophagy-inflammation-cell death axis in organismal aging. Science 333:1109–1112. doi:10.1126/science.1201940.

Greenfield, R.B., M.J. Cecava, T.R. Johnson, and S.S. Donkin. 2000. Impact of dietary protein amount and rumen undegradability on intake, peripartum liver triglyceride, plasma metabolites, and milk production in transition dairy cattle. J. Dairy Sci. 83:703–710. doi:10.3168/jds.S0022-0302(00)74932-0.

Groehn, J.A., J.B. Kaneene, and D. Foster. 1992. Risk factors associated with lameness in lactating dairy cattle in Michigan. Prev. Vet. Med. 14:77–85. doi:https://doi.org/10.1016/0167-5877(92)90086-U.

Grum, D.E., J.K. Drackley, and J.H. Clark. 2002. Fatty acid metabolism in liver of dairy cows fed supplemental fat and nicotinic acid during an entire lactation. J. Dairy Sci. 85:3026–3034. doi:https://doi.org/10.3168/jds.S0022-0302(02)74388-9.

Grum, D.E., J.K. Drackley, R.S. Younker, D.W. LaCount, and J.J. Veenhuizen. 1996. Nutrition during the dry period and hepatic lipid metabolism of periparturient dairy cows. J. Dairy Sci. 79:1850–1864.

Grum, D.E., L.R. Hansen, and J.K. Drackley. 1994. Peroxisomal β-oxidation of fatty acids in bovine and rat liver. Comp. Biochem. Physiol. Part B Comp. Biochem. 109:281–292. doi:https://doi.org/10.1016/0305-0491(94)90012-4.

Grummer, R.R. 1995. Impact of changes in organic nutrient metabolism on feeding the transition dairy cow. J. Anim. Sci. 73:2820–2833. doi:10.2527/1995.7392820x.

Guo, G., M. Huss, G.Q. Tong, C. Wang, L. Li Sun, N.D. Clarke, and P. Robson. 2010. Resolution of cell fate decisions revealed by single-cell gene expression analysis from zygote to blastocyst. Dev. Cell 18:675–685. doi:10.1016/j.devcel.2010.02.012.

Gutgesell, A., R. Ringseis, and K. Eder. 2009. Short communication: dietary conjugated linoleic acid down-regulates fatty acid transporters in the mammary glands of lactating rats. J. Dairy Sci.

92:1169–1173. doi:https://doi.org/10.3168/jds.2008-1640.

Hardie, D.G., F.A. Ross, and S.A. Hawley. 2012. AMPK: a nutrient and energy sensor that maintains energy homeostasis. Nat. Rev. Mol. Cell Biol. 13:251–262. doi:10.1038/nrm3311.

Harmon, D.L., K.L. Gross, C.R. Krehbiel, K.K. Kreikemeier, M.L. Bauer, and R.A. Britton. 1991. Influence of dietary forage and energy intake on metabolism and acyl-CoA synthetase activity in bovine ruminal epithelial tissue. J. Anim. Sci. 69:4117–4127. doi:10.2527/1991.69104117x.

Harrison, D.E., R. Strong, Z.D. Sharp, J.F. Nelson, C.M. Astle, K. Flurkey, N.L. Nadon, J.E. Wilkinson, K. Frenkel, C.S. Carter, M. Pahor, M.A. Javors, E. Fernandez, and R.A. Miller. 2009. Rapamycin fed late in life extends lifespan in genetically heterogeneous mice. Nature 460:392–395. doi:10.1038/nature08221.

Hegardt, F.G. 1999. Mitochondrial 3-hydroxy-3-methylglutaryl-CoA synthase: a control enzyme in ketogenesis. Biochem. J. 338:569–582. doi:10.1042/bj3380569.

Herdt, T.H. 2000. Ruminant adaptation to negative energy balance: influences on the etiology of ketosis and fatty liver. Vet. Clin. Food Anim. Pract. 16:215–230. doi:10.1016/S0749-0720(15)30102-X.

Herrera, E., and G. Desoye. 2016. Maternal and fetal lipid metabolism under normal and gestational diabetic conditions. Horm. Mol. Biol. Clin. Investig. 26:109–127. doi:https://doi.org/10.1515/hmbci-2015-0025.

Hirche, F., M. Fischer, J. Keller, and K. Eder. 2009. Determination of carnitine, its short chain acyl esters and metabolic precursors trimethyllysine and γ-butyrobetaine by quasi-solid phase extraction and MS/MS detection. J. Chromatogr. B 877:2158–2162.

Hiss, S., M. Mielenz, R.M. Bruckmaier, and H. Sauerwein. 2004. Haptoglobin concentrations in blood and milk after endotoxin challenge and quantification of mammary Hp mRNA expression. J. Dairy Sci. 87:3778–3784. doi:10.3168/jds.S0022-0302(04)73516-X.

Hoeben, D., C. Burvenich, E. Trevisi, G. Bertoni, J. Hamann, R.M. Bruckmaier, and J.W. Blum. 2000. Role of endotoxin and TNF-α in the pathogenesis of experimentally induced coliform mastitis in periparturient cows. J. Dairy Res. 67:503–514.

Holmes, R.S., and J. Hempel. 2011. Comparative studies of vertebrate aldehyde dehydrogenase 3: sequences, structures, phylogeny and evolution. Evidence for a mammalian origin for the ALDH3A1 gene. Chem. Biol. Interact. 191:113–121. doi:https://doi.org/10.1016/j.cbi.2011.01.014.

Hoppel, C.L. 1982. Carnitine and carnitine palmitoyltransferase in fatty acid oxidation and ketosis. Pages 2853–2857 in Federation proceedings.

Horton, J.D., J.L. Goldstein, and M.S. Brown. 2002. SREBPs: Transcriptional mediators of lipid homeostasis. Cold Spring Harb. Symp. Quant. Biol. 67:491–498. doi:10.1101/sqb.2002.67.491.

Hosack, D.A., G. Dennis, B.T. Sherman, H.C. Lane, and R.A. Lempicki. 2003. Identifying biological themes within lists of genes with EASE. Genome Biol. 4:R70. doi:10.1186/gb-2003-4-10-r70.

Hotamisligil, G.S. 2006. Inflammation and metabolic disorders. Nature 444:860–867. doi:10.1038/nature05485.

Hotamisligil, G.S., and E. Erbay. 2008. Nutrient sensing and inflammation in metabolic diseases. Nat. Rev. Immunol. 8:923–934. doi:10.1038/nri2449.

Houten, S.M., and R.J.A. Wanders. 2010. A general introduction to the biochemistry of mitochondrial fatty acid β-oxidation. J. Inherit. Metab. Dis. 33:469–477. doi:10.1007/s10545-010-9061-2.

Houtkooper, R.H., and J. Auwerx. 2012. Exploring the therapeutic space around NAD+. J. Cell Biol. 199:205–209. doi:10.1083/jcb.201207019.

Houtkooper, R.H., C. Canto, R.J. Wanders, and J. Auwerx. 2010a. The secret life of NAD+: an old metabolite controlling new metabolic signaling pathways. Endocr. Rev. 31:194–223. doi:10.1210/er.2009-0026.

Houtkooper, R.H., E. Pirinen, and J. Auwerx. 2012. Sirtuins as regulators of metabolism and healthspan. Nat. Rev. Mol. Cell Biol. 13:225–238. doi:10.1038/nrm3293.

Houtkooper, R.H., R.W. Williams, and J. Auwerx. 2010b. Metabolic networks of longevity. Cell 142:9–14.

Hsu, M.H., Ü. Savas, K.J. Griffin, and E.F. Johnson. 2001. Identification of peroxisome proliferator-responsive human genes by elevated expression of the peroxisome proliferator-activated receptor α in HepG2 cells. J. Biol. Chem. 276:27950–27958. doi:10.1074/jbc.M100258200.

Hu, Y., T. Deng, L. Chen, H. Wu, and S. Zhang. 2016. Selection and validation of reference genes for qRT-PCR in cycas elongata. PLoS One 11:e0154384.

Hunt, M.C., V. Tillander, and S.E.H. Alexson. 2014. Regulation of peroxisomal lipid metabolism: The role of acyl-CoA and coenzyme A metabolizing enzymes. Biochimie 98:45–55. doi:https://doi.org/10.1016/j.biochi.2013.12.018.

Ikeda, Y., K. Okamura-Ikeda, and K. Tanaka. 1985. Purification and characterization of short-chain, medium-chain, and long-chain acyl-CoA dehydrogenases from rat liver mitochondria. Isolation of the holo- and apoenzymes and conversion of the apoenzyme to the holoenzyme. J. Biol. Chem. 260:1311–1325.

Imai, S., C.M. Armstrong, M. Kaeberlein, and L. Guarente. 2000. Transcriptional silencing and longevity protein Sir2 is an NAD-dependent histone deacetylase. Nature 403:795–800. doi:10.1038/35001622.

Inagaki, T., P. Dutchak, G. Zhao, X. Ding, L. Gautron, V. Parameswara, Y. Li, R. Goetz, M. Mohammadi, V. Esser, J.K. Elmquist, R.D. Gerard, S.C. Burgess, R.E. Hammer, D.J. Mangelsdorf, and S.A. Kliewer. 2007. Endocrine regulation of the fasting response by PPARα-mediated induction of fibroblast growth factor 21. Cell Metab. 5:415–425. doi:https://doi.org/10.1016/j.cmet.2007.05.003.

Ingvartsen, K.L. 2006. Feeding- and management-related diseases in the transition cow: Physiological adaptations around calving and strategies to reduce feeding-related diseases. Anim. Feed Sci. Technol. 126:175–213. doi:https://doi.org/10.1016/j.anifeedsci.2005.08.003.

Iqbal, S., Q. Zebeli, A. Mazzolari, G. Bertoni, S.M. Dunn, W.Z. Yang, and B.N. Ametaj. 2009. Feeding barley grain steeped in lactic acid modulates rumen fermentation patterns and increases milk fat content in dairy cows. J. Dairy Sci. 92:6023–6032. doi:https://doi.org/10.3168/jds.2009-2380.

Iyer, S., K. Bergquist, K. Young, E. Gnaiger, R.R. Rao, and J.P.J. Bennett. 2012. Mitochondrial gene therapy improves respiration, biogenesis, and transcription in G11778A Leber's hereditary optic neuropathy and T8993G Leigh's syndrome cells. Hum. Gene Ther. 23:647–657. doi:10.1089/hum.2011.177.

Izai, K., Y. Uchida, T. Orii, S. Yamamoto, and T. Hashimoto. 1992. Novel fatty acid beta-oxidation enzymes in rat liver mitochondria. I. Purification and properties of very-long-chain acyl-coenzyme A dehydrogenase. J. Biol. Chem. 267:1027–1033.

Jenkins, T.C., and K.J. Harvatine. 2014. Lipid feeding and milk fat depression. Vet. Clin. Food Anim. Pract. 30:623–642.

Jerred, M.J., D.J. Carroll, D.K. Combs, and R.R. Grummer. 1990. Effects of fat supplementation and immature alfalfa to concentrate ratio on lactation performance of dairy cattle. J. Dairy Sci. 73:2842–2854.

Jesse, B.W., R.S. Emery, and J.W. Thomas. 1986. Control of bovine hepatic fatty acid oxidation. J.

Dairy Sci. 69:2290–2297.

Jia, H., X. Li, G. Liu, J.J. Loor, R. Bucktrout, X. Sun, G. Li, X. Shu, J. Dong, Y. Wang, R. Zuo, Z. Wang, and X. Li. 2019. Perilipin 5 promotes hepatic steatosis in dairy cows through increasing lipid synthesis and decreasing very low density lipoprotein assembly. J. Dairy Sci. 102:833–845. doi:https://doi.org/10.3168/jds.2018-15208.

Jóźwik, A., N. Strzałkowska, E. Bagnicka, W. Grzybek, J. Krzyżewski, E. Poławska, A. Kołataj, and J.O. Horbańczuk. 2012. Relationship between milk yield, stage of lactation, and some blood serum metabolic parameters of dairy cows. Czech J. Anim. Sci. 57:353–360.

Jungi, T.W., K. Farhat, I.A. Burgener, and D. Werling. 2011. Toll-like receptors in domestic animals. Cell Tissue Res. 343:107–120.

Kadenbach, B., M. Hüttemann, S. Arnold, I. Lee, and E. Bender. 2000. Mitochondrial energy metabolism is regulated via nuclear-coded subunits of cytochrome c oxidase. Free Radic. Biol. Med. 29:211–221. doi:https://doi.org/10.1016/S0891-5849(00)00305-1.

Kahn, B.B., T. Alquier, D. Carling, and D.G. Hardie. 2005. AMP-activated protein kinase: ancient energy gauge provides clues to modern understanding of metabolism. Cell Metab. 1:15–25.

Katoh, N. 2002. Relevance of apolipoproteins in the development of fatty liver and fatty liver-related peripartum diseases in dairy cows. J. Vet. Med. Sci. 64:293–307. doi:10.1292/jvms.64.293.

Kazantzis, M., and A. Stahl. 2012. Fatty acid transport proteins, implications in physiology and disease. Biochim. Biophys. Acta - Mol. Cell Biol. Lipids 1821:852–857. doi:https://doi.org/10.1016/j.bbalip.2011.09.010.

Kelley, K.W., D.A. Weigent, and R. Kooijman. 2007. Protein hormones and immunity. Brain. Behav. Immun. 21:384–392. doi:https://doi.org/10.1016/j.bbi.2006.11.010.

Kelly, D.P., and R.C. Scarpulla. 2004. Transcriptional regulatory circuits controlling mitochondrial biogenesis and function. Genes Dev. 18:357–368. doi:10.1101/gad.1177604.

Kenyon, C.J. 2010. The genetics of ageing. Nature 464:504–512.

Kersten, S., J. Seydoux, J.M. Peters, F.J. Gonzalez, B. Desvergne, and W. Wahli. 1999. Peroxisome proliferator-activated receptor alpha mediates the adaptive response to fasting. J. Clin. Invest. 103:1489–1498. doi:10.1172/JCI6223.

Kessler, E.C., J.J. Gross, R.M. Bruckmaier, and C. Albrecht. 2014. Cholesterol metabolism, transport, and hepatic regulation in dairy cows during transition and early lactation. J. Dairy Sci. 97:5481–

5490. doi:https://doi.org/10.3168/jds.2014-7926.

Khafipour, E., D.O. Krause, and J.C. Plaizier. 2009. A grain-based subacute ruminal acidosis challenge causes translocation of lipopolysaccharide and triggers inflammation. J. Dairy Sci. 92:1060–1070. doi:https://doi.org/10.3168/jds.2008-1389.

Khazanehei, H., S. Li, E. Khafipour, and J.C. Plaizier. 2015. Effects of dry period management and parity on rumen fermentation, blood metabolites, and liver triacylglyceride in dairy cows. Can. J. Anim. Sci. 95:445–453. doi:10.4141/cjas-2014-157.

Kim, J.J., M. Wang, and R. Paschke. 1993. Crystal structures of medium-chain acyl-CoA dehydrogenase from pig liver mitochondria with and without substrate. Proc. Natl. Acad. Sci. 90:7523–7527.

Kim, K.H., and M.-S. Lee. 2014. FGF21 as a stress hormone: The roles of FGF21 in stress adaptation and the treatment of metabolic diseases. Diabetes Metab J 38:245–251.

Kim, K.H., and M.S. Lee. 2015. FGF21 as a mediator of adaptive responses to stress and metabolic benefits of anti-diabetic drugs. J. Endocrinol. 226:R1–R16. doi:10.1530/JOE-15-0160.

Knapp, J.R., and R.L. Baldwin Jr. 1990. Regulation of ketogenesis in dairy cattle. J. Anim. Sci 68:522.

Koepsell, H., K. Lips, and C. Volk. 2007. Polyspecific organic cation transporters: Structure, function, physiological roles, and biopharmaceutical implications. Pharm. Res. 24:1227–1251. doi:10.1007/s11095-007-9254-z.

Kulinski, A., S. Rustaeus, and J.E. Vance. 2002. Microsomal triacylglycerol transfer protein is required for lumenal accretion of triacylglycerol not associated with ApoB, as well as for ApoB lipidation. J. Biol. Chem. 277:31516–31525. doi:10.1074/jbc.M202015200.

Kulkarni, R.G., G. Achaiah, and G. Narahari Sastry. 2006. Novel targets for antiinflammatory and antiarthritic agents. Curr. Pharm. Des. 12:2437–2454.

Kumar, A., S. Ashraf, T.S. Goud, A. Grewal, S. V Singh, B.R. Yadav, and R.C. Upadhyay. 2015. Expression profiling of major heat shock protein genes during different seasons in cattle (Bos indicus) and buffalo (Bubalus bubalis) under tropical climatic condition. J. Therm. Biol. 51:55–64. doi:https://doi.org/10.1016/j.jtherbio.2015.03.006.

Kumar, H., T. Kawai, and S. Akira. 2011. Pathogen recognition by the innate immune system. Int. Rev. Immunol. 30:16–34.

Kvidera, S.K., M.J. Dickson, M. Abuajamieh, D.B. Snider, M.V.S. Fernandez, J.S. Johnson, A.F. Keating, P.J. Gorden, H.B. Green, K.M. Schoenberg, and L.H. Baumgard. 2017a. Intentionally

induced intestinal barrier dysfunction causes inflammation, affects metabolism, and reduces productivity in lactating Holstein cows. J. Dairy Sci. 100:4113–4127. doi:10.3168/jds.2016-12349.

Kvidera, S.K., E.A. Horst, M. Abuajamieh, E.J. Mayorga, M.V.S. Fernandez, and L.H. Baumgard. 2017b. Glucose requirements of an activated immune system in lactating Holstein cows. J. Dairy Sci. 100:2360–2374. doi:https://doi.org/10.3168/jds.2016-12001.

LaCount, D.W., L.S. Emmert, and J.K. Drackley. 1996. Dose response of dairy cows to abomasal administration of four amounts of L-carnitine. J. Dairy Sci. 79:591–602.

Lagouge, M., C. Argmann, Z. Gerhart-Hines, H. Meziane, C. Lerin, F. Daussin, N. Messadeq, J. Milne, P. Lambert, P. Elliott, B. Geny, M. Laakso, P. Puigserver, and J. Auwerx. 2006. Resveratrol improves mitochondrial function and protects against metabolic disease by activating SIRT1 and PGC-1alpha. Cell 127:1109–1122. doi:10.1016/j.cell.2006.11.013.

Laguna, J.G., M.S. Cardoso, J.A. Lima, R.B. Reis, A.U. Carvalho, H.M. Saturnino, and S.M.R. Teixeira. 2017. Expression of hepatic genes related to energy metabolism during the transition period of Holstein and F1 Holstein-Gir cows. J. Dairy Sci. 100:9861–9870. doi:https://doi.org/10.3168/jds.2016-12459.

Lahjouji, K., G.A. Mitchell, and I.A. Qureshi. 2001. Carnitine transport by organic cation transporters and systemic carnitine deficiency. Mol. Genet. Metab. 73:287–297. doi:https://doi.org/10.1006/mgme.2001.3207.

Lan, Y.-L., J.-C. Lou, W. Lyu, and B. Zhang. 2019. Update on the synergistic effect of HSL and insulin in the treatment of metabolic disorders. Ther. Adv. Endocrinol. Metab. 10:2042018819877300–2042018819877300. doi:10.1177/2042018819877300.

Lane, R.H., D.E. Kelley, V.H. Ritov, A.E. Tsirka, and E.M. Gruetzmacher. 2001. Altered expression and function of mitochondrial β-oxidation enzymes in juvenile intrauterine-growth-retarded rat skeletal muscle. Pediatr. Res. 50:83–90.

Laplante, M., and D.M. Sabatini. 2009. mTOR signaling at a glance. J. Cell Sci. 122:3589 LP – 3594. doi:10.1242/jcs.051011.

Laplante, M., and D.M. Sabatini. 2012. mTOR signaling in growth control and disease. Cell 149:274–293.

LeBlanc, S.J., K.D. Lissemore, D.F. Kelton, T.F. Duffield, and K.E. Leslie. 2006. Major advances in disease prevention in dairy cattle. J. Dairy Sci. 89:1267–1279. doi:10.3168/jds.S0022-0302(06)72195-6.

Lehner, R., and A. Kuksis. 1996. Biosynthesis of triacylglycerols. Prog. Lipid Res. 35:169–201. doi:https://doi.org/10.1016/0163-7827(96)00005-7.

Lehtolainen, T., S. Suominen, T. Kutila, and S. Pyörälä. 2003. Effect of intramammary Escherichia coli endotoxin in early-vs. late-lactating dairy cows. J. Dairy Sci. 86:2327–2333.

Lei, S., R. Sun, D. Wang, M. Gong, X. Su, F. Yi, and Z. Peng. 2016. Increased hepatic fatty acids uptake and oxidation by LRPPRC-driven oxidative phosphorylation reduces blood lipid levels. Front. Physiol. 7:270.

Leroy, J.L.M.R., T. Vanholder, B. Mateusen, A. Christophe, G. Opsomer, A. de Kruif, G. Genicot, and A. Van Soom. 2005. Non-esterified fatty acids in follicular fluid of dairy cows and their effect on developmental capacity of bovine oocytes in vitro. Reproduction 130:485–495. doi:10.1530/rep.1.00735.

Li, J.L., Q.Y. Wang, H.Y. Luan, Z.C. Kang, and C.B. Wang. 2012. Effects of L-carnitine against oxidative stress in human hepatocytes: involvement of peroxisome proliferator-activated receptor alpha. J. Biomed. Sci. 19:32. doi:10.1186/1423-0127-19-32.

Li, Y., J.-S. Park, J.-H. Deng, and Y. Bai. 2006. Cytochrome c oxidase subunit IV is essential for assembly and respiratory function of the enzyme complex. J. Bioenerg. Biomembr. 38:283–291. doi:10.1007/s10863-006-9052-z.

Li, Y., S. Xu, M.M. Mihaylova, B. Zheng, X. Hou, B. Jiang, O. Park, Z. Luo, E. Lefai, and J.Y.-J. Shyy. 2011. AMPK phosphorylates and inhibits SREBP activity to attenuate hepatic steatosis and atherosclerosis in diet-induced insulin-resistant mice. Cell Metab. 13:376–388.

Li, Z., G. Xu, Y. Qin, C. Zhang, H. Tang, Y. Yin, X. Xiang, Y. Li, J. Zhao, M. Mulholland, and W. Zhang. 2014. Ghrelin promotes hepatic lipogenesis by activation of mTOR-PPARγ signaling pathway. Proc. Natl. Acad. Sci. 111:13163 LP – 13168. doi:10.1073/pnas.1411571111.

Liang, H., and W.F. Ward. 2006. PGC-1α: a key regulator of energy metabolism. Adv. Physiol. Educ. 30:145–151. doi:10.1152/advan.00052.2006.

Liang, W.C., and I. Nishino. 2010. State of the art in muscle lipid diseases. Acta Myol. 29:351.

Liu, T.-Y., X.-Q. Xiong, X.-S. Ren, M.-X. Zhao, C.-X. Shi, J.-J. Wang, Y.-B. Zhou, F. Zhang, Y. Han, X.-Y. Gao, Q. Chen, Y.-H. Li, Y.-M. Kang, and G.-Q. Zhu. 2016. FNDC5 alleviates hepatosteatosis by restoring AMPK/mTOR-mediated autophagy, fatty acid oxidation, and lipogenesis in mice. Diabetes 65:3262 LP – 3275. doi:10.2337/db16-0356.

Locher, L., S. Haussler, L. Laubenthal, S.P. Singh, J. Winkler, A. Kinoshita, A. Kenez, J. Rehage, K. Huber, H. Sauerwein, and S. Danicke. 2015. Effect of increasing body condition on key regulators of fat metabolism in subcutaneous adipose tissue depot and circulation of nonlactating dairy cows. J. Dairy Sci. 98:1057–1068. doi:10.3168/jds.2014-8710.

Longo, N., M. Frigeni, and M. Pasquali. 2016. Carnitine transport and fatty acid oxidation. Biochim. Biophys. Acta - Mol. Cell Res. 1863:2422–2435. doi:https://doi.org/10.1016/j.bbamcr.2016.01.023.

Lüderitz, O., K. Tanamoto, C. Galanos, G.R. McKenzie, H. Brade, U. Zähringer, E.T. Rietschel, S. Kusumoto, and T. Shiba. 1984. Lipopolysaccharides: Structural principles and biologic activities. Rev. Infect. Dis. 6:428–431. doi:10.1093/clinids/6.4.428.

Lumeng, C.N., and A.R. Saltiel. 2011. Inflammatory links between obesity and metabolic disease. J. Clin. Invest. 121:2111–2117.

Marchitti, S.A., Y. Chen, D.C. Thompson, and V. Vasiliou. 2011. Ultraviolet radiation: cellular antioxidant response and the role of ocular aldehyde dehydrogenase enzymes. Eye Contact Lens 37:206–213. doi:10.1097/ICL.0b013e3182212642.

Marcos, E., A. Mazur, P. Cardot, and Y. Rayssiguier. 1990. Serum apolipoproteins B and A-I and naturally occurring fatty liver in dairy cows. Lipids 25:575–577. doi:10.1007/BF02537168.

Mattison, J.A., G.S. Roth, T.M. Beasley, E.M. Tilmont, A.M. Handy, R.L. Herbert, D.L. Longo, D.B. Allison, J.E. Young, M. Bryant, D. Barnard, W.F. Ward, W. Qi, D.K. Ingram, and R. de Cabo. 2012. Impact of caloric restriction on health and survival in rhesus monkeys from the NIA study. Nature 489:318–321. doi:10.1038/nature11432.

McGarry, J.D., and N.F. Brown. 1997. The mitochondrial carnitine palmitoyltransferase system—from concept to molecular analysis. Eur. J. Biochem. 244:1–14.

Memon, R.A., K.R. Feingold, A.H. Moser, W. Doerrler, S. Adi, C.A. Dinarello, and C. Grunfeld. 1992. Differential effects of interleukin-1 and tumor necrosis factor on ketogenesis. Am. J. Physiol. Metab. 263:E301–E309. doi:10.1152/ajpendo.1992.263.2.E301.

Meyer, J., S.U. Daniels, S. Grindler, J. Tröscher-Mußotter, M. Alaedin, J. Frahm, L. Hüther, J. Kluess, S. Kersten, D. von Soosten, U. Meyer, E. Most, K. Eder, H. Sauerwein, J. Seifert, K. Huber, J. Rehage, and S. Dänicke. 2020. Effects of a dietary L-carnitine supplementation on performance, energy metabolism and recovery from calving in dairy cows. Animals 10:342. doi:10.3390/ani10020342.

Meyer, J., S.U. Kononov, S. Grindler, J. Tröscher-Mußotter, M. Alaedin, J. Frahm, L. Hüther, J. Kluess, S. Kersten, D. von Soosten, U. Meyer, E. Most, K. Eder, H. Sauerwein, J. Seifert, K. Huber, A. Wegerich, J. Rehage, and S. Dänicke. 2021. Dietary L-carnitine supplementation modifies the lipopolysaccharide-induced acute phase reaction in dairy cows. Animals 10:3390.

Michalik, L., J. Auwerx, J.P. Berger, V.K. Chatterjee, C.K. Glass, F.J. Gonzalez, P.A. Grimaldi, T. Kadowaki, M.A. Lazar, S. O'Rahilly, C.N.A. Palmer, J. Plutzky, J.K. Reddy, B.M. Spiegelman, B. Staels, and W. Wahli. 2006. Peroxisome proliferator-activated receptors. Pharmacol. Rev. 58:726–741. doi:10.1124/pr.58.4.5.

Mittal, M., M.R. Siddiqui, K. Tran, S.P. Reddy, and A.B. Malik. 2013. Reactive oxygen species in inflammation and tissue injury. Antioxid. Redox Signal. 20:1126–1167. doi:10.1089/ars.2012.5149.

Mizutani, H., T. Sako, Y. Toyoda, T. Kawabata, N. Urumuhang, H. Koyama, and S. Motoyoshi. 1999. Preliminary studies on hepatic carnitine palmitoyltransferase in dairy cattle with or without fatty liver. Vet. Res. Commun. 23:475–480. doi:10.1023/A:1006358222037.

Moe, P.W. 1981. Energy metabolism of dairy cattle. J. Dairy Sci. 64:1120–1139.

Morrison, E.I., H. Reinhardt, H. Leclerc, T.J. DeVries, and S.J. LeBlanc. 2018. Effect of rumen-protected B vitamins and choline supplementation on health, production, and reproduction in transition dairy cows. J. Dairy Sci. 101:9016–9027. doi:https://doi.org/10.3168/jds.2018-14663.

Moseti, D., A. Regassa, and W. K. Kim. 2016. Molecular regulation of adipogenesis and potential anti-adipogenic bioactive molecules. Int. J. Mol. Sci. 17. doi:10.3390/ijms17010124.

Musso, G., M. Cassader, and R. Gambino. 2016. Non-alcoholic steatohepatitis: emerging molecular targets and therapeutic strategies. Nat. Rev. Drug Discov. 15:249–274. doi:10.1038/nrd.2015.3.

Muzio, G., M. Maggiora, E. Paiuzzi, M. Oraldi, and R.A. Canuto. 2012. Aldehyde dehydrogenases and cell proliferation. Free Radic. Biol. Med. 52:735–746. doi:https://doi.org/10.1016/j.freeradbiomed.2011.11.033.

Muzio, G., A. Trombetta, M. Maggiora, G. Martinasso, V. Vasiliou, N. Lassen, and R.A. Canuto. 2006. Arachidonic acid suppresses growth of human lung tumor A549 cells through down-regulation of ALDH3A1 expression. Free Radic. Biol. Med. 40:1929–1938. doi:10.1016/j.freeradbiomed.2006.01.020.

Naeem, A., J.K. Drackley, J. Stamey, and J.J. Loor. 2012. Role of metabolic and cellular proliferation genes in ruminal development in response to enhanced plane of nutrition in neonatal Holstein

calves1. J. Dairy Sci. 95:1807–1820. doi:https://doi.org/10.3168/jds.2011-4709.

Nafikov, R.A., J.P. Schoonmaker, K.T. Korn, K. Noack, D.J. Garrick, K.J. Koehler, J. Minick-Bormann, J.M. Reecy, D.E. Spurlock, and D.C. Beitz. 2013. Association of polymorphisms in solute carrier family 27, isoform A6 (SLC27A6) and fatty acid-binding protein-3 and fatty acid-binding protein-4 (FABP3 and FABP4) with fatty acid composition of bovine milk. J. Dairy Sci. 96:6007–6021. doi:https://doi.org/10.3168/jds.2013-6703.

Nakamura, M.T., B.E. Yudell, and J.J. Loor. 2014. Regulation of energy metabolism by long-chain fatty acids. Prog. Lipid Res. 53:124–144. doi:10.1016/j.plipres.2013.12.001.

Narkar, V.A., M. Downes, R.T. Yu, E. Embler, Y. X. Wang, E. Banayo, M.M. Mihaylova, M.C. Nelson, Y. Zou, H. Juguilon, H. Kang, R.J. Shaw, and R.M. Evans. 2008. AMPK and PPARdelta agonists are exercise mimetics. Cell 134:405–415. doi:10.1016/j.cell.2008.06.051.

Nelson, D. L., Cox, M. M., and Lehninger, A.L. 2017. Lehninger Principles of Biochemistry. 7th ed. W.H. Freeman and Company, New York, NY.

Nightingale, C.R., M.D. Sellers, and M.A. Ballou. 2015. Elevated plasma haptoglobin concentrations following parturition are associated with elevated leukocyte responses and decreased subsequent reproductive efficiency in multiparous Holstein dairy cows. Vet. Immunol. Immunopathol. 164:16–23.

Nita, M., and A. Grzybowski. 2016. The role of the reactive oxygen species and oxidative stress in the pathomechanism of the age-related ocular diseases and other pathologies of the anterior and posterior eye segments in adults. Oxid. Med. Cell. Longev. 2016:3164734. doi:10.1155/2016/3164734.

Nulton-Persson, A.C., and L.I. Szweda. 2001. Modulation of mitochondrial function by hydrogen peroxide. J. Biol. Chem. 276:23357–23361. doi:10.1074/jbc.M100320200.

Nunnari, J., and A. Suomalainen. 2012. Mitochondria: in sickness and in health. Cell 148:1145–1159.

Oltenacu, P.A., and I. Ekesbo. 1994. Epidemiological study of clinical mastitis in dairy cattle.

Olzmann, J.A., and P. Carvalho. 2019. Dynamics and functions of lipid droplets. Nat. Rev. Mol. Cell Biol. 20:137–155. doi:10.1038/s41580-018-0085-z.

Osorio, J.S., P. Ji, J.K. Drackley, D. Luchini, and J.J. Loor. 2013. Supplemental Smartamine M or MetaSmart during the transition period benefits postpartal cow performance and blood neutrophil function. J. Dairy Sci. 96:6248–6263. doi:https://doi.org/10.3168/jds.2012-5790.

Owen, K.Q., J.L. Nelssen, R.D. Goodband, M.D. Tokach, and K.G. Friesen. 2001. Effect of dietary L-carnitine on growth performance and body composition in nursery and growing-finishing pigs. J. Anim. Sci. 79:1509–1515. doi:10.2527/2001.7961509x.

Owens, F.N., D.S. Secrist, W.J. Hill, and D.R. Gill. 1998. Acidosis in cattle: a review. J. Anim. Sci. 76:275–286. doi:10.2527/1998.761275x.

Palmquist, D.L. 1994. The role of dietary fats in efficiency of ruminants. J. Nutr. 124:1377S-1382S.

Palmquist, D.L., and T.C. Jenkins. 2017. A 100-year review: Fat feeding of dairy cows. J. Dairy Sci. 100:10061–10077. doi:https://doi.org/10.3168/jds.2017-12924.

Pappa, A., C. Chen, Y. Koutalos, A.J. Townsend, and V. Vasiliou. 2003. ALDH3A1 protects human corneal epithelial cells from ultraviolet- and 4-hydroxy-2-nonenal-induced oxidative damage. Free Radic. Biol. Med. 34:1178–1189. doi:https://doi.org/10.1016/S0891-5849(03)00070-4.

Patil, R.K., B.U. Mahajan, S.B. Unger, N.S. Goyal, S. Belemkar, J.S. Surana, S. Ojha, and R.C. Patil. 2019. Animal models of inflammation for screening of anti-inflammatory drugs: Implications for the discovery and development of phytopharmaceuticals. Int. J. Mol. Sci. 20. doi:10.3390/ijms20184367.

Patki, G., F. Atrooz, I. Alkadhi, N. Solanki, and S. Salim. 2015. High aggression in rats is associated with elevated stress, anxiety-like behavior, and altered catecholamine content in the brain. Neurosci. Lett. 584:308–313. doi:https://doi.org/10.1016/j.neulet.2014.10.051.

Petrov, D., I. Pedrós, G. Artiach, F.X. Sureda, E. Barroso, M. Pallàs, G. Casadesús, C. Beas-Zarate, E. Carro, I. Ferrer, M. Vazquez-Carrera, J. Folch, and A. Camins. 2015. High-fat diet-induced deregulation of hippocampal insulin signaling and mitochondrial homeostasis deficiences contribute to Alzheimer disease pathology in rodents. Biochim. Biophys. Acta - Mol. Basis Dis. 1852:1687–1699. doi:https://doi.org/10.1016/j.bbadis.2015.05.004.

Piantoni, P., A.L. Lock, and M.S. Allen. 2015. Saturated fat supplementation interacts with dietary forage neutral detergent fiber content during the immediate postpartum and carryover periods in Holstein cows: Production responses and digestibility of nutrients. J. Dairy Sci. 98:3309–3322.

Pieklik, J.R., and R.W. Guynn. 1975. Equilibrium constants of the reactions of choline acetyltransferase, carnitine acetyltransferase, and acetylcholinesterase under physiological conditions. J. Biol. Chem. 250:4445–4450.

Pinedo, P.J., A. De Vries, and D.W. Webb. 2010. Dynamics of culling risk with disposal codes reported by dairy herd improvement dairy herds. J. Dairy Sci. 93:2250–2261.

Plaizier, J.C., E. Khafipour, S. Li, G.N. Gozho, and D.O. Krause. 2012. Subacute ruminal acidosis (SARA), endotoxins and health consequences. Anim. Feed Sci. Technol. 172:9–21. doi:https://doi.org/10.1016/j.anifeedsci.2011.12.004.

Ramsay, R.R., and A. Arduini. 1993. The carnitine acyltransferases and their role in modulating Acyl-CoA pools. Arch. Biochem. Biophys. 302:307–314. doi:https://doi.org/10.1006/abbi.1993.1216.

Recknagel, P., F.A. Gonnert, E. Halilbasic, M. Gajda, N. Jbeily, A. Lupp, I. Rubio, R.A. Claus, A. Kortgen, and M. Trauner. 2013. Mechanisms and functional consequences of liver failure substantially differ between endotoxaemia and faecal peritonitis in rats. Liver Int. 33:283–293.

Remick, D.G., and P.A. Ward. 2005. Evaluation of endotoxin models for the study of sepsis. Shock 24:7–11.

Renner, K., A. Amberger, G. Konwalinka, R. Kofler, and E. Gnaiger. 2003. Changes of mitochondrial respiration, mitochondrial content and cell size after induction of apoptosis in leukemia cells. Biochim. Biophys. Acta - Mol. Cell Res. 1642:115–123. doi:https://doi.org/10.1016/S0167-4889(03)00105-8.

Ringseis, R., J. Keller, and K. Eder. 2018. Regulation of carnitine status in ruminants and efficacy of carnitine supplementation on performance and health aspects of ruminant livestock: a review. Arch. Anim. Nutr. 72:1–30. doi:10.1080/1745039X.2017.1421340.

Ringseis, R., J.O. Zeitz, A. Weber, C. Koch, and K. Eder. 2019. Hepatic transcript profiling in early-lactation dairy cows fed rumen-protected niacin during the transition from late pregnancy to lactation. J. Dairy Sci. 102:365–376. doi:10.3168/jds.2018-15232.

Roche, J.R., A.W. Bell, T.R. Overton, and J.J. Loor. 2013. Nutritional management of the transition cow in the 21st century–a paradigm shift in thinking. Anim. Prod. Sci. 53:1000–1023.

Roche, J.R., N.C. Friggens, J.K. Kay, M.W. Fisher, K.J. Stafford, and D.P. Berry. 2009. Invited review: Body condition score and its association with dairy cow productivity, health, and welfare. J. Dairy Sci. 92:5769–5801. doi:10.3168/jds.2009-2431.

Rosen, E.D., and O.A. MacDougald. 2006. Adipocyte differentiation from the inside out. Nat. Rev. Mol. Cell Biol. 7:885–896. doi:10.1038/nrm2066.

Roth, J.A., M.L. Kaeberle, and W.H. Hsu. 1982. Effect of estradiol and progesterone on lymphocyte and neutrophil functions in steers. Infect. Immun. 35:997 LP – 1002.

Ruegsegger, G.J., and L.H. Schultz. 1985. Response of high producing dairy cows in early lactation to

the feeding of heat-treated whole soybeans. J. Dairy Sci. 68:3272–3279.

Saggerson, D. 2008. Malonyl-CoA, a key signaling molecule in mammalian cells. Annu. Rev. Nutr. 28:253–272. doi:10.1146/annurev.nutr.28.061807.155434.

Saremi, B., A. Al-Dawood, S. Winand, U. Müller, J. Pappritz, D. von Soosten, J. Rehage, S. Dänicke, S. Häussler, M. Mielenz, and H. Sauerwein. 2012. Bovine haptoglobin as an adipokine: Serum concentrations and tissue expression in dairy cows receiving a conjugated linoleic acids supplement throughout lactation. Vet. Immunol. Immunopathol. 146:201–211. doi:https://doi.org/10.1016/j.vetimm.2012.03.011.

Sato, H., M. Matsumoto, and S. Hanasaka. 1999. Relations between plasma acetate, 3-hydroxybutyrate, FFA, glucose levels and energy nutrition in lactating dairy cows. J. Vet. Med. Sci. 61:447–451.

Sato, S. Subacute ruminal acidosis (SARA) challenge, ruminal condition and cellular immunity in cattle. Jpn. J. Vet. Res. 63:S25–S36. doi:10.14943/jjvr.63.suppl.s25.

Savage, D.B., C.S. Choi, V.T. Samuel, Z.-X. Liu, D. Zhang, A. Wang, X.-M. Zhang, G.W. Cline, X.X. Yu, J.G. Geisler, S. Bhanot, B.P. Monia, and G.I. Shulman. 2006. Reversal of diet-induced hepatic steatosis and hepatic insulin resistance by antisense oligonucleotide inhibitors of acetyl-CoA carboxylases 1 and 2. J. Clin. Invest. 116:817–824. doi:10.1172/JCI27300.

Saxton, R.A., and D.M. Sabatini. 2017. mTOR signaling in growth, metabolism, and disease. Cell 168:960–976. doi:https://doi.org/10.1016/j.cell.2017.02.004.

Schaap, F.G., A.E. Kremer, W.H. Lamers, P.L.M. Jansen, and I.C. Gaemers. 2013. Fibroblast growth factor 21 is induced by endoplasmic reticulum stress. Biochimie 95:692–699. doi:https://doi.org/10.1016/j.biochi.2012.10.019.

Schäff, C., S. Börner, S. Hacke, U. Kautzsch, H. Sauerwein, S.K. Spachmann, M. Schweigel-Röntgen, H.M. Hammon, and B. Kuhla. 2013. Increased muscle fatty acid oxidation in dairy cows with intensive body fat mobilization during early lactation. J. Dairy Sci. 96:6449–6460. doi:https://doi.org/10.3168/jds.2013-6812.

Schlegel, G., J. Keller, F. Hirche, S. Geißler, F.J. Schwarz, R. Ringseis, G.I. Stangl, and K. Eder. 2012a. Expression of genes involved in hepatic carnitine synthesis and uptake in dairy cows in the transition period and at different stages of lactation. BMC Vet. Res. 8:28. doi:10.1186/1746-6148-8-28.

Schlegel, G., R. Ringseis, J. Keller, F.J. Schwarz, W. Windisch, and K. Eder. 2013. Expression of fibroblast growth factor 21 in the liver of dairy cows in the transition period and during lactation.

J. Anim. Physiol. Anim. Nutr. (Berl). 97:820–829. doi:10.1111/j.1439-0396.2012.01323.x.

Schlegel, G., R. Ringseis, W. Windisch, F.J. Schwarz, and K. Eder. 2012b. Effects of a rumen-protected mixture of conjugated linoleic acids on hepatic expression of genes involved in lipid metabolism in dairy cows. J. Dairy Sci. 95:3905–3918.

Schoenberg, K.M., K.L. Perfield, J.K. Farney, B.J. Bradford, Y.R. Boisclair, and T.R. Overton. 2011. Effects of prepartum 2,4-thiazolidinedione on insulin sensitivity, plasma concentrations of tumor necrosis factor-α and leptin, and adipose tissue gene expression. J. Dairy Sci. 94:5523–5532. doi:https://doi.org/10.3168/jds.2011-4501.

Schooneman, M.G., N. Achterkamp, C.A. Argmann, M.R. Soeters, and S.M. Houten. 2014. Plasma acylcarnitines inadequately reflect tissue acylcarnitine metabolism. Biochim. Biophys. Acta - Mol. Cell Biol. Lipids 1841:987–994. doi:https://doi.org/10.1016/j.bbalip.2014.04.001.

Schooneman, M.G., F.M. Vaz, S.M. Houten, and M.R. Soeters. 2013. Acylcarnitines. Diabetes 62:1 LP – 8. doi:10.2337/db12-0466.

Schroeder, F., A.D. Petrescu, H. Huang, B.P. Atshaves, A.L. McIntosh, G.G. Martin, H.A. Hostetler, A. Vespa, D. Landrock, K.K. Landrock, H.R. Payne, and A.B. Kier. 2008. Role of fatty acid binding proteins and long chain fatty acids in modulating nuclear receptors and gene transcription. Lipids 43:1–17. doi:10.1007/s11745-007-3111-z.

Schuh, K., H. Sadri, S. Haussler, L.A. Webb, C. Urh, M. Wagner, C. Koch, J. Frahm, S. Danicke, G. Dusel, and H. Sauerwein. 2019. Comparison of performance and metabolism from late pregnancy to early lactation in dairy cows with elevated v. normal body condition at dry-off. Animal 13:1478–1488. doi:10.1017/S1751731118003385.

Seemann, S., F. Zohles, and A. Lupp. 2017. Comprehensive comparison of three different animal models for systemic inflammation. J. Biomed. Sci. 24:60. doi:10.1186/s12929-017-0370-8.

Serhan, C.N. 2009. Systems approach to inflammation resolution: identification of novel anti-inflammatory and pro-resolving mediators. J. Thromb. Haemost. 7:44–48. doi:10.1111/j.1538-7836.2009.03396.x.

Shahzad, K., H. Akbar, M. Vailati-Riboni, L. Basiricò, P. Morera, S.L. Rodriguez-Zas, A. Nardone, U. Bernabucci, and J.J. Loor. 2015. The effect of calving in the summer on the hepatic transcriptome of Holstein cows during the peripartal period. J. Dairy Sci. 98:5401–5413. doi:https://doi.org/10.3168/jds.2015-9409.

Sheldon, I.M., J.G. Cronin, M. Pospiech, and M.L. Turner. 2018. Symposium review: Mechanisms

linking metabolic stress with innate immunity in the endometrium. J. Dairy Sci. 101:3655–3664. doi:https://doi.org/10.3168/jds.2017-13135.

Shi, L., L. Liu, Z. Ma, X. Lv, C. Li, L. Xu, B. Han, Y. Li, F. Zhao, and Y. Yang. 2019. Identification of genetic associations of ECHS 1 gene with milk fatty acid traits in dairy cattle. Anim. Genet. 50:430–438.

Shi, Z., X.B. Li, Z.C. Peng, S.P. Fu, C.X. Zhao, X.L. Du, Z.Y. Fang, Z. Wang, G.W. Liu, and X.W. Li. 2018. Berberine protects against NEFA-induced impairment of mitochondrial respiratory chain function and insulin signaling in bovine hepatocytes. Int. J. Mol. Sci. 19:1691. doi:10.3390/ijms19061691.

Singh, I. 1997. Biochemistry of peroxisomes in health and disease. Mol. Cell. Biochem. 167:1–29.

Skibiel, A.L., M. Zachut, B.C. do Amaral, Y. Levin, and G.E. Dahl. 2018. Liver proteomic analysis of postpartum Holstein cows exposed to heat stress or cooling conditions during the dry period. J. Dairy Sci. 101:705–716. doi:https://doi.org/10.3168/jds.2017-13258.

Song, B. J., M.A. Abdelmegeed, L.E. Henderson, S. H. Yoo, J. Wan, V. Purohit, J. P. Hardwick, and K. H. Moon. 2013. Increased nitroxidative stress promotes mitochondrial dysfunction in alcoholic and nonalcoholic fatty liver disease. Oxid. Med. Cell. Longev. 2013:781050. doi:10.1155/2013/781050.

Song, M.J., K.H. Kim, J.M. Yoon, and J.B. Kim. 2006. Activation of Toll-like receptor 4 is associated with insulin resistance in adipocytes. Biochem. Biophys. Res. Commun. 346:739–745. doi:https://doi.org/10.1016/j.bbrc.2006.05.170.

Sordillo, L.M. 2016. Nutritional strategies to optimize dairy cattle immunity1. J. Dairy Sci. 99:4967–4982. doi:https://doi.org/10.3168/jds.2015-10354.

Sordillo, L.M., and S.L. Aitken. 2009. Impact of oxidative stress on the health and immune function of dairy cattle. Vet. Immunol. Immunopathol. 128:104–109.

Sordillo, L.M., G.A. Contreras, and S.L. Aitken. 2009. Metabolic factors affecting the inflammatory response of periparturient dairy cows. Anim. Heal. Res. Rev. 10:53–63.

Sordillo, L.M., and V. Mavangira. 2014. The nexus between nutrient metabolism, oxidative stress and inflammation in transition cows. Anim. Prod. Sci. 54:1204–1214.

Sordillo, L.M., and W. Raphael. 2013. Significance of metabolic stress, lipid mobilization, and inflammation on transition cow disorders. Vet. Clin. Food Anim. Pract. 29:267–278.

Spaniol, M., P. Kaufmann, K. Beier, J. Wüthrich, M. Török, H. Scharnagl, W. März, and S. Krähenbühl. 2003. Mechanisms of liver steatosis in rats with systemic carnitine deficiency due to treatment with trimethylhydraziniumpropionate. J. Lipid Res. 44:144–153. doi:10.1194/jlr.M200200-JLR200.

Stahl, A. 2004. A current review of fatty acid transport proteins (SLC27). Pflügers Arch. 447:722–727. doi:10.1007/s00424-003-1106-z.

Steiger, M., M. Senn, G. Altreuther, D. Werling, F. Sutter, M. Kreuzer, and W. Langhans. 1999. Effect of a prolonged low-dose lipopolysaccharide infusion on feed intake and metabolism in heifers1. J. Anim. Sci. 77:2523–2532. doi:10.2527/1999.7792523x.

Stortz, J. A., S. L. Raymond, J. C. Mira, L. L. Moldawer, A. M. Mohr, and P. A. Efron. 2017. Murine models of sepsis and trauma: Can we bridge the gap?. ILAR J. 58:90–105. doi:10.1093/ilar/ilx007.

Strucken, E., Y. Laurenson, and G. Brockmann. 2015. Go with the flow - Biology and genetics of the lactation cycle. Front. Genet. 6. doi:10.3389/fgene.2015.00118.

Sugden, M.C., K. Bulmer, and M.J. Holness. 2001. Fuel-sensing mechanisms integrating lipid and carbohydrate utilization. Biochem. Soc. Trans. 29:272–278. doi:10.1042/bst0290272.

Sumner, J.M., and J.P. McNamara. 2007. Expression of lipolytic genes in the adipose tissue of pregnant and lactating Holstein dairy cattle. J. Dairy Sci. 90:5237–5246.

Sunny, N.E., F. Bril, and K. Cusi. 2017. Mitochondrial adaptation in nonalcoholic fatty liver disease: Novel mechanisms and treatment strategies. Trends Endocrinol. Metab. 28:250–260. doi:https://doi.org/10.1016/j.tem.2016.11.006.

Swank, V.A., W.S.B. Yoho, K.M. O'Diam, M.L. Eastridge, A.J. Niehaus, and K.M. Daniels. 2013. Jersey calf performance in response to high-protein, high-fat liquid feeds with varied fatty acid profiles: Blood metabolites and liver gene expression. J. Dairy Sci. 96:3845–3856. doi:https://doi.org/10.3168/jds.2012-6100.

Swigoňová, Z., A.-W. Mohsen, and J. Vockley. 2009. Acyl-CoA dehydrogenases: dynamic history of protein family evolution. J. Mol. Evol. 69:176–193.

Tanaka, K., and I.M. Armitage. 1975. Investigation of 13C-valine metabolism in methylmalonic acidemia using nuclear magnetic resonance: Identification of propionate as an obligate intermediate. United States.

Tanaka, T., J. Yamamoto, S. Iwasaki, H. Asaba, H. Hamura, Y. Ikeda, M. Watanabe, K. Magoori, R.X.

Ioka, K. Tachibana, Y. Watanabe, Y. Uchiyama, K. Sumi, H. Iguchi, S. Ito, T. Doi, T. Hamakubo, M. Naito, J. Auwerx, M. Yanagisawa, T. Kodama, and J. Sakai. 2003. Activation of peroxisome proliferator-activated receptor δ induces fatty acid β-oxidation in skeletal muscle and attenuates metabolic syndrome. Proc. Natl. Acad. Sci. 100:15924 LP – 15929. doi:10.1073/pnas.0306981100.

Taylor, R. 1990. Interpretation of the correlation coefficient: a basic review. J. Diagnostic Med. Sonogr. 6:35–39. doi:10.1177/875647939000600106.

Tein, I. 2003. Carnitine transport: Pathophysiology and metabolism of known molecular defects. J. Inherit. Metab. Dis. 26:147–169. doi:10.1023/A:1024481016187.

Thorpe, C., and J.J. Kim. 1995. Structure and mechanism of action of the acyl-CoA dehydrogenases. FASEB J. 9:718–725.

Tontonoz, P., E. Hu, R.A. Graves, A.I. Budavari, and B.M. Spiegelman. 1994. mPPAR gamma 2: tissue-specific regulator of an adipocyte enhancer. Genes Dev. 8:1224–1234. doi:10.1101/gad.8.10.1224.

Torrens, J.M., J.M. Orellana-Gavaldà, M. Palou, J. Sánchez, L. Herrero, C. Picó, D. Serra, and A. Palou. 2014. Enhancing hepatic fatty acid oxidation as a strategy for reversing metabolic disorders programmed by maternal undernutrition during gestation. Cell. Physiol. Biochem. 33:1498–1515. doi:10.1159/000358714.

Tyburczy, C., A.L. Lock, D.A. Dwyer, F. Destaillats, Z. Mouloungui, L. Candy, and D.E. Bauman. 2008. Uptake and utilization of trans octadecenoic acids in lactating dairy cows. J. Dairy Sci. 91:3850–3861. doi:https://doi.org/10.3168/jds.2007-0893.

Uchida, Y., K. Izai, T. Orii, and T. Hashimoto. 1992. Novel fatty acid beta-oxidation enzymes in rat liver mitochondria. II. Purification and properties of enoyl-coenzyme A (CoA) hydratase/3-hydroxyacyl-CoA dehydrogenase/3-ketoacyl-CoA thiolase trifunctional protein. J. Biol. Chem. 267:1034–1041.

Um, J.H., S.J. Park, H. Kang, S. Yang, M. Foretz, M.W. McBurney, M.K. Kim, B. Viollet, and J.H. Chung. 2010. AMP-activated protein kinase-deficient mice are resistant to the metabolic effects of resveratrol. Diabetes 59:554–563. doi:10.2337/db09-0482.

Um, S.H., D. D'Alessio, and G. Thomas. 2006. Nutrient overload, insulin resistance, and ribosomal protein S6 kinase 1, S6K1. Cell Metab. 3:393–402. doi:https://doi.org/10.1016/j.cmet.2006.05.003.

Vailati-Riboni, M., M. Kanwal, O. Bulgari, S. Meier, N. V Priest, C.R. Burke, J.K. Kay, S. McDougall, M.D. Mitchell, C.G. Walker, M. Crookenden, A. Heiser, J.R. Roche, and J.J. Loor. 2016. Body condition score and plane of nutrition prepartum affect adipose tissue transcriptome regulators of metabolism and inflammation in grazing dairy cows during the transition period. J. Dairy Sci. 99:758–770. doi:https://doi.org/10.3168/jds.2015-10046.

Valko, M., D. Leibfritz, J. Moncol, M.T.D. Cronin, M. Mazur, and J. Telser. 2007. Free radicals and antioxidants in normal physiological functions and human disease. Int. J. Biochem. Cell Biol. 39:44–84. doi:https://doi.org/10.1016/j.biocel.2006.07.001.

Vandesompele, J., K. De Preter, F. Pattyn, B. Poppe, N. Van Roy, A. De Paepe, and F. Speleman. 2002. Accurate normalization of real-time quantitative RT-PCR data by geometric averaging of multiple internal control genes. Genome Biol. 3:research0034.1. doi:10.1186/gb-2002-3-7-research0034.

Vaz, F.M., and R.J.A. Wanders. 2002. Carnitine biosynthesis in mammals. Biochem. J. 361:417–429. doi:10.1042/bj3610417.

VDLUFA. 2007. Verband Deutscher Landwirtschaftlicher Untersuchungs-und Forschungsanstalten. Handbuch der Landwirtschaftlichen Versuchs-und Untersuchungsmethodik (VDLUFA-Methodenbuch), Bd. III. Die Chemische Untersuchung von Futtermitteln.

Veldhoven, P.P. Van. 2010. Biochemistry and genetics of inherited disorders of peroxisomal fatty acid metabolism. J. Lipid Res. 51:2863–2895. doi:10.1194/JLR.R005959.

Vilà-Brau, A., A.L. De Sousa-Coelho, C. Mayordomo, D. Haro, and P.F. Marrero. 2011. Human HMGCS2 regulates mitochondrial fatty acid oxidation and FGF21 expression in HepG2 cell line. J. Biol. Chem. 286:20423–20430. doi:10.1074/jbc.M111.235044.

Virmani, A., and A. Diedenhofen. 2015. The possible mechanisms involved in the protection strategies against radiation-induced cellular damage by carnitines. Int. J. Clin. Med. 06:71–80. doi:10.4236/ijcm.2015.62011.

Viscomi, C., E. Bottani, G. Civiletto, R. Cerutti, M. Moggio, G. Fagiolari, E.A. Schon, C. Lamperti, and M. Zeviani. 2011. In vivo correction of COX deficiency by activation of the AMPK/PGC-1alpha axis. Cell Metab. 14:80–90. doi:10.1016/j.cmet.2011.04.011.

Viturro, E., C. Altenhofer, B. Zölch, A. Burgmaier, I. Riedmaier, and M.W. Pfaffl. 2014. Microfluidic high-throughput reverse-transcription quantitative PCR analysis of liver gene expression in lactating animals. Microchim. Acta 181:1725–1732. doi:10.1007/s00604-014-1205-x.

Wajner, M., and A.U. Amaral. 2016. Mitochondrial dysfunction in fatty acid oxidation disorders:

insights from human and animal studies. Biosci. Rep. 36. doi:10.1042/BSR20150240.

Waldron, M.R., T. Nishida, B.J. Nonnecke, and T.R. Overton. 2003. Effect of lipopolysaccharide on indices of peripheral and hepatic metabolism in lactating cows. J. Dairy Sci. 86:3447–3459. doi:https://doi.org/10.3168/jds.S0022-0302(03)73949-6.

Wanders, R.J.A. 2013. Peroxisomes in human health and disease: Metabolic pathways, metabolite transport, interplay with other organelles and signal transduction BT - peroxisomes and their key role in cellular signaling and metabolism. L.A. del Río, ed. Springer Netherlands, Dordrecht.

Wanders, R.J.A. 2014. Metabolic functions of peroxisomes in health and disease. Biochimie 98:36–44. doi:https://doi.org/10.1016/j.biochi.2013.08.022.

Wanders, R.J.A., and H.R. Waterham. 2006. Biochemistry of mammalian peroxisomes revisited. Annu. Rev. Biochem. 75:295–332. doi:10.1146/annurev.biochem.74.082803.133329.

Wang, M.-F., C.-L. Han, and S.-J. Yin. 2009. Substrate specificity of human and yeast aldehyde dehydrogenases. Chem. Biol. Interact. 178:36–39. doi:https://doi.org/10.1016/j.cbi.2008.10.002.

Wehner, G., C. Balko, K. Humbeck, E. Zyprian, and F. Ordon. 2016. Expression profiling of genes involved in drought stress and leaf senescence in juvenile barley. BMC Plant Biol. 16:3.

Weiss, W.P., and J.M. Pinos-Rodríguez. 2009. Production responses of dairy cows when fed supplemental fat in low-and high-forage diets. J. Dairy Sci. 92:6144–6155.

Westermann, B. 2010. Mitochondrial fusion and fission in cell life and death. Nat Rev Mol Cell Biol 11:872-884. Nat. Rev. Mol. Cell Biol. 11:872–884. doi:10.1038/nrm3013.

Wetterau, J.R., R.E. Gregg, T.W. Harrity, C. Arbeeny, M. Cap, F. Connolly, C.H. Chu, R.J. George, D.A. Gordon, and H. Jamil. 1998. An MTP inhibitor that normalizes atherogenic lipoprotein levels in WHHL rabbits. Science (80). 282:751–754.

Wheeler, L.J., Z.L. Watson, L. Qamar, T.M. Yamamoto, B.T. Sawyer, K.D. Sullivan, S. Khanal, M. Joshi, V. Ferchaud-Roucher, H. Smith, L.A. Vanderlinden, S.W. Brubaker, C.M. Caino, H. Kim, J.M. Espinosa, J.K. Richer, and B.G. Bitler. 2019. Multi-omic approaches identify metabolic and autophagy regulators important in ovarian cancer dissemination. Science 19:474–491. doi:https://doi.org/10.1016/j.isci.2019.07.049.

White, H.M. 2015. The role of TCA cycle anaplerosis in ketosis and fatty liver in periparturient dairy cows. Anim. an open access J. from MDPI 5:793–802. doi:10.3390/ani5030384.

Van Wijk, R., and W.W. van Solinge. 2005. The energy-less red blood cell is lost: erythrocyte enzyme

abnormalities of glycolysis. Blood 106:4034–4042. doi:10.1182/blood-2005-04-1622.

Wipperman, M.F., M. Yang, S.T. Thomas, and N.S. Sampson. 2013. Shrinking the FadE proteome of Mycobacterium tuberculosis: insights into cholesterol metabolism through identification of an α2β2 heterotetrameric acyl coenzyme A dehydrogenase family. J. Bacteriol. 195:4331–4341.

Wolfrum, C., C.M. Borrmann, T. Börchers, and F. Spener. 2001. Fatty acids and hypolipidemic drugs regulate peroxisome proliferator-activated receptors α- and γ-mediated gene expression via liver fatty acid binding protein: A signaling path to the nucleus. Proc. Natl. Acad. Sci. 98:2323 LP – 2328. doi:10.1073/pnas.051619898.

Xu, T., F.C. Cardoso, A. Pineda, E. Trevisi, X. Shen, F. Rosa, J.S. Osorio, and J.J. Loor. 2017. Grain challenge affects systemic and hepatic molecular biomarkers of inflammation, stress, and metabolic responses to a greater extent in Holstein than Jersey cows. J. Dairy Sci. 100:9153–9162. doi:https://doi.org/10.3168/jds.2017-13321.

Xu, T., H. Tao, G. Chang, K. Zhang, L. Xu, and X. Shen. 2015. Lipopolysaccharide derived from the rumen down-regulates stearoyl-CoA desaturase 1 expression and alters fatty acid composition in the liver of dairy cows fed a high-concentrate diet. BMC Vet. Res. 11:52. doi:10.1186/s12917-015-0360-6.

Yan, S., X.F. Yang, H.L. Liu, N. Fu, Y. Ouyang, and K. Qing. 2015. Long-chain acyl-CoA synthetase in fatty acid metabolism involved in liver and other diseases: an update. World J. Gastroenterol. WJG 21:3492.

Yang, J., L. Craddock, S. Hong, and Z.M. Liu. 2009. AMP-activated protein kinase suppresses LXR-dependent sterol regulatory element-binding protein-1c transcription in rat hepatoma McA-RH7777 cells. J. Cell. Biochem. 106:414–426. doi:10.1002/jcb.22024.

Yang, L.Y., and A. Kuksis. 1991. Apparent convergence (at 2-monoacylglycerol level) of phosphatidic acid and 2-monoacylglycerol pathways of synthesis of chylomicron triacylglycerols. J. Lipid Res. 32:1173–1186.

Yang, Y., H. Sadri, C. Prehn, J. Adamski, J. Rehage, S. Dänicke, B. Saremi, and H. Sauerwein. 2019. Acylcarnitine profiles in serum and muscle of dairy cows receiving conjugated linoleic acids or a control fat supplement during early lactation. J. Dairy Sci. 102:754–767. doi:https://doi.org/10.3168/jds.2018-14685.

Yeaman, S.J. 2004. Hormone-sensitive lipase - new roles for an old enzyme. Biochem. J. 379:11–22. doi:10.1042/bj20031811.

Yoshino, J., K.F. Mills, M.J. Yoon, and S. Imai. 2011. Nicotinamide mononucleotide, a key NAD(+) intermediate, treats the pathophysiology of diet- and age-induced diabetes in mice. Cell Metab. 14:528–536. doi:10.1016/j.cmet.2011.08.014.

You, M., M. Matsumoto, C.M. Pacold, W.K. Cho, and D.W. Crabb. 2004. The role of AMP-activated protein kinase in the action of ethanol in the liver. Gastroenterology 127:1798–1808. doi:https://doi.org/10.1053/j.gastro.2004.09.049.

Youle, R.J., and D.P. Narendra. 2011. Mechanisms of mitophagy. Nat. Rev. Mol. cell Biol. 12:9–14.

Zammit, V.A., C.G. Corstorphine, and S.R. Gray. 1984. Changes in the ability of malonyl-CoA to inhibit carnitine palmitoyltransferase I activity and to bind to rat liver mitochondria during incubation in vitro. Differences in binding at 0°C and 37°C with a fixed concentration of malonyl-CoA. Biochem. J. 222:335–342. doi:10.1042/bj2220335.

Zarrin, M., O. Wellnitz, H.A. van Dorland, J.J. Gross, and R.M. Bruckmaier. 2014. Hyperketonemia during lipopolysaccharide-induced mastitis affects systemic and local intramammary metabolism in dairy cows. J. Dairy Sci. 97:3531–3541. doi:10.3168/JDS.2013-7480.

Zeng, J., and D. Li. 2005. Intrinsic isomerase activity of medium-chain Acyl-CoA dehydrogenase. Biochemistry 44:6715–6722. doi:10.1021/bi047363m.

Zhang, Y.K., Y.Y. Qu, Y. Lin, X.H. Wu, H.Z. Chen, X. Wang, K.Q. Zhou, Y. Wei, F. Guo, C.F. Yao, X. Di He, L.X. Liu, C. Yang, Z.Y. Guan, S.D. Wang, J. Zhao, D.P. Liu, S.M. Zhao, and W. Xu. 2017. Enoyl-CoA hydratase-1 regulates mTOR signaling and apoptosis by sensing nutrients. Nat. Commun. 8:464. doi:10.1038/s41467-017-00489-5.

Zhao, F.F., T.Y. Wu, H.R. Wang, L.Y. Ding, G. Ahmed, H.W. Li, W. Tian, and Y.Z. Shen. 2018. Jugular arginine infusion relieves lipopolysaccharide-triggered inflammatory stress and improves immunity status of lactating dairy cows. J. Dairy Sci. 101:5961–5970. doi:https://doi.org/10.3168/jds.2017-13850.

Zhou, G., R. Myers, Y. Li, Y. Chen, X. Shen, J. Fenyk-Melody, M. Wu, J. Ventre, T. Doebber, N. Fujii, N. Musi, M.F. Hirshman, L.J. Goodyear, and D.E. Moller. 2001. Role of AMP-activated protein kinase in mechanism of metformin action. J. Clin. Invest. 108:1167–1174. doi:10.1172/JCI13505.

Zhou, L., L. Xu, J. Ye, D. Li, W. Wang, X. Li, L. Wu, H. Wang, F. Guan, and P. Li. 2012. Cidea promotes hepatic steatosis by sensing dietary fatty acids. Hepatology 56:95–107.

Zhu, Y., G. Liu, X. Du, Z. Shi, M. Jin, X. Sha, X. Li, Z. Wang, and X. Li. 2019. Expression patterns of hepatic genes involved in lipid metabolism in cows with subclinical or clinical ketosis. J. Dairy

Sci. 102:1725–1735. doi:10.3168/jds.2018-14965.

Zoncu, R., A. Efeyan, and D.M. Sabatini. 2011. mTOR: from growth signal integration to cancer, diabetes and ageing. Nat. Rev. Mol. Cell Biol. 12:21–35. doi:10.1038/nrm3025.

9 ACKNOWLEDGMENTS

Foremost, I would like to express my sincere gratitude to my advisor Professor Dr. Dr. Helga Sauerwein, for her guidance and support throughout my Ph.D. studies. I am grateful to her for giving me the unique opportunity of working in her amazing group and on an exciting topic. I have gained priceless knowledge and skills from her.

I am grateful to Professor Dr. Karl-Heinz Südekum for accepting to co-reference this thesis. I am thankful for his supervision throughout my Ph.D. study.

I would also like to thank the team of scientists from different locations in Germany who worked for hand in hand on the MitoCow project. It was a great chance for me to work with such an interdisciplinary group of recognized scientists, technicians, and students.

My sincere thanks also go to Dr. Morteza Hosseini Ghaffari for supporting me not only as my mentor but also as a big brother through my scientific and personal life. I thank him for sharing his ideas with me and guiding me through the research project.

I would like to thank all my colleagues from the institute for animal science, especially the section of Physiology, and highlighting Inga Hofs as a colleague and friend for all her support inside and outside of my Ph.D. project, and also, Isabella Israel, Arash Veshkini, Laura Webb, Thomas Blees, Barbara Heitkönig, Katharina Kustwan and all the other colleagues who for the lack of space, I am not able to name here.

My thorough appreciation goes to Dr. Hassan Sadri. He has always been very supportive of me and his strong personality and knowledge were an inspiration for me to start my life in Germany and accomplish my Ph.D.

I would like to thank Dr. Jan Bergerhoff for his supports in the final stages of my study, exactly at the time when I needed them the most.

I would like to thank the nice people in the Institute of Genome Biology, genomics unit, Leibniz Institute for Farm Animal Biology in Dummerstorf, Germany for technical support and providing the facilities for carrying out the Fluidigm mRNA profiling.

I would like to thank my master thesis supervisor Professor Dr. Hamid Kohram who left this world when I was writing this Ph.D. thesis. Without his contribution to my scientific life, I would not have gotten into the position to prepare this thesis.

My last and very warmly felt special thanks to my wonderful family, baba Kazem, maman Zarifeh, abji Fatemeh, dadash Ahmad, dadash Ali, and the little Diana. Words can never express how grateful I am to them for their never-ending supports in my life and for giving me the opportunity to follow my dreams. My sincere love goes to them for their love and all the moral help.